UNIVERSITY OF WASHINGTON

Department of Orthopaedics and Sports Medicine

2001 Research Report

Helping People Become Winners

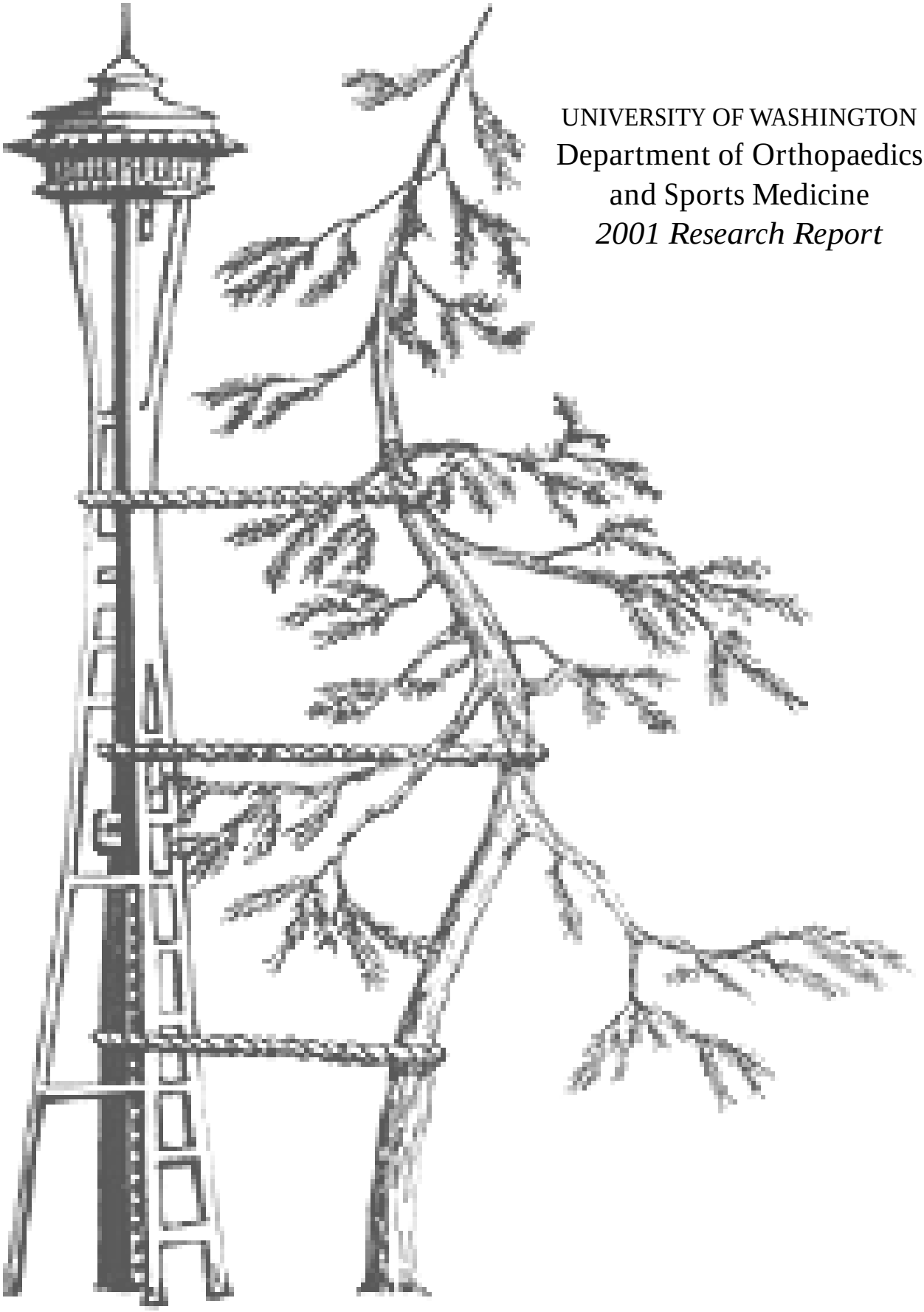

UNIVERSITY OF WASHINGTON

Department of Orthopaedics and Sports Medicine

2001 Research Report

UNIVERSITY OF WASHINGTON SCHOOL OF MEDICINE

Department of Orthopaedics and Sports Medicine
University of Washington
Seattle, WA 98195

EDITORS:
Fred Westerberg
Frederick A. Matsen III, M.D.
ASSOCIATE EDITORS:
Howard A. Chansky, M.D.
Ernest U. Conrad III, M.D.
Ted S. Gross, Ph.D.
M.L. Chip Routt, M.D.
Peter T. Simonian, M.D.
Kit M. Song, M.D.

DESIGN & LAYOUT:
Fred Westerberg

Cover Illustration: "The Beggars"
by Pieter Brueghel, the Elder, 1568
Collection of The Louvre, Paris, France
Reprinted with permission of
Reunion des Musees Nationaux/Art Resource, New York

Contents

Foreword 1

Sigvard T. Hansen, Jr., M.D., 2001 Distinguished Alumnus 2

Assessment of NTx and Col2CTx Urine Assay in Endurance Athletes 3

John O'Kane, M.D., Lynne Atley, Ph.D., Chris Hawley, M.D., Carol Teitz, M.D., and David Eyre, Ph.D.

Identification of Matrilin-3 in Adult Human Articular Cartilage 6

Jiann-Jiu Wu, Ph.D. and David Eyre, Ph.D.

TLS / CHOP Inhibits RNA Splicing Mediated by YB-1 8

Timothy Rapp, M.D., Liu Yang, Ph.D., Ernest U. Conrad III, M.D., and Howard A. Chansky, M.D.

Depth of Countersinking Modulates Cartilage Remodeling in Sheep Osteochondral Autografts 10

Fred Huang, M.D., Peter Simonian, M.D., Anthony Norman, B.S.E., and John Clark, M.D., Ph.D.

Distal Femoral Tunnel Placement for Multiple Ligament Reconstruction: Three Dimensional Computer Modeling and Cadaveric Correlation 13

William J. Mills, M.D. and Randy Ching, Ph.D.

Intramedullary Nailing of Distal Metaphyseal Tibial Fractures 16

Sean E. Nork, M.D., Alexandra K. Schmitt, M.D., Julie Agel, M.A., Sarah K. Holt, M.P.H., Jason L. Schrick, B.S., and Robert A. Winquist, M.D.

The Association Between Supracondylar Intercondylar Distal Femoral Fractures and Hoffa Fractures 19

Sean E. Nork, M.D., Kamran Aflatoon, D.O ., Daniel N. Segina, M.D., Stephen K. Benirschke, M.D., M.L. Chip Routt, Jr., M.D, and M. Bradford Henley, M.D., M.B.A.

Triangular Osteosynthesis and Iliosacral Screw Fixation For Unstable Sacral Fractures: A Biomechanical Evaluation Under Cyclic Loads 22

T.A. Schildhauer, W.R. Ledoux, Jens R. Chapman, M.D., M.B. Henley, M.D., Allan F. Tencer, Ph.D., and M.L.Chip Routt, M.D.

Effect of Cervical Lesions on Neural Space Integrity 25

Sohail K. Mirza, M.D., D.J. Nuckley, M.A. Konodi, and Randy P. Ching, Ph.D.

Vertebroplasty with a Cavitation Drill 27

A.J. Mirza, M.A. Konodi, Jens R. Chapman, M.D., Carlo Bellabarba, M.D., Randy P. Ching, Ph.D., Allan F. Tencer, Ph.D., and Sohail K. Mirza, M.D.

The Development and Validation of a Computational Foot and Ankle Model 31

William R. Ledoux, Ph.D., Daniel L. A. Camacho, M.D., Ph.D., Randal P. Ching, Ph.D., and Bruce J. Sangeorzan, M.D.

Mechanical Testing to Characterize the Performance of Shock Absorbing Pylons Used in Transtibial Prostheses 33

Jocelyn S. Berge, B.S., Glenn K. Klute, Ph.D., Carol F. Kallfelz, M.S., and Joseph M. Czerniecki, M.D.

The Distribution of Shoulder Replacements Among Surgeons and Hospitals is Significantly Different than that of Hip or Knee Replacements 35

Samer S. Hasan, M.D., Ph.D., Jordan M. Leith, M.D., F.R.C.S.C., Kevin L. Smith, M.D., and Frederick A. Matsen III, M.D.

Hereditary Multiple Exostoses: Is There a Correlation Between Phenotype and Genotype? 37
Gregory A. Schmale, M.D., Ernest U. Conrad III, M.D., and Wendy H. Raskind, M.D., Ph.D.

Intralesional Treatment of Symptomatic Enchondromas and Low-Grade Chondrosarcomas 40
Scott Helmers, M.D. and Ernest U. Conrad III, M.D..

The Orthopedic Implications of Chemotherapy to Growth in Children 42
Scott Helmers, M.D. and Ernest U. Conrad III, M.D.

Technique of Scapulothoracic Fusion in Facioscapulohumeral Muscular Dystrophy 44
Mohammad Diab, M.D. and Frederic Shapiro, M.D.

Effects of Growth Factors in Combination on In Vivo Flexor Tendon Healing 47
Christopher H. Allan, M.D., Sang-Gil P. Lee, M.D., Robert A. Mintzer, B.S., Ho-Jung Kang, M.D., and Daniel P. Mass, M.D.

Randomized Prospective Trial of Active versus Passive Motion after Zone II Flexor Tendon Repair 49
Thomas E. Trumble, M.D., Richard S. Idler, M.D., James W. Strickland, M.D., Peter J. Stern, M.D., Shelly Sailer, O.T.R./C.H.T., and Mary M. Gilbert, M.A.

Department of Orthopaedics and Sports Medicine Faculty 52

Incoming Residents 53

Graduating Residents 54

New Faculty 55

Research Grants 56

Contributors to Departmental Research and Education 60

2001 AAOS Alumni Pictures 62

Foreword

This year, our cover features the Beggars, painted by Pieter Brueghel the elder 433 years ago. This small painting on wood is shown here in the same size as it is seen on the second floor of the Richelieu wing of the Louvre. Closer inspection reveals that at least three of these beggars have had amputations of both their legs. As a result, they need to use their arms for support and getting around. This makes it impossible for them to work - thus they are reduced to begging. Their prostheses serve primarily to protect their shins from the ground, but one has tried to build himself up a bit with an added post. These individuals are being totally ignored by the figure passing them by. In contrast, let us consider the life of Ernest Burgess (1911-2000) who did not pass by individuals who lost their legs, but rather spent much of his life designing and providing limbs that enabled them to get back up on their feet, to free up their arms, to work, to play and to have families. The systems he put in place will continue to serve, not only in the United States where limbs are lost from trauma, infection and tumors, but in Vietnam, Cambodia, and Afghanistan where land mines continue to truncate limbs and the quality of peoples' lives.

Ernest M. Burgess, M.D., Ph.D.

This has been a most exiting year for our Department. We now have a new name: Orthopaedics and Sports Medicine, indicating our commitment to prevention and to the prompt return of our patients to optimal function after injury or surgery. Thanks to the generosity of a select group of Seattle citizens, we have established the first Endowed Chair for Women's Sports Medicine and Lifetime Fitness and are now well along in our search for the first holder. The Department and the Chair were featured in the University's Showcase event on May 2 and we formally opened our new Sports Medicine Clinic in the Hec Edmundson Pavilion with the help of Rose Bowl-winning Coach Rick Neuheisel on May 16.

On the research front, our faculty continue to achieve at the highest level, with extramural funding, peer-reviewed publications, and recognitions, such as the Kappa Delta Clinical Research Award presented this year to Bruce Sangeorzan, Allan Tencer and Randy Ching. David Eyre's group in the Burgess Laboratories continues their pace-setting work in collagen biology - using the Col2CTx marker of cartilage turnover along with the NTx marker of bone turnover. Ted Gross and his team in the Orthopaedic Science Laboratories are exploring bone's ability to self-regulate its mass and morphology in response to hormonal, metabolic, and physical stimuli. John Clark has just returned from a sabbatical in Switzerland where he explored new methods of acetabular reconstruction. John Sidles continues his widely recognized work on magnetic resonance force microscopy. Howard Chansky and Liu Yang have formed a new molecular biology laboratory at the VA where they are joined by Sohail Mirza and his spine research program - soon to be supported by a spine research chair. Steve Benirschke, holder of the Debs Chair, has now returned from his New Zealand sabbatical and will bring his foot trauma research team to action. Countless other laboratory and clinical research programs are underway in our Department, a sampling of which are presented in the pages that follow. We hope you enjoy these articles. If you have thoughts or questions, please be sure to share them with me.

As this Research Report demonstrates, we have an inherently curious team of faculty, residents and staff, all striving to improve the care of our patients through a commitment to rigorous investigation. With changes in reimbursement for health care and with changes in the federal support for research, many orthopaedic departments across the country are progressively curtailing their commitment to research. Thanks to the dedication of the UW Orthopaedics and Sports Medicine faculty and to the generosity of the caring individuals in our region, our investigative programs have never been stronger.

Best wishes,

Frederick A. Matsen III, M.D.
Chairman

Sigvard T. Hansen, Jr., M.D.
2001 Distinguished Alumnus
University of Washington School of Medicine

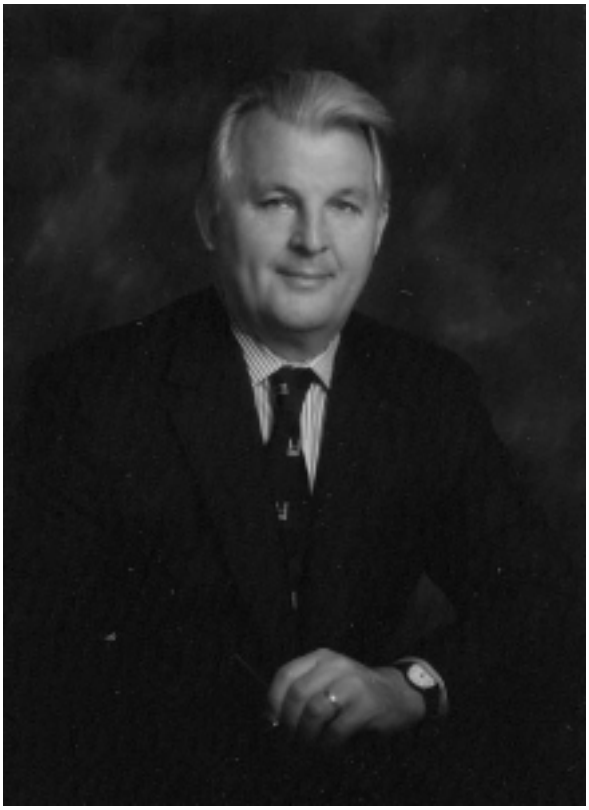

Ted is generally credited for establishing the field of Orthopaedic Traumatology-the aggressive and immediate fixation of all major fractures in multiple injured individuals. His approach enables severely traumatized individuals to get out of bed soon after their accident, avoiding atelectasis, pneumonia, deep venous thrombosis, pulmonary emboli, urinary track infections, and bed sores. His philosophy and techniques have saved vast numbers of lives not only here, but also across the globe, thanks to his worldwide teaching efforts and to the traumatology fellowships he has initiated here.

His attention is now turned to foot and ankle reconstruction. Simply stated, he is the world's most respected authority in this field. His fundamental understanding of the alignment and motion of the complex foot, subtalar, and ankle joints have enabled him to master the most complex of reconstructive problems, whether from arthritis, injury, or degenerative conditions such as Charcot Marie Tooth's disease. He now does more total ankle replacements than any other individual surgeon in the country. As was the case during his "traumatology period", his impact is not confined to the patients he treats. He is in heavy demand as a lecturer across the world and teaches students, residents, fellows and practicing physicians from all over the globe. Following him on rounds is a bit like being at the United Nations, with accents from Europe, Asia, Africa and, South America. His sentinel book, *Functional Reconstruction of the Foot and Ankle*, was published in March 2000. On July 20, 2000 the Sigvard T. Hansen Foot & Ankle Institute was officially opened at Harborview Medical Center with Dr. Hansen as its inaugural Director.

We should mention some of his many other contributions to the University of Washington. His consistent presence at Harborview has provided the stamp of credibility on what used to be King County Hospital, helping convert it to one of the best known medical centers in the land. Thanks to his consistent leadership and stabilizing presence, Harborview Orthopaedics is now ranked as the best Orthopaedic program in the Western United States and the best public Orthopaedic program in the country! (see http://www.usnews.com/usnews/nycu/health/hosptl/specorth.htm)

He served the UW School of Medicine as Chair of Orthopaedics for five years and as acting Chair on two other occasions. He served as Chief of Orthopaedics at Harborview for many years. On two occasions when there were massive defections of faculty, he single-handedly held the service together. Thanks to the effect of his "deep keel", the Orthopaedic service is now in its longest period of faculty stability and has the reputation of being the best traumatology service in the world.

Dr. Hansen's excellence has been recognized by patients, former residents, former fellows, fellow faculty, and industry in the establishment of the Sigvard T. Hansen Endowed Chair for Traumatology Research. This chair, of which he was the inaugural holder, provides perpetual support for innovative research leading to improved care for injured individuals worldwide. In the near future we hope to have completed the fund-raising needed to endow a new Hansen Chair that will be permanently directed to improving the care of those individuals with severe foot and ankle arthritis and deformities. Those interested in knowing more are invited to contact me at matsen@u.washington.edu.

As a conclusion of our salute, we recognize that Ted Hansen is not only the Distinguished Alumnus of the University of Washington School of Medicine, but also the Distinguished Alumnus of the Department of Orthopaedics' Residency Program that he completed in 1969. I will always remember his three admonitions:

- Stick your neck out for what you believe in.
- If it doesn't look good, it probably isn't.
- If it's worth doing, it's worth doing right.

By the way, Ted, thanks for coming in at 3 am to help me with that tibia fracture 26 years ago and all the other help you've given!

Best wishes,

F. A. Matsen III

Frederick A. Matsen III, M.D.
Chairman

Assessment of NTx and Col2CTx Urine Assay in Endurance Athletes

JOHN O'KANE, M.D., LYNNE ATLEY, PH.D., CHRIS HAWLEY, M.D., CAROL TEITZ, M.D., AND DAVID EYRE, PH.D.

Rowing, cross-country running, or swimming competitively at the college level requires outstanding aerobic fitness and extensive aerobic training. In all three sports, most of the training is sport specific. While the cardiovascular challenges for the three sports are similar, the musculoskeletal challenges vary significantly. Runners expose their lower extremity bones and joints to large repetitive axial loads. Crew athletes expose their entire skeleton to both axial and non-axial loads but by virtue of their being seated, their lower extremity bones and joints experience lower axial loads than those of runners. Swimmers' joints experience the least compressive force, and their bones experience the lowest axial loads.

Biological markers exist that can provide an index of the rate of bone and cartilage turnover in a living human. Cross-linked N-telopeptides of type I collagen (NTx) can be measured in blood or urine as an index of osteoclastic bone resorption (Calvo et al., 1996). Cathepsin K, a protease abundantly expressed by osteoclasts, cleaves type I collagen to generate the NTx neoepitope (Atley et al., 2000). NTx levels are elevated in postmenopausal women, in patients with metabolic bone disease and in growing children (Calvo et al., 1996).

Matrix metalloproteinases (MMP) have been implicated in the proteolytic degradation of cartilage collagen, a hallmark of osteoarthritis. The cross-linked C-telopeptide of type II collagen (Col2CTx) assay measures a proteolytic neoepitope of MMP cleavage as a marker of cartilage degradation (Atley et al., 1998). Higher levels of Col2CTx have been demonstrated in growing children from growth plate degradation and in adults with rheumatoid arthritis and osteoarthritis, diseases characterized by the destruction of articular cartilage (Atley et al., 1998).

Although NTx and Col2CTx assays have been applied to patients with skeletal pathologies, these assays have not been used to assess healthy but highly trained individuals in different sports. This study evaluates NTx and Col2CTx levels in college athletes, all participating in high intensity aerobic training, but experiencing very different degrees of skeletal stress.

Figure 1: Crew.

METHODS

A cross-sectional study of sixty collegiate athletes representing crew (C), cross-country runners (XC) and swimmers (S) was undertaken. Twenty athletes per training regimen, 10 males and 10 females, volunteered to participate. Data were collected in the early fall and during which time all of the athletes were in active training for their sports. Athletes were weighed and their height measured, then body mass index (BMI) was calculated. Spot urine samples were collected and assayed for NTx (bone resorption) and Col2CTx (cartilage degradation) by competition enzyme-linked immunosorbant assays on 96-well microtiter plates. The NTx and Col2CTx assays are based on monoclonal antibodies that recognize specific telopeptide sequences of type I and type II collagen, respectively. Biomarker values were reported as a ratio of urinary creatinine excretion. Data were analyzed by ANOVA and pair wise comparisons made by Tukey's Test using SigmaStat software.

RESULTS

NTx control ranges comparisons are gender specific while men and woman are combined in the Col2CTx analysis. Compared to controls, 70% of the rowers, 40% of the runners, and 10% of the swimmers had NTx values more than two standard deviations above the average.

Runners and rowers both had significantly elevated NTx values compared to swimmers. For Col2CTx, swimmers and rowers did not differ significantly from the controls, and only runners were significantly elevated. Age and urinary creatinine, variables which might affect the assay levels, did not vary significantly between the groups. Runners did have lower BMI than swimmers or rowers.

DISCUSSION

The data indicate significant differences in bone remodeling and cartilage degradation between the three sports. High NTx levels are consistent with increased bone remodeling. With

Figure 2: Cross Country Running.

Figure 3: Swimming.

remodeling the potential exists for net bone loss or gain depending on the relative activity of osteoclasts (resorption) and osteoblasts (formation). An increase in bone remodeling in response to training most likely reflects an adaptive response of the skeleton to the stresses and strains applied to it. Many studies have reported a positive association between load-bearing exercise and bone mineral density. The Col2CTx assay is clinically less well studied, but elevations appear to be secondary to cartilage degradation, either from active growth plate degradation in children or in adults with rheumatoid or osteoarthritis.

In our study groups, crew NTx values are the highest, likely secondary to axial and non-axial forces applied to the entire skeleton. Runners have high values as well compared to the general population secondary to high-impact loading of the lower skeleton despite little stress to the upper body. Swimming clearly stresses the entire body, but apparently through forces resulting in significantly less bone remodeling.

One might postulate that the Col2CTx data would parallel the NTx . Interestingly though, the Col2CTx data suggest that while swimming minimally stresses the joints as well as the bones, rowing which has the highest NTx value, causes significantly less cartilage degradation than running. Running is also the only sport with a Col2CTx value significantly elevated over controls. There is some evidence that professional participation in running sports such as soccer can result in early OA changes to weight-bearing joints, but the influence of injury versus joint loading alone is hard to separate. Once articular cartilage is injured, continued loading can result in more rapid progression of degenerative changes. Clinical studies are mixed regarding the risk of developing osteoarthritis from long term participation in regular exercise with some studies suggesting a modest increased risk (Lane et al, 1999). In Lane's study weight-bearing exercise was not any more likely than other forms of exercise to cause changes. Our data suggests that distance runners are stressing their joints sufficiently to cause cartilage degradation beyond that seen in the other sports, but clinical studies do not suggest runners are at significant increased risk for premature OA provided they do not have pre-existing knee injuries.

These results may have implications for exercise counseling. There is ample evidence that aerobic exercise is important for disease prevention, improving longevity and quality of life. One disease positively affected by exercise is osteoporosis; a debilitating age related loss of bone density resulting in crippling deformity and life threatening fractures. Weight-bearing exercise is specifically recommended to prevent osteoporosis because it is known to stimulate bone turnover with a net increase in bone density. It is common though for elderly individuals to have arthritis of their weight-bearing joints making weight-bearing exercise difficult and high impact exercise contraindicated. These results suggest that for this population, rowing may be an ideal exercise, stimulating bone turnover with less stress to weight-bearing joints. Whether or not rowing maintains bone density to the same extent as walking, jogging, or running should be the subject of future research.

	Age	BMI	NTx	Col2CTx	Creatinine
	yrs	kg/m2	nM BCE/mM Cr	ng/mg Cr	nM
Cross Country	19.3 +/- 1.3	21.3 +/- 1.9	61.9 +/- 31.0	35.1 +/- 14.5	11.6 +/- 8.3
Swimming	19.4 +/-1.6	25.9 +/-2.7	38.8 +/- 22.7	19.0 +/- 7.8	12.7 +/- 5.6
Crew	19.8 +/- 1.0	26.6 +/-2.7	85.8 +/-35.7	26.5 +/- 7.8	13.7 +/- 4.9
Control Women	36		35 +/- 15		
Control Men	46		27 +/- 12		
Control	33			24.5 +/- 8.4	

Table 1: Assessment data table.

Recommended Reading

Atley LM, Shao P, Ochs V, Shaffer K, Eyre DR. 1998. Matrixmetalloproteinase-mediated release of immunoreactive telopeptides from cartilage type II collagen. Trans. Orthop. Res. Soc. 23:850.

Atley LM, Mort JS, Lalumiere M, Eyre DR. 2000. Proteolysis of human bone collagen by cathepsin K: Characterization of the cleavage sites generating the cross-linked N-telopeptide neoepitope. Bone 26:241-247.

Calvo MS, Eyre DR, Gundberg CM. 1996. Molecular basis and clinical application of biological markers of bone turnover. Endocrine reviews 17:333-368.

Lane NE et al. 1999. Recreational physical activity and the risk of osteoarthritis of the hip in elderly women. Journal of Rheumatology. 26: 849-54.

Larsen E, Jensen PK, Jensen PR. 1999. Long-term outcome of knee and ankle injuries in elite football. Scand J Med Sci Sports. 9(5): 285-9.

Identification of Matrilin-3 in Adult Human Articular Cartilage

JIANN-JIU WU, PH.D. AND DAVID EYRE, PH.D.

Matrilin-3 is a recently identified matrix protein of cartilage that shows sequence homology to matrilin-1 (cartilage matrix protein or CMP). Matrilin-1 and -3 are both prominently expressed within growth cartilage matrix. They have several molecular features in common including a signalling peptide, either one or two von Willebrand factor type A-like domain(s), one or more EGF-like domain(s), and a COOH-terminal coiled-coil (-helix. Matrilin-1 consists of two vWFA-like modules connected by one EGF-like domain, whereas matrilin-3 cDNA predicts a single vWFA-like module separated from the C-terminal coiled-coil by four EGF-like modules (Fig. 1). We recently reported the identification of matrilin-3 at the protein level in extracts of bovine and human growth cartilages. The findings established that matrilin-3 is a subunit with matrilin-1 in disulfide-bonded heterotetrameric molecules. Using specific antibodies to human matrilin-1 and -3, we here define further the molecular properties of matrilin-3 in human fetal cartilage and demonstrate the presence of matrilin-3, but not matrilin-1, in normal adult human articular cartilage.

MATERIALS AND METHODS

Cartilage slices from fetal human epiphyseal cartilage (humerus and femur, 96-122 days, medical terminations, Central Laboratories for Human Embryology, University of Washington, Seattle) and adult human articular cartilage (banked normal tissue from a male donor 25 yr of age, Northwest Tissue Center, Seattle) were digested with chondroitinase ABC. Extracted proteins were resolved by SDS-PAGE and transblotted to PVDF membrane for Western blot analysis. Western blot analysis was performed with two polyclonal antisera. One was generated in rabbits against a mixture of two synthetic peptides, matching sequences in the A1 domain (-EAGAREPSSNIPKV-) and the carboxy-terminal domain (-LEKLKINEYGQIHR-) of the human matrilin-3 cDNA translation product. The polyclonal antiserum against matrilin-1 was made similarly against a mixture of two synthetic peptides (-AEGGRSRSPDISKV-) and (-AVSKRLAILENTVV-), also from A1 and carboxy-terminal domains.

RESULTS AND DISCUSSION

Electrophoresis of the disulfide-bonded matrilin tetramers from fetal cartilage on a low percentage polyacrylamide gel (SDS-5%PAGE) resolved a series of bands that were immunoreactive for matrilin-3 (Fig. 2, lane 2). The faster migrating of these bands also reacted with matrilin-1 antibody (Fig. 2, lane 1). Fetal growth cartilage therefore contains a mixture of molecular forms of mat-1/mat-3 heterotetramers. An extra band migrating slower than the mat-1/mat-3 heterotetramers reacted for matrilin-3 only, suggesting the presence of the homotetrameric molecule of matrilin-3. Therefore, fetal growth cartilage contains homotrimeric molecules of matrilin-1, homotetrameric molecules of matrilin-3 and the various heterotetrameric chain combinations of matrilins-1 and -3. Western blot analysis of matrix proteins extracted from adult articular cartilage showed a disulfide-bonded high molecular weight band migrating slower than the mat-1/mat-3 tetramers, reacting with the matrilin-3 antibody but not the matrilin-1 antibody and running in the position of the homotetrameric molecule of matrilin-3 from fetal cartilage (Fig 2, lane 4). At the protein level, it has previously been shown that both matrilin-1 and matrilin-3 are prominent matrix components of bovine and human epiphyseal growth cartilages but not of adult articular cartilage. By developing specific antisera to the individual subunits we were able to further characterize the mixture of molecular forms of the matrilin-1/matrilin-3 complex in growth cartilage and demonstrate that normal adult articular cartilage is distinct in containing the matrilin-3 homotetramer. Matrilin-1 is known to bind to type II collagen fibrils and to aggrecan and also to form a filamentous polymer by self interaction. The function of matrilin-3 is unknown but its content of a single vWFA-like domain and multiple EGF-like domains and difference in pattern of tissue expression suggests that matrilin-3 will differ from matrilin-1 in its interactive properties in the matrix. Its distribution, changes with age and potential effects on its expression in joints undergoing osteoarthritic

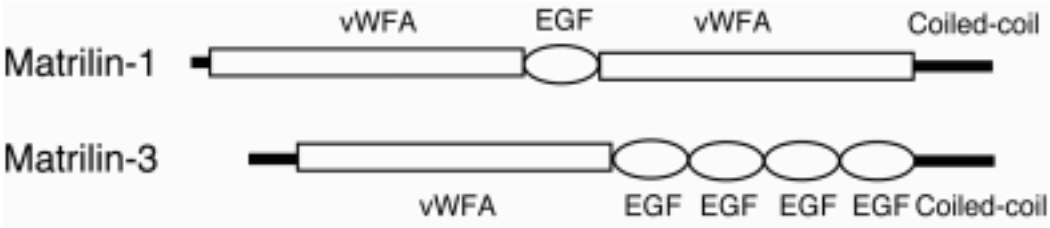

Figure 1: Modular structures of matrilin-1 and matrilin-3 monomers.

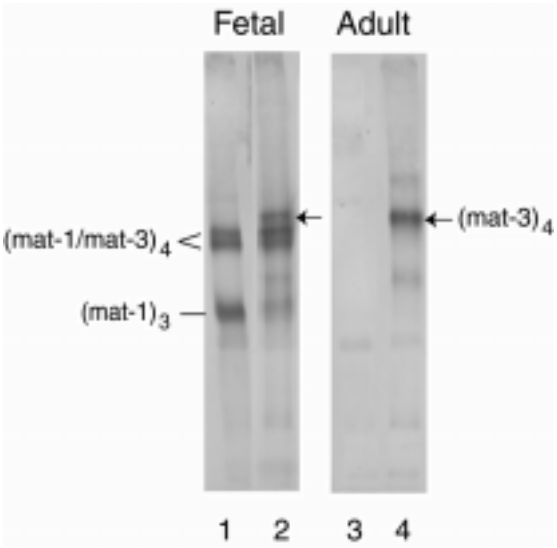

Figure 2: Western blot analysis of matrilin-1/matrilin-3 oligomers extracted from fetal human epiphyseal cartilage (lanes 1 and 2) and adult human articular cartilage (lanes 3 and 4) Matrilin samples were run under non-reducing conditions on SDS-5% PAGE then blotted to PVDF membrane and developed with the anti-matrilin-1 (lanes1 and 3) and anti-matrilin-3 (lanes 2 and 4) sera.

changes will be important to define.

Recommended Reading

Wu, J. J., and Eyre, D. R. (1998). Matrilin-3 forms disulfide-linked oligomers with matrilin-1 in bovine epiphyseal cartilage. J Biol Chem 273, 17433-17438.

Belluoccio, D., Schenker, T., Baici, A., and Trueb, B. (1998). Characterization of human matrilin-3 (MATN3). Genomics 53, 391-394.

Wagener, R., Kobbe, B., and Paulsson, M. (1997). Primary structure of matrilin-3, a new member of a family of extracellular matrix proteins related to cartilage matrix protein (matrilin-1) and von Willebrand factor. FEBS Lett 413, 129-134

Chen, Q., Johnson, D. M., Haudenschild, D. R., Tondravi, M. M. and Goetinck, P. F. (1995) Cartilage matrix protein forms a type II collagen-independent filamentous network:Analysis in primary cell cultures with retrovirus expression system. Mol. Biol. Cell 6, 1743-1753.

Paulsson, M. and Heinegard, D. (1982) Radioimmunoassay of the 148-kilodalton cartilage protein. Distribution of the protein among bovine tissues. Biochem. J. 207, 207-213.

TLS / CHOP Inhibits RNA Splicing Mediated by YB-1

TIMOTHY RAPP, M.D., LIU YANG, PH.D., ERNEST U. CONRAD III, M.D., AND HOWARD A. CHANSKY, M.D.

Liposarcomas are the second most common diagnosed malignant soft tissue sarcoma. The clinical management of liposarcomas is primarily surgical. High grade liposarcomas occasionally lead to metastatic disease and death as there is no proven effective systemic treatment. A better understanding of the basic biology of these sarcomas is essential if better treatments are to be developed.

The molecular mechanisms that permit normal fat cells to undergo malignant differentiation are unknown. Chromosomal translocations are a common feature of malignancy. Translocations often result in the formation of novel fusion genes, and thereby fusion proteins, that in some manner alter the normal function of the host cell. Several sarcomas are thought to arise as a direct result of a translocation resulting in expression of a fusion protein. Human myxoid liposarcomas consistently have a characteristic chromosomal translocation, t(12;16)(q13;p11) (Figure 1). This translocation creates a fusion gene consisting of a DNA sequence encoding a portion of the gene TLS (translocated in liposarcoma) and the gene CHOP, a member of the C/EBP family of regulatory transcription factors. Our current study addresses the mechanism by which this fusion gene (protein), TLS/CHOP, contributes to malignant transformation of normal lipocytes.

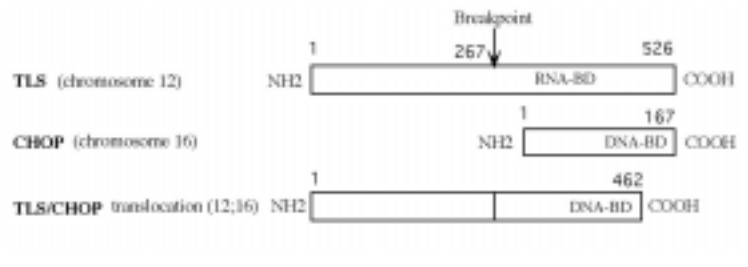

Figure 1: Human myxoid liposarcomas have a characteristic chromosomal transloccation, t(12;16) that results in fusion of the amino terminal domain of TLS to CHOP. The fused CHOP gene includes some DNA from the 5' untranslated region. TLS/CHOP is shorter than TLS but runs more slowly on a gel due to changes in conformation and charge. DNA-BD = DNA binding domain; RNA-BD = RNA binding domain.

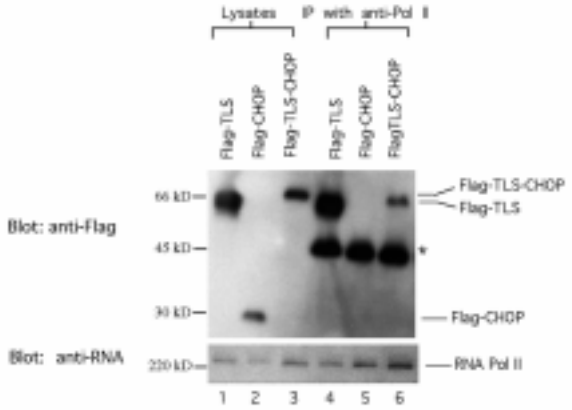

Figure 2: COS-7 cells transfected with either Flag-tagged TLS, TLS/CHOP, or CHOP (lanes 1-3) were used for immunoprecipitation with the anti-RNA Pol II followed by blotting with either anti-Flag or anti-RNA Pol II. RNA Pol II binds to TLS (lane 4) and to TLS/CHOP (lane 6) but not to CHOP (lane 5). The asterisk indicates the position of the anti-RNA Pol II antibody.

The N-terminal domain of the native TLS protein has been shown to associate with RNA polymerase II (Pol II); the C-terminal domain of TLS interacts with several members of a family of proteins (splicing factors) that mediate RNA splicing. Thus TLS is believed to function as a molecule that spatially and temporally links the processes of transcription and splicing. In myxoid liposarcoma the fusion partner of TLS, in this case CHOP, replaces the C-terminal domain of normal TLS. YB-1 is an evolutionarily conserved protein involved in transcription and translation. Earlier work in our laboratory suggested that YB-1 also interacted with the C-terminal domain of TLS in a manner similar to splicing factors. Our hypothesis was that the fusion protein TLS/CHOP, missing the normal intact C-terminal domain of TLS, would not bind YB-1 thus resulting in aberrant splicing of messenger RNA (mRNA).

RESULTS

Immunoprecipitation and Western analysis of lysates from transfected COS-7 cells were used to determine whether the TLS/CHOP fusion protein can bind to RNA Pol II and to the putative RNA splicing factor YB-1. The cells were transfected with a series of plasmids containing gene inserts encoding either TLS, TLS-CHOP, or CHOP. Our results show that native TLS and the fusion protein TLS/CHOP both associate with RNA Pol II (Figure 2). Further, our assays showed that binding of TLS to YB-1 is dependent upon the C-terminal domain of TLS. Native TLS was shown to co-immunoprecipitate with the splicing factor YB-1. YB-1 and TLS/CHOP did not co-immunoprecipitate, consistent with our hypothesis that the fusion protein TLS/CHOP is unable to bind to YB-1 due to substitution of the C-terminal domain of TLS by CHOP (Figure 3).

Although our immunoprecipitation assays show that TLS/CHOP interacts with RNA Pol II and not with YB-1, we further needed to analyze whether this observation has any effect on RNA

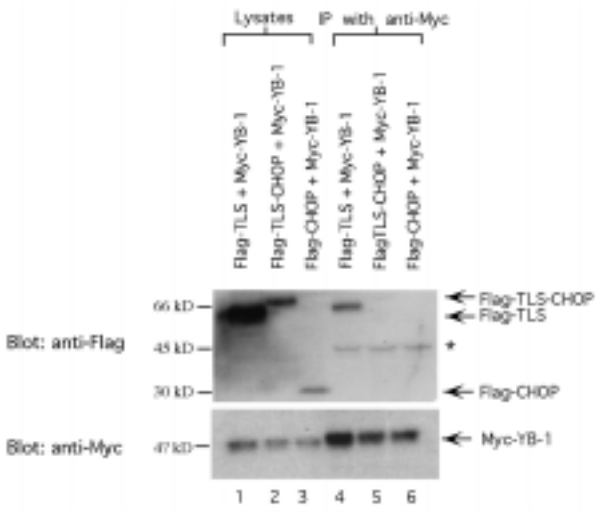

Figure 3: COS-7 cell lysates expressing Myc-tagged YB-1 and either Flag-tagged TLS, TLS/CHOP, or CHOP (lanes 1-3) were immunoprecipitated with anti-Myc. Blotting was then performed with either anti-Myc or anti-Flag. YB-1binds to TLS (lane 4) but does not bind to either TLS/CHOP or CHOP (lanes 5 and 6). The bottom gel is a control to ensure that the proteins were expressed at comparable levels. The asterisk indicates position of the anti-myc antibody used in the immunoprecipitation.

splicing. To evaluate the effect that TLS/CHOP has on YB-1-mediated RNA splicing, we performed reverse-transcriptase polymerase chain reaction (RT-PCR) and RNase protection assay. Alternative splicing of the adenovirus E1A pre-mRNA normally resulted in the generation of three different splicing isoforms. YB-1 expression increased the 13S isoform in our assay. While co-expression of TLS or CHOP did not alter YB-1-mediated splicing pattern of E1A mRNA, TLS/CHOP expression inhibited this splicing effect of YB-1 (results not shown).

Discussion

The chimeric fusion protein TLS/CHOP is a hallmark of the most common subtype of liposarcoma. However, little is known about the effects this translocation has on the biology and pathogenesis of liposarcomas. Our studies focused on important molecular mechanisms that may be altered by the creation of this novel fusion protein.

RNA Pol II is the crucial enzyme responsible for the transcription and processing of mRNA from the DNA template. The results of our immunoprecipitation studies indicate that wild-type protein TLS, and the fusion protein TLS/CHOP that is present in myxoid liposarcoma cells, retain the ability to bind RNA Pol II. However, TLS/CHOP loses its affinity for YB-1, a transcriptional modifier and splicing factor. We presume that the interaction of native TLS with RNA Pol II and YB-1 is crucial for the normal functioning of the RNA Pol II enzyme. Though TLS/CHOP preserves its interaction with RNA Pol II, it is possible that the replacement of the C-terminus of wild-type TLS with CHOP interferes with normal RNA processing and splicing.

RT-PCR and the RNase protection assay (RPA) are very sensitive techniques that permit identification and quantification of very small amounts of RNA. Our RT-PCR and RPA experiments further support the hypothesis that RNA processing is affected by the fusion gene TLS/CHOP. Our results show that splicing of E1A RNA is inhibited in cells transfected with TLS/CHOP when compared to cells transfected with native TLS.

These results advance our understanding of sarcoma biology in several ways. The fusion gene TLS/CHOP cannot bind to the splicing factor YB-1 and in our in vivo assays, this has marked effects on splicing of mRNA. Aberrant splicing and altered protein expression are general features of tumors and this may be one of the mechanisms by which they occur. We have published similar findings for a fusion gene found in Ewing's sarcoma tissue (EWS/Fli-1); our experiments suggest that disruption of RNA splicing may be an important generalized feature of sarcomas with fusion proteins.

Recommended Reading

Yang L, Embree LJ, Tsai S, Hickstein DD: Oncoprotein TLS interacts with serine-arginine proteins involved in RNA splicing. J Biol Chem. 1998 Oct 23;273(43):27761-4.

Hisaoka M, Tsuji S, Morimitsu Y, Hashimoto H, Shimajiri S, Komiya S, Ushijima M.: Detection of TLS/FUS-CHOP fusion transcripts in myxoid and round cell liposarcomas by nested reverse transcription-polymerase chain reaction using archival paraffin-embedded tissues. Diagn Mol Pathol. 1998 Apr;7(2):96-101.

Ron D.: TLS-CHOP and the role of RNA-binding proteins in oncogenic transformation. Curr Top Microbiol Immunol. 1997 220:131-42. Review.

Crozat A, Aman P, Mandahl N, Ron D.: Fusion of CHOP to a novel RNA-binding protein in human myxoid liposarcoma. Nature. 1993 Jun 17;363(6430):640-4.

Depth of Countersinking Modulates Cartilage Remodeling in Sheep Osteochondral Autografts

FRED HUANG, M.D., PETER T. SIMONIAN, M.D., ANTHONY NORMAN, B.S.E., AND JOHN CLARK, M.D., PH.D.

Animal studies suggest that step-offs created by displacement of osteochondral fragments can remodel. However, the mechanism by which remodeling occurs is unknown, and large incongruities seldom, if ever, heal completely. This issue complicates the surgical technique of osteochondral autografting — so-called "mosaicplasty" — because cylindrical plugs do not lend themselves to exact articular reconstruction of traumatic defects. Mosaicplasty, which is a relatively new procedure, is gaining widespread popularity for the treatment of focal chondral and osteochondral defects. It entails harvesting one or multiple plugs from either the periphery of the distal femoral articular surface or the intercondylar notch. Surprisingly, the basic science literature on osteochondral autografts is quite limited. Many questions remain regarding the viability and remodeling potential of the articular cartilage present on these cylindrical autografts. In this study, we asked whether thin articular cartilage on grafts harvested from the joint periphery could enlarge to reduce and/or eliminate incongruities created when a graft was countersunk.

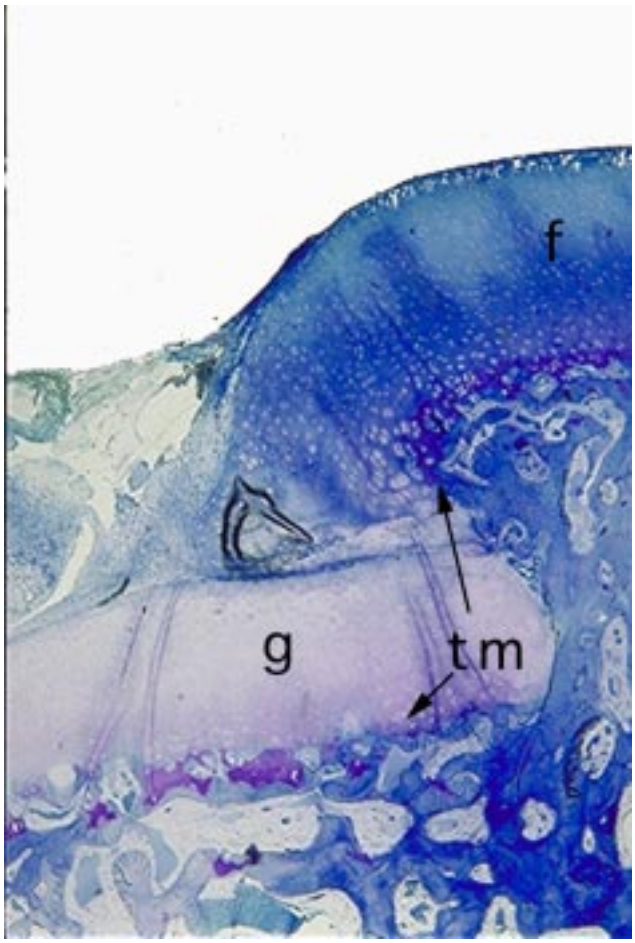

Figure 1: Specimen countersunk approximately two millimeters shows differential matrix staining of the grafted cartilage (g) in comparison to the recipient site cartilage (f). The tidemarks (tm) are linear and have not duplicated or advanced. The grafted cartilage has not enlarged. Magnification 25X.

METHODS

Following guidelines of our IACUC and under adequate anesthesia, medial parapatellar arthrotomy and partial fat pad resection were performed to allow for collection of fresh osteochondral plugs 5mm in diameter from the medial trochlear facet of skeletally mature male sheep. A trephine drill bit was utilized to harvest the autografts, which were immediately transplanted into matching drill holes in the ipsilateral medial femoral condyles. In three animals the periphery of the autograft surface was placed flush with the surrounding cartilage (Group I). In three others countersinking exceeded 1.5 mm (Group II), and in three sheep the surface was countersunk approximately 1mm (Group III). Initial congruity/incongruity of the surface was assessed with a silicone cast (Aquasil, Dentsply, Milford, DE) made intraoperatively. As markers of bone formation, the sheep received an injection of oxy-tetracycline perioperatively, and calcein or oxy-tetracycline at two and four weeks post-operatively. Immediate ad lib activity was permitted.

RESULTS

On the basis of high-resolution microscopy and fluorescent markers, all grafts had rapidly revascularized at six weeks. Viable osteocytes were present throughout the grafted bone. Blood vessels and foci of new bone formation were present in all areas, including the subchondral region. The appearance of the cartilage and subchondral plate depended on the level at which the graft was placed.

Group I: Grafts fitted flush with the surrounding cartilage surface showed little change in the structure of the articular cartilage. The grafted cartilage underwent limited enlargement to assume a slight convexity that matched the contour of the surrounding medial femoral condyle. With the numbers available, this enlargement was not statistically significant ($p=0.78$). Proteoglycan staining of the articular cartilage in this group matched both the

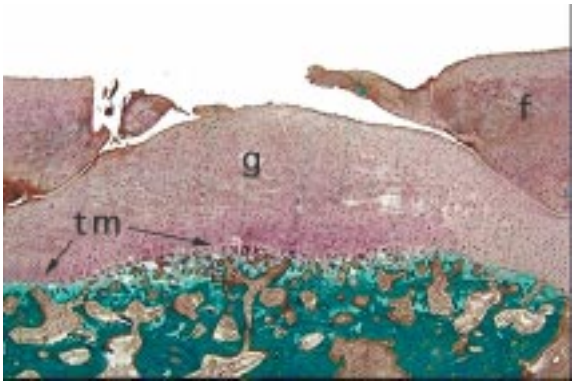

Figure 2: Graft countersunk one millimeter demonstrates significant cartilage growth centrally (g). Recipient site cartilage (f) has deformed to create an overlapping rim at the periphery of the graft. The tidemark of the graft has advanced centrally but not peripherally (tm). Magnification 25X.

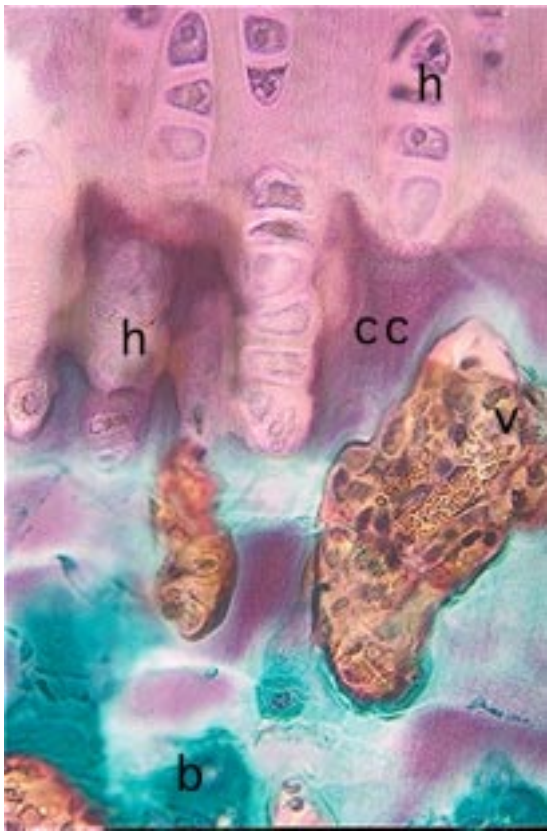

Figure 3: Higher power view shows a wide layer of calcified cartilage (cc) with adjacent chondrones (h) and neo-vascularity (v). Mature bone is present in the deeper layers (b). Magnification 400X.

surrounding cartilage and control cartilage samples. In comparison to intact samples from the donor site, the tidemark was slightly irregular, but there was no evidence of tidemark dissolution or duplication. No layer of the grafted cartilage exhibited chondrocyte hyperplasia or cloning.

Group II: Cartilage on plugs countersunk 1.5 mm or more appeared to be dormant despite vascularity in the adjacent subchondral region. In one case complete chondrolysis occurred. In the remaining two specimens in this group, the cartilage did not swell, chondrocyte nuclei were often pyknotic, and proteoglycan staining was less intense compared to the other groups. The architecture of the tidemark remained unchanged from the pre-transplant configuration. Vessels invaded the graft, but followed no consistent pattern and were not associated with chondrocyte hyperplasia. The grafted cartilage surface was irregular and overgrown with fibrous tissue.

Group III: Through hypertrophy and hyperplasia, the central cartilage on grafts that had been countersunk approximately 1 mm grew to match the pre-existing surface level. The average cartilage thickness (versus controls) increased by 55% ($p=0.046$). Multiple tidemarks were visible, and the zone of calcified cartilage was wide and indistinct. The cellularity of the deepest layers increased, and many of the hyperplastic chondrocytes were organized in individual cell strings (chondrones). Vertically-oriented capillaries penetrated into the basal layer of the cartilage, following the plane of the chondrones in a pattern reminiscent of endochondral ossification in a physis. New bone was present along the path of these capillaries.

Discussion

This is the first description of a remodeling process in malreduced osteochondral fragments. Cartilage on grafts sunk below a critical level becomes quiescent, whereas cartilage placed in a minimally countersunk environment remodels impressively. This remodeling occurs via a process that closely resembles endochondral ossification, in that it involves chondrocyte hyperplasia and hypertrophy, invasion of capillaries from the subchondral bone, and new bone formation. It is not clear why the cartilage on deeply countersunk grafts becomes atrophic, but its failure to remodel suggests that some minimum amount of loading is necessary to maintain metabolic activity of articular cartilage in cylindrical autografts.

Clinical Relevance: Osteochondral autografting is an attractive restorative procedure for the treatment of focal chondral and osteochondral defects. One of the difficulties that surgeons face when performing this procedure is the imperfect match between the surface contours of grafts and the areas

to be grafted. It is unclear if grafts should be placed slightly proud, flush, or slightly countersunk to yield optimal clinical results. Based on the results of this pilot study, we recommend that grafts be inserted either flush or slightly countersunk, but not countersunk more than the thickness of the surrounding cartilage. Deeply countersunk grafts should be avoided for fear of cartilage atrophy due to insufficient mechanical loading. When countersunk minimally, grafted articular cartilage exhibits significant remodeling and growth via a process that mimics the endochondral ossification associated with a physis. Such cartilage growth increases the thickness of the grafted cartilage and minimizes surface incongruities that are created by plug countersinking and/or the inherent mismatch between grafts and the sites to be grafted. These findings are relevant to other conditions that produce acute articular incongruities, namely intra-articular fractures.

Recommended Reading

Kish, G.; Modis, L.; and Hangody, L.: Osteochondral mosaicplasty for the treatment of focal chondral and osteochondral lesions of the knee and talus in the athlete. Rationale, indications, techniques, and results. Clin. Sports Med., 18(1): 45-66, 1999.

Lefkoe, T.; Walsh, W.; Anastasatos, J.; Ehrlich, M.; and Barrach, H.: Remodeling of articular step-offs. Is osteoarthrosis dependent on defect size? Clin. Orthop. 314: 253-265, 1995.

Llinas, A.; McKellop, H.; Marshall, G.; Sharpe, F.; Kirchen, M.; and Sarmiento, A.: Healing and remodeling of articular incongruities in a rabbit fracture model. J. Bone Joint Surg Am. 75(10): 1508-1523, 1993.

Distal Femoral Tunnel Placement for Multiple Ligament Reconstruction: Three Dimensional Computer Modeling and Cadaveric Correlation

WILLIAM J. MILLS, M.D. AND RANDY P. CHING, PH.D.

Reconstruction of the multiligament knee injury or knee dislocation frequently requires a combination of ligament repair, augmentation and reconstruction. Our experience with reconstruction and augmentation of combined medial collateral ligament (MCL), lateral collateral ligament (LCL) and anterior cruciate ligament (ACL) injuries suggests the space available for graft fixation in the distal femur is limited by the multi-planar irregular surfaces of the distal femur and the requirement for multiple screws or tunnels. Posterior cruciate ligament reconstruction is often performed as well in this setting, yet due to the medial femoral condyle location of the usual PCL tunnel(s) this graft does not create a logistical problem.

The optimal placement of the ACL femoral tunnel is well defined. Subsequent screws or tunnels for LCL and MCL grafts or augmentations must avoid the ACL tunnel. If one limits drill passage or tunnel depth to the width of the condyle, then avoidance of the ACL graft or tunnel is not an issue. However for greater screw purchase or tunnel length and interference fixation, we frequently drill beyond the midline of the distal femur, thus threatening encroachment on the ACL graft. We are currently using more tunnel fixation than washered screw and post fixation for many of our collateral repairs and reconstructions as many patients have complaints regarding the prominence of the washered screws at the level of the epicondyles. It is clear from clinical and anatomic studies that drill paths perpendicular to the distal femur from either epicondyle (collateral origins) will enter 1) the femoral notch and pierce the ACL graft or 2) the femoral tunnel and potentially compromise ACL fixation. This investigation was designed to define safe screw and tunnel placement in the distal femur for multiligament reconstruction.

METHODS

A three dimensional model of the distal femur was created using transverse computed tomographic (CT) images from a 28 year old female. Digital 1 mm image slices (DICOM format) were transferred from the CT workstation (HighSpeed Advantage CT, General Electric Medical Systems, Milwaukee, WI) to a personal desktop computer (PowerMacintosh, Apple Computer Company, Cupertino, CA) for model generation. Segmentation of the 2-D model geometry was performed using digital image processing and analysis software (NIH Image, US National Institutes of Health, Bethesda, MD) with the aid of custom macros. The segmented files were imported into a 3-D computer aided design (CAD) environment (Formoz, Autodessys Inc.), Columbus, OH) where the model was meshed and investigated. A standard 10 mm ACL femoral tunnel was incorporated into the 3-D model, preserving a typical 1 mm posterior wall. A 7 mm diameter lateral epicondyle tunnel (that most commonly used by us clinically) was incorporated into the model, as was a 10 mm diameter medial epicondyle tunnel. Optimal tunnel placement was investigated by digitally inserting potential MCL and LCL tunnels around an existing ACL tunnel with the goal of defining tunnel locations and trajectories that did not overlap one another or penetrate the articular surfaces of the distal femur. The limiting landmarks for tunnel placement was the anatomic origin of the collateral ligaments at the femoral epicondyles. Based on this computer model, safe tunnels trajectories were defined.

To assess the accuracy of the 3-D CT modeling ACL, MCL and LCL tunnels were then created in 3 different cadaver knees rigidly mounted allowing knee manipulation. Standard arthroscopic instruments were used to create a 10 mm diameter femoral ACL tunnel 30 mm deep retaining one mm of femoral notch back wall. Forty (40) mm length lateral (7mm diameter) and medial (10 mm diameter) epicondylar tunnels

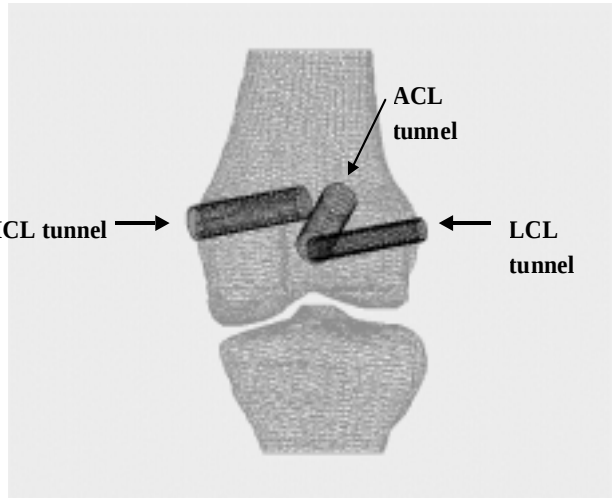

Figure 1: CT model demonstrating "safe" ACL, MCL, and LCL trajectories in the coronal plane.

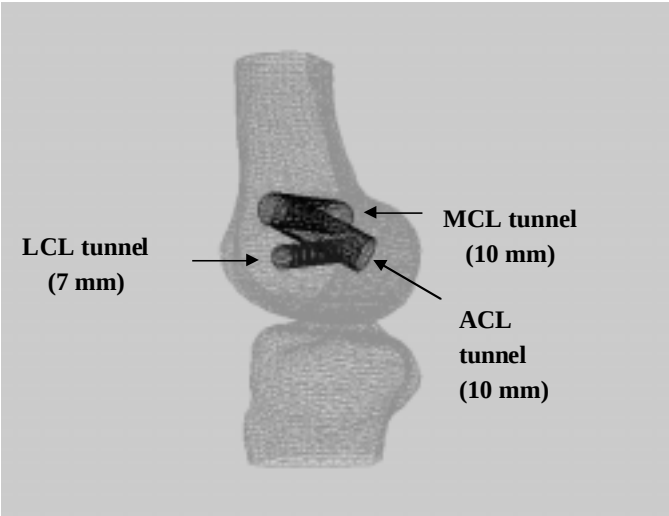

Figure 2: CT model demonstrating "safe" ACL, MCL, and LCL trajectories in the sagittal plane.

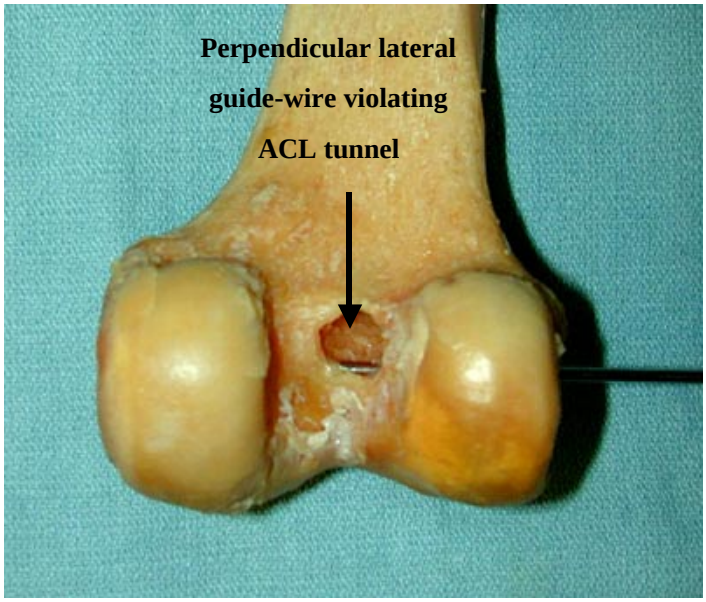

Figure 3: Guide-wire or drill for LCL graft fixation perpendicular to the long axis of the femur.

were created over guide wires placed at angles defined by the CT model. After drilling the initial tunnels, all tunnel diameters were sequentially expanded 1 mm until tunnel overlap occurred.

Results

The 3-D computer generated model defined "safe" LCL or lateral epicondylar tunnels as those angled 30° anteriorly and 10° distally (Figures 1 and 2). Flatter trajectories, or those not angled distally entered either the femoral notch or the ACL graft. This was readily confirmed by the cadaver dissection (Figure 3). Greater anterior or distal angulation encroached on the femoral trochlea. MCL or medial epicondylar tunnels were "safe" if angled 20° anteriorly with 10° proximal angulation (Figures 1 and 2). Greater proximal angulation of the MCL tunnel caused cut-out of the cortex proximal to the medial epicondyle especially as larger diameter tunnels were created. 10 mm tunnels based on this model avoided violating articular surfaces in all cadaver specimens. Increasing the ACL tunnel diameter to 12 mm produced no encroachment on either the LCL or MCL tunnel. Increasing the diameter of the MCL tunnel to 11 mm created MCL/LCL tunnel overlap in the midline of the femur in one cadaver, while a 12 mm MCL tunnel and 11 mm LCL tunnel created overlap in the midline in the remaining two cadavers (Figure 4).

Discussion and Conclusions

The 3-D CAD model accurately predicted safe tunnel placements in the distal femur when applied to cadaver specimens. There is greater freedom for ACL than MCL or LCL tunnel diameter. Fairly straightforward trajectory corrections (LCL: 30° anterior, 10° distal; MCL: 20° anterior, 10° proximal) from both epicondyles should allow safe drill paths and tunnel creation in the distal femur. Cross sectioning of the cadaver specimens suggests that collateral tunnels greater than 10 mm diameter, in order to avoid the ACL graft and the articular surface, will eventually converge when crossing the midline. We have incorporated this information in clinical practice, and have had no apparent instances of tunnel encroachment, femoral notch or articular surface violation in our patient population. The 3-D CAD model may prove useful in other areas where non-linear anatomy and limited space for fixation provide surgical challenges.

Recommended Reading

Fineberg MS, Zarins B, Sherman OH. Practical considerations in anterior cruciate ligament replacement surgery. Arthroscopy 2000 16(7): 715-24.

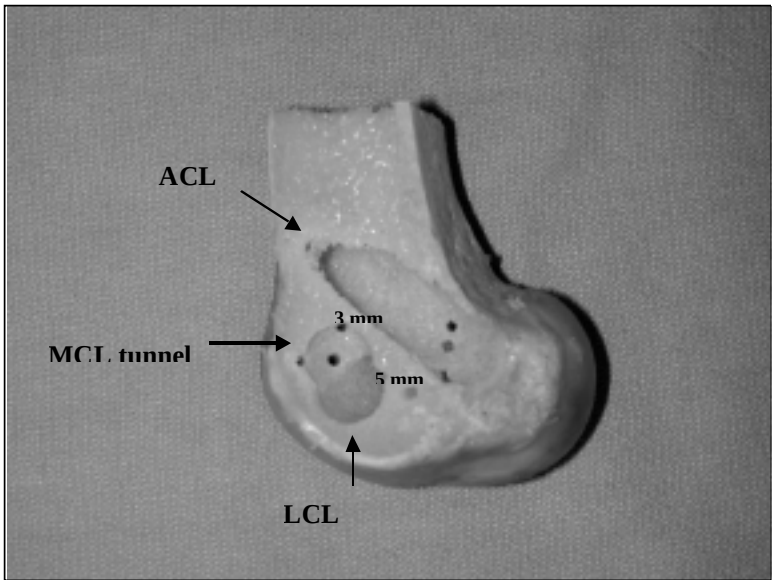

Figure 4: Cadaveric sagittal cross-section.

Sommer C, Friedrich NF, Muller W. Improperly placed anterior cruciate ligament grafts: correlation between radiological parameters and clinical results. Knee Surg Sports Traumatol Arthrosc 2000 8(4): 207-13.

Veltri DM and Warren RF. Operative treatment of posterolateral instability of the knee. Clin Sports Med 1994 13(3): 599-614.

Intramedullary Nailing of Distal Metaphyseal Tibial Fractures

SEAN E. NORK, M.D., ALEXANDRA K. SCHMITT, M.D., JULIE AGEL, M.A., SARAH K. HOLT, M.P.H., JASON L. SCHRICK, B.S., AND ROBERT A. WINQUIST, M.D.

The optimal treatment of distal tibial metaphyseal fractures remains controversial. While intramedullary nailing has gained acceptance as a method of stabilization of diaphyseal tibia fractures, its use has not become widely accepted for distal metaphyseal fractures. Fixation with an intrameduallary device spares the extaosseous blood supply, allows for load-sharing, avoids extensive soft tissue dissection, and is a technique familiar to most surgeons. Recent advances in the design of intramedullary nails have extended the spectrum of fractures amenable to this fixation. The purpose of this study was to evaluate reamed intramedullary nailing of distal tibial metaphyseal fractures located within five centimeters of the ankle joint.

MATERIALS AND METHODS

During a sixteen months period, 243 skeletally mature patients with tibia fractures were treated with intramedullary nailing at two institutions. Thirty-six patients with involvement of the distal five centimeters of the tibia and were treated with reamed intramedullary nailing and formed the study group. There were 24 male and 12 female patients, ranging in age from 18 to 82 years (mean 30 years). These tibial fractures were classified according to AO/OTA guidelines as 43A1 (n=8), 43A2 (n=5), 43A3 (n=13), 43C1 (n=6), 43C2 (n=2), and 43C3 (n=2). Fourteen fractures (39%) were open. An associated fracture of the fibula was present in 35 of 36 patients. Four patients had a concomitant leg compartmental syndrome and were treated with four compartment fasciotomies.

The ten 43C fractures (28%) with articular extensions were treated with supplementary percutaneous fixations prior to intramedullary nailings (Figure 1). Fibular fractures felt to have an effect on ankle joint or distal tibiofibular syndesmosis stability were treated with open reduction and internal fixation prior to intramedullary nailing. The tibial fractures were treated with reamed intramedullary nailing systems that optimize distal fixation, allowing placement three biplanar distal interlocking screws through the distal three centimeters of the nail. The primary reduction aid for obtaining length, alignment and rotation of the distal tibial segment was fibular plating in 19 patients (54%). Additional reduction techniques included use of a femoral distractor, temporary percutaneous clamp fixation, percutaneous manipulation with Schantz pins, and open reduction and temporary unicortical tibial plating. The surgical goals of obtaining and maintaining anatomical alignment during nailing was further accomplished with central placement of the guide wire and all reamers, and maintenance of the reduction at the time of nail passage.

In order to evaluate the functional outcome and health status of this group of patients, we administered the Short-Form 36 (SF-36), a generic health status measure and the Musculoskeletal Function Assessment (MFA), a functional outcome measure.

Category	Study Population		Normative Values		p-value
	Avg	SD	Avg	SD	
Physical Function	65.0	31.6	83.5	23.5	**0.007**
Role Limitations Physical	61.8	41.8	83.1	32.3	**0.02**
Bodily Pain	66.2	28.3	77.4	24.5	**0.03**
General Health	70.4	29.6	71.4	20.3	0.87
Vitality	57.9	34.8	62.7	21.9	0.45
Social Functioning	81.3	18.8	87.0	21.7	0.37
Role Limitations Emotional	90.9	30.2	86.2	30.3	0.59
Mental Health	74.4	18.4	76.5	18.8	0.99

Table 1: Comparison of Study Population and SF-36 Normative Values.

RESULTS

The average distance from the distal extent of the tibial fracture to the plafond was 35 millimeters (range 0 to 45 mm). The average distance between the distal nail tip and the articular surface of the plafond was 6.2 mm (range 2 - 10 mm). The average sagittal plane deformity was 0.9 degrees (range 0 - 5 degrees). The average coronal plane deformity was 0.3 degrees (range 0 - 5 degrees). Acceptable alignment was obtained in 33 patients (92%) and no patient had a malalignment of greater than five degrees. Two patients had a five degree recurvatum deformity and one patient had a five degree valgus deformity.

Of the thirty-six patients in our study, radiographic follow-up to union was obtained in thirty patients. Five patients were lost to follow-up and one patient died on postoperative day number three from pulmonary complications. Three patients with open fractures with associated bone loss required staged iliac crest autograft at an average of 6.7 weeks (range, 6 - 8 weeks) postoperatively. Four patients underwent dynamization of their nail

(1a)

(1b)

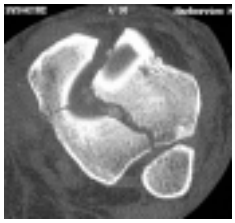

(1c)

(1d)

(1e)

Figure 1: This 58 year old female with a history of diabetes sustained this distal tibial fracture with extension into the ankle joint. She was treated with limited open reduction of the articular surface and intramedullary nailing of the tibia.

Category	Study Population			Normative Values		p-value
	Avg	SD	Range	Avg	SD	
Mobility	37.9	27.1	0-70	11.9	12.7	**< 0.001**
Housework	34.3	28.2	0-77.8	7.8	15.4	**< 0.001**
Self-Care	14.8	20.8	0-66.7	1.7	4.4	**< 0.001**
Sleep & Rest	13.9	23.4	0-66.7	15.5	21.8	0.81
Leisure &Recreation	58.3	28.9	25-100	10.0	21.9	**< 0.001**
Family Relationships	6.7	17.2	0-60	7.9	16.6	0.81
Cognition & Thinking	10.4	29.1	0-100	6.1	17.3	0.44
Emotional Adjustments	31.0	18.6	5.6-61.1	15.6	12.8	**< 0.001**
Employment	16.7	34.3	0-100	5.3	16.7	**0.047**

Table 2: Comparison of Study Population and MFA* Normative Values.

at three months postoperatively to encourage healing.

In these thirty patients, there was no change in final alignment when compared to the immediate postoperative radiographs. Fracture union occurred in all thirty patients at an average of 23.5 weeks (range, 13 - 57 weeks) from the date of intramedullary nailing. In the three patients with associated bone loss requiring a staged autograft procedure, the average time to healing was significantly longer at 44.3 weeks (range, 33 - 57 weeks) ($p = .034$).

Outcomes Evaluation

The average scores in the eight categories of the SF-36 were: PF, 65.0; RP, 61.8; BP, 66.2; GH, 70.4; VT, 57.9; SF, 81.3; RE, 90.9; MH, 76.4. These values were compared to published normative values for the general population (Table 1). A significant difference was found in three of the eight categories which included physical functioning, role limitations physical, and bodily pain.

The distribution of values in each of the ten categories of the MFA is tabulated in Table 2 with the normative values from uninjured patients. The average MFA for our group of patients was 23.8 (standard deviation, 14.67) (range, 2 - 44). The total function MFA score for patients with isolated knee, leg and ankle injuries after a year of follow-up is 22.9 (range 2 - 59). For comparison, the total function MFA score for uninjured patients is 9.3 (range, 0 - 59).

Discussion

Intramedullary nailing of open and closed tibial shaft fractures has been associated with high rates of radiographic and clinical success. Fractures distal to the tibial diaphysis within five centimeters of the ankle joint may represent a different injury and have therefore been excluded from reports on tibial shaft fractures. Potential difficulties associated with fractures in this location include wound problems associated with limited soft tissue coverage, the associated amplification of the bending moment of the short distal segment of the tibia above the ankle joint, and the voluminous anatomy of the tibial methaphysis in the plafond. Because of the large diameter of the distal tibia relative to the intramedullary nail the interface between the cortex of the tibia and the nail cannot be used to assist in fracture reduction in this location.

In our series of patients, the articular extension was addressed prior to intramedullary nailing of the tibia. This was performed to prevent additional displacement and to assist in reduction of the distal fragment. Loss of reduction of the articular segment was not seen with nail insertions. Strategic placement of periarticular lag screws may help prevent this potential complication. Articular fractures

patients had loss of alignment or length. All intraarticular fractures healed without displacement. The need for bone graft was seen only in those fractures with severe bony comminution in conjunction with soft tissue defects.

Recommended Reading

Konrath, G. Moed, B. R. Watson, J. T. Kaneshiro, S. Karges, D. E., and Cramer, K. E.: Intramedullary nailing of unstable diaphyseal fractures of the tibia with distal intraarticular involvement. J Orthop Trauma, 11: 200-205, 1997.

Krettek, C. Stephan, C. Schandelmaier, P. Richter, M. Pape, H. C., and Miclau, T.: The use of Poller screws as blocking screws in stabilising tibial fractures treated with small diameter intramedullary nails. J Bone Joint Surg [Br], 81: 963-968, 1999.

Mosheiff, R. Safran, O. Segal, D., and Liebergall, M.: The unreamed tibial nail in the treatment of distal metaphyseal fractures. Injury, 30: 83-90, 1999.

Puno, R. M. Vaughan, J. J. Stetten, M. L., and Johnson, J. R.: Long-term effects of tibial angular malunion on the knee and ankle joints. J Orthop Trauma, 5: 247-254, 1991.

Robinson, C. M. McLauchlan, G. J. McLean, I. P., and Court-Brown, C. M.: Distal metaphyseal fractures of the tibia with minimal involvement of the ankle. Classification and treatment by locked intramedullary nailing. J Bone Joint Surg [Br], 77: 781-787, 1995.

Ting, A. J. Tarr, R. R. Sarmiento, A. Wagner, K., and Resnick, C.: The role of subtalar motion and ankle contact pressure changes from angular deformities of the tibia. Foot Ankle, 7: 290-299, 1987.

Study performed at Harborview Medical Center, Seattle, Washington, USA

The Association Between Supracondylar Intercondylar Distal Femoral Fractures and Hoffa Fractures

SEAN E. NORK, M.D., KAMRAN AFLATOON, D.O., DANIEL N. SEGINA, M.D.,
STEPHEN K. BENIRSCHKE, M.D., M.L. CHIP ROUTT, JR., M.D, AND M. BRADFORD HENLEY, M.D., M.B.A.

The isolated coronal fracture of the femoral condyle was originally described by Hoffa in 1904. This fracture involves the lateral femoral condyle more commonly, but fractures of the medial condyle have been described as well. Nonoperative treatment has been associated with displacement and poor functional results. Operative treatment of these fractures has therefore been recommended. These fractures represent a diagnostic dilemma, are frequently missed, and are associated with further displacement if unrecognized. Computed tomography has been recommended as an adjunct in the diagnosis of condylar involvement in intraarticular distal femoral fractures.

For combined supracondylar and intercondylar femoral fractures, operative treatment is recommended to provide stable restoration of the articular surface and facilitate early range of motion. The association between intercondylar distal femoral fractures and coronal split fractures has received little mention despite numerous publications on distal femoral fractures. The purposes of this study are to identify the association between supracondylar intercondylar distal femoral fractures and coronal split fractures, and to describe the radiographic evaluation of these injuries.

Figure 1: Injury radiographs and CT scans of a patient with a supracondylar intercondylar distal femoral fracture with an associated Hoffa fracture. The coronal fracture line is visible on the lateral radiograph. The axial and sagittal reformations further define the injury.

MATERIALS AND METHODS

Over a 60 months period from May, 1994 to April, 1999, all patients sustaining an intraarticular fracture of the distal femur were collected from a prospectively designed orthopaedic database and reviewed retrospectively. One hundred twelve patients with 117 intraarticular distal femoral fractures were identified and included in the initial review. Patients with unicondylar (OTA type 33B) injuries (n = 26) were excluded. The remaining 86 patients with 91 supracondylar intercondylar distal femoral fractures survived their initial resuscitation and were treated operatively at Harborview Medical Center, a level one trauma center in Seattle, Washington.

All Supracondylar Intercondylar Fractures

There were 60 male and 26 female patients ranging in age from 15 to 88 years (average 44.7 years). These 91 fractures were classified according to AO and OTA guidelines and included 33C1 (n = 8), 33C2 (n = 29), and 33C3 (n = 54) injuries. Five patients had bilateral intraarticular distal femoral fractures. All injuries with a sagittal intercondylar split associated with a coronal fragment of either condyle were classified as 33C3. Forty-eight fractures were open (53%) and included 13 Type II, 32 Type IIIA, 1 Type IIIB, and 2 Type IIIC injuries.

Fractures with Associated Coronal Split Fragments (Hoffa Fractures)

Thirty-seven distal femoral fractures in thirty-six patients had an associated Hoffa fracture. There were twenty-seven male and nine female patients ranging in age from fifteen to eighty-eight years (average 38.0 years). Twenty-eight of thirty-seven distal femoral fractures with an associated Hoffa fracture (76%) were open and classified as Type II (n = 7), Type IIIA (n = 18), Type IIIB (n = 1), and Type IIIC (n = 2).

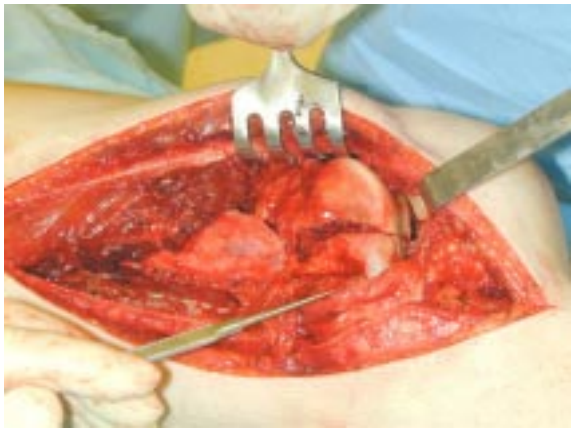

Figure 2: Intraoperative clinical image of the coronal fracture line of the lateral femoral condyle.

Results

Hoffa fractures were diagnosed in thirty-seven of ninety-one (41%) supracondylar intercondylar distal femoral fractures. One patient had bilateral intraarticular distal femoral fractures with medial and lateral coronal split fragments in each knee (four independent condylar fragments). Nine patients had bicondylar coronal split fractures (medial and lateral) in the same extremity. Twenty-seven patients had unicondylar coronal split fractures with 85% (n = 23) located laterally and 15% (n = 4) located medially. This combined for a total of forty-seven coronal split fragments in thirty-seven knees.

Overall, 53% of distal femoral fractures (AO/OTA type 33C1, 33C2, and 33C3 fractures) were open and 67% of AO/OTA Type 33C3 fractures were open. Open fractures occurred in 90% (nine of ten) of extremities with medial and lateral (bicondylar) Hoffa fragments. In fractures with at least one Hoffa fragment, 76% (28 of 37) were open compared to 37% (20 of 54) of intraarticular distal femoral fractures without a coronal split fragment ($p = .00022$).

The average Injury Severity Score (ISS) in these eighty-six patients was 18.2 (range, 9-50). The average ISS in patients with a Hoffa fracture was 20.6 (range, 9-50), compared to 16.1 (range, 9-50) in patients without a Hoffa fracture ($p = 0.028$). Similarly, in patients with bicondylar Hoffa fractures the ISS with significantly higher (24.3) than in the remaining patients (17.1) ($p = .019$).

A dedicated CT scan of the distal femur was obtained in twenty-seven of the ninety-one knees. In patients with a Hoffa fragment, preoperative CT scans were obtained in thirteen patients and identified seventeen of these Hoffa fractures. Of the forty-seven Hoffa fragments, biplanar distal femur plain radiographs were diagnostic in only thirty-four (72%). Eight additional Hoffa fractures were identified with the aid of the CT scan (Figure 1). In six patients, the diagnosis of a Hoffa fracture was discovered intraoperatively. In two of these patients, the coronal split fracture was appreciated during insertion of the angled blade plate seating chisel as the fracture displaced in presumed 33C2 type fractures (Figure 2). In both patients, the Hoffa fractures was then reduced and stabilized. The surgical implant was changed to a lateral condylar buttress plate.

Of the forty-seven coronal split fractures, twenty six were displaced while twenty-one were non-displaced. According to the classification system of Letteneur et al, there were eight Type I fractures and thirty-nine Type III fractures 13. Five Hoffa were segmental injuries with multiple condylar fragments.

Discussion

The presence of a Hoffa fragment in association with intraarticular distal femoral fractures has received little attention, despite numerous publications on distal femoral fractures. Temporary fixation of the Hoffa fragment followed by rigid fixation the of the distal femoral fracture with an angled blade plate has been recommended in the past. However, based upon the experience in our study population, fixation of the Hoffa fragment prior to stabilization of the supracondylar and intercondylar fracture fragments is recommended (Figure 3).

The complexity of the fractures in this series reflects the patient population at this primary and tertiary referral Level one trauma center. Of ninety-one supracondylar-intercondylar distal femoral fractures, only eight were true "T" intercondylar fractures without articular or metaphyseal-diaphyseal comminution (Type 33C1 fractures). Overall, only seventeen of fifty-four (31%) 33C3 distal femoral fractures did not have a coronal split fracture. The presence of a coronal split fracture in over 40% of all supracondylar-intercondylar distal femoral fractures is concerning, as implant choice may be altered based on this finding.

The lateral condyle is involved more frequently than the medial condyle in both unicondylar fractures, as well as isolated Hoffa fractures. In all thirteen cases of two combined series, the isolated Hoffa fracture was of the lateral condyle. In our series, 85% (23/27) of patients with unicondylar coronal split fractures had lateral condyle injuries. However, 36% (14/47) of coronal split fractures were of the medial condyle in all patients with at least one Hoffa fragment.

The largest series of isolated coronal unicondylar fractures (OTA type 33B3) was reported by Letenneur et al and consists of twenty cases. Surgical treatment of displaced fractures was recommended and produced better results than nonoperative care. The fate of untreated or unrecognized coronal split fragments has been described in two series. Lewis et al reported on subsequent malreduction in two patients with unrecognized, initially nondisplaced coronal split fractures. Similarly, Butler et al reported on two patients with unrecognized Hoffa fragments which ultimately required a second surgical procedure for reduction and fixation. In our series, all recognized Hoffa fragments were

(3a) (3b)

Figure 3: Postoperative radiographs after fixation of the Hoffa fracture and the distal femoral supracondylar intercondylar fractures.

stabilized at the time of distal femoral fixation.

Recognition of these injuries, especially nondisplaced fractures, is often difficult with AP and lateral plain radiographs. The potential complication of a missed Hoffa fracture includes displacement intraoperatively or postoperativley. More importantly, the implant choice based on the preoperative plan can be appropriately adjusted in the presence of a Hoffa fragment. Orthogonal plain radiographs, even during retrospective review, demonstrated the fracture in only thirty-four of the forty-seven coronal split fragments, emphasizing that non-displaced Hoffa fractures may be overlooked easily. CT scans, which were obtained in only 27 of 91 cases, demonstrated the fragment in seven additional cases. Six fragments (13%) were identified at the time of surgical stabilization. None of these six patients had a preoperative CT scan. Given the incidence of coronal plane fractures in high energy distal femoral fractures, combined with the frequency of nondisplaced fragments, preoperative CT scans may be helpful in identifying these injuries. This is especially true in fractures where the planned approach does not include direct visualization of the articular surface.

In this series of predominately blunt trauma patients (96.5%), the majority of these injuries were open (53%). The incidence of associated open traumatic wounds in patients with distal femoral fractures ranged from 17 - 31%. However, in reports of comminuted distal femoral fractures, open wounds occur in 40 - 56% of patients. Our open fracture incidence of 67% of AO type 33C3 fractures and 53% of all AO Type 33C fractures is reflective of the high energy patient population reviewed. Consistent with the incidence of comminution in combined distal femur and coronal split fractures, the incidence of associated open wounds increased to 70% (19/27) in patients with unicondylar involvement and 90% (9/10) of patients with combined medial and lateral coronal split fractures. The presence of at least one Hoffa fragment with an intercondylar distal femoral fracture was associated with a higher rate of associated open wounds. Similarly, an open fracture was associated with an increased risk of a coronal split fragment.

Conclusions

The 41% incidence of Hoffa fractures in association with supracondylar-intercondylar distal femoral fractures is higher than expected. Involvement of both the medial and lateral condyles occurred in 27% of these injuries. In unicondylar injuries, the lateral condyle was affected much more frequently (85%) than the medial condyle. Open associated wounds occurred in 76% of these fractures. In our patients, an open injury was associated with an increased risk of a Hoffa fracture. The diagnosis is often difficult and CT scanning may be required in supracondylar fractures with intercondylar extension.

Recommended Reading

Bolhofner, B. R. Carmen, B., and Clifford, P.: The results of open reduction and Internal fixation of distal femur fractures using a biologic (indirect) reduction technique. J Orthop Trauma, 10: 372-377, 1996.

Johnson, E. E.: Combined direct and indirect reduction of comminuted four-part intraarticular T-type fractures of the distal femur. Clin Orthop, 231: 154-162, 1988.

Letenneur, J. Labour, P. E. Rogez, J. M. Lignon, J., and Bainvel, J. V.: [Hoffa's fractures. Report of 20 cases (author's transl)]. Ann Chir, 32: 213-219, 1978.

Lewis, S. L. Pozo, J. L., and Muirhead-Allwood, W. F.: Coronal fractures of the lateral femoral condyle. J Bone Joint Surg [Br], 71: 118-120, 1989.

Ostermann, P. A. Neumann, K. Ekkernkamp, A., and Muhr, G.: Long term results of unicondylar fractures of the femur. J Orthop Trauma, 8: 142-146, 1994.

Sanders, R. Swiontkowski, M. Rosen, H., and Helfet, D.: Double-plating of comminuted, unstable fractures of the distal part of the femur. J Bone Joint Surg [Am], 73: 341-346, 1991.

Triangular Osteosynthesis and Iliosacral Screw Fixation For Unstable Sacral Fractures: A Biomechanical Evaluation Under Cyclic Loads

T.A. Schildhauer, William .R. Ledoux, Ph.D., Jens R. Chapman, M.D., M.B. Henley, M.D., Allan F. Tencer, Ph.D., and M.L.Chip Routt, M.D.

Operative fixation techniques for unstable sacrum fractures include open or percutaneous iliosacral screw osteosynthesis, tension band transiliac plate osteosynthesis, transiliac bars and local plate osteosynthesis. Each allows early postoperative patient mobilization with only partial weight-bearing. However, patient non-compliance, accidental full weight-bearing, poor bone quality and delayed union for various reasons result in loss of reduction in up to 26% of patients.

Some sacral fracture fixation techniques were evaluated with biomechanical testing, and proved to be similar in immediate stability. Nevertheless, these biomechanical tests involved only load to failure under constraint conditions or stability testing with only a few loading cycles simulating the immediate postoperative time period. The majority of these tests were performed in a double-leg stance model, which fails to account for the larger loads across the fracture during single limb stance. Cyclic loading simulating pelvic fixation loading during the postoperative period of bony healing under full weight-bearing conditions has not been performed.

Triangular osteosynthesis for unstable sacrum fractures has been recently described. This fixation technique combines lumbopelvic distraction osteosynthesis with a transverse fixation (iliosacral screw osteosynthesis or tension band transiliac plate osteosynthesis) providing clinically sufficient multiplanar stability. This posterior pelvic stability uniquely allows early postoperative full weight-bearing.

The purpose of our study was (1) to create a biomechanical set-up allowing for cyclic loading of pelvic specimens in a single-leg stance model, and (2) to compare the stabilities of triangular lumbopelvic and iliosacral screw osteosyntheses for unstable transforaminal sacral fractures, both at initial loading and through 10,000 cycles.

Materials and Methods

Twelve embalmed human cadaveric pelvic specimens including the lumbar spine were obtained. Soft tissues were removed, retaining all ligamentous structures. The specimens were randomly assigned to two test groups. An unstable transforaminal sacral fracture was created by osteotomizing the sacrum at the foramina, and also at the ipsilateral superior and inferior pubic ramus. Specimens in group I were stabilized posteriorly with a 7 mm cannulated cancellous fully threaded iliosacral screw, and anteriorly with a 4.5 mm medullary superior ramus screw. Specimens in group II were stabilized as in group I, but underwent additional triangular lumbopelvic fixation. For that, an USS spinal fixation system was applied between the L5 pedicle (7 mm x 50 mm screw) and the ipsilateral posterior ilium. A posterior iliac screw (8 mm x 120 mm screw) was inserted into the PSIS and directed towards the AIIS. Plain pelvic anteroposterior radiographs were obtained after placement of the implants to document proper fixation.

The specimens were mounted in a custom frame designed to simulate single limb stance. The ipsilateral acetabulum was attached to a proximal femoral hemiarthroplasty. The shaft of the prosthesis was rigidly secured to a base plate, allowing adjustments in the horizontal plane. Hip flexor, abductor and extensor muscles were simulated with adjustable cables attached to the ipsilateral iliac crest. The vertebral body of L3 was potted in an aluminum container. An axial force was applied to the container centered on the posterior longitudinal ligament. The axial force was applied with a pneumatic air controller and cylinder. The cylinder actuator had a ball-tip only allowing forces to be applied in the axial direction. A load cell in series with the ball-tip and actuator measured the applied force. A constant force of 100 N (approximately 16% body weight (BW) in a 50 kg person) was applied to the contralateral acetabulum to account for the contralateral leg weight. Motions across the fracture site were measured using the Polhemus FastTrak electromagnetic motion sensor system. Two motion sensors were attached to the posterior sacrum at the level of S2 on each side of the fracture. All motions were related to the cranial ridge of the ipsilateral anterior S1 foramen, the point of interest.

With the unloaded specimen positioned in the frame, the initial position of the point of interest was recorded. For initial stability testing, the specimens were loaded cyclically from 175 N (35% BW) to 375 N (75% BW) and the total displacement at the point

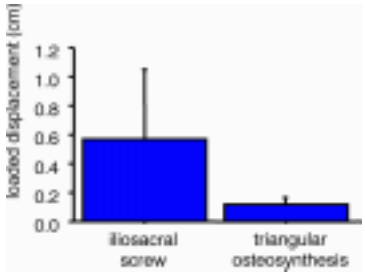

Table 1: The loaded displacement for the iliosacral screw (0.565 cm, S.D. 0.488) and triangular osteosynthesis (0.121 cm, S.D. 0.055).

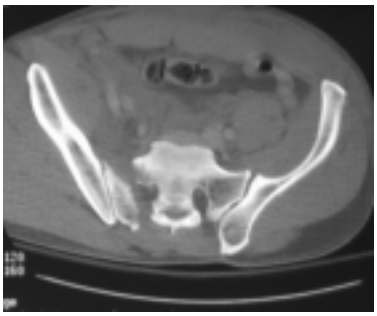

Figure 1: Unstable sacral fracture.

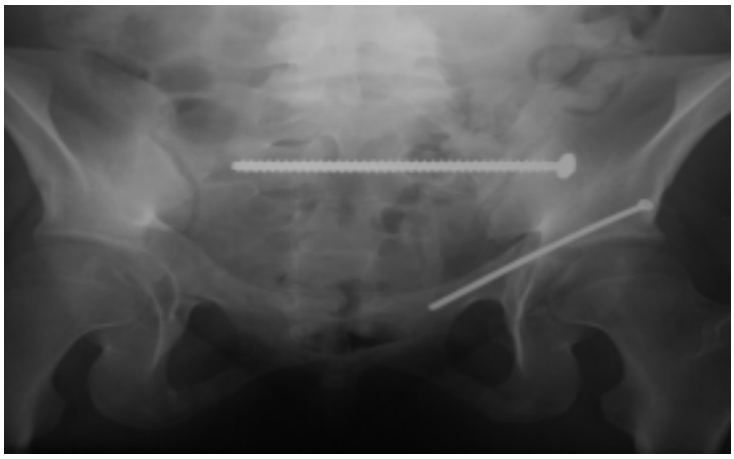

Figure 2a: Iliosacral screws: AP view.

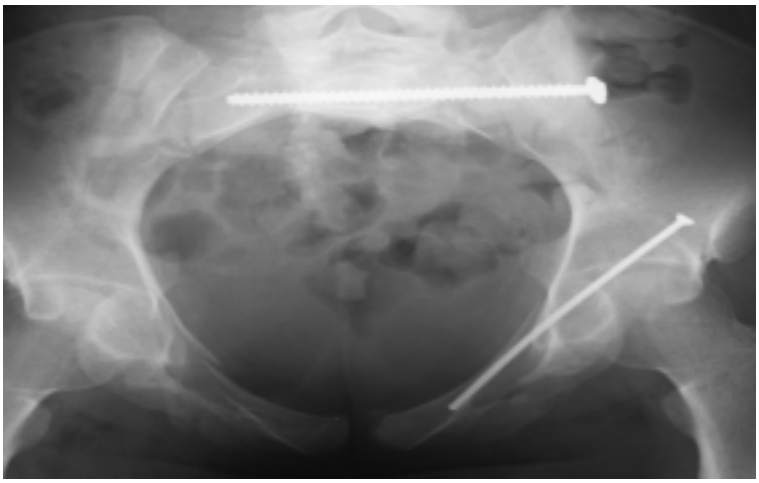

Figure 2b: Iliosacral screws: Pelvic outlet view.

of interest on the fracture site was measured. Pilot research demonstrated that there was little change in motion at the fracture site over this range, therefore the average displacement during one cycle was obtained. The specimens were loaded for 10,000 cycles, with data collected every 1000 cycles. If the fracture displaced more than 1 cm prior to 10,000 cycles, the specimen and fixation were considered to have failed. Macroscopic fracture behavior was noted. For several of the specimens, the cyclic loading caused the pelves to rotate within the testing frame, moving the Polhemus sensors out of the calibrated field. As such, only initial loading displacement and macroscopic fracture behavior at 10,000 cycles or at failure, are reported. The effect of fixation and age was studied with an unpaired t-test.

Results

Randomization of the specimens in the two groups resulted in 3 male and 3 female specimens in group I (iliosacral screw fixation), as well as in 4 male and 2 female specimens in group II (triangular osteosynthesis). The average age was 73 (S.D. 7.4, range 64 - 82) years and 73.7 (S.D. 9.7, range 56 - 84) years, respectively.

For initial loading, simulating the immediate postoperative situation, specimens in group II had a statistically significantly smaller displacement at the point of interest ($p = 0.05$) and therefore greater stability than specimens in group I. The triangular osteosynthesis construct provided a higher degree of stability, independent of age or sex. Two specimens in group I failed catastrophically under initial loading, resulting in large variability in this group. If these specimens were not included, there is still a significant difference in displacement ($p=0.0275$) between the two groups with higher stability for specimens in group II.

Macroscopic fracture behavior was classified as type 1 - minimal motion at the sacral and pubic ramus fractures, type 2 - considerable sacral fracture motion and complete displacement of the inferior pubic ramus, and type 3 - immediate, catastrophic failure. All specimens with the triangular osteosynthesis (group II) demonstrated type 1 fracture behavior. The iliosacral screw fixation performance (group I) was not as repeatable, with one type 1, three type 2 and two type 3. Specimen failure was in flexion of the injured hemipelvis with cephalad translation and internal rotation.

Discussion

In this evaluation, the triangular osteosynthesis construct provided a significantly higher degree of stability than iliosacral screw fixation, in both initial load bearing and macroscopic fracture behavior after 10,000 cycles. These data support early clinical results of triangular osteosynthesis for unstable sacrum fractures. These results also indicate that such patients could be allowed earlier full weight bearing and that the fixation technique may prevent secondary displacement.

Biomechanical testing of posterior pelvic operative fixation techniques is often criticized for not appropriately simulating the clinical situation, e.g. often only the immediate postoperative condition is examined. In the clinical situation, the hardware-bone constructs of various fixation techniques that performed similarly at initial loading, might react differently after the fracture has been repetitively loaded. For this reason, we tested specimens up to 10,000 cycles. However, cyclic loading still does not perfectly simulate the postoperative clinical situation, as fracture healing would result in increased stability,

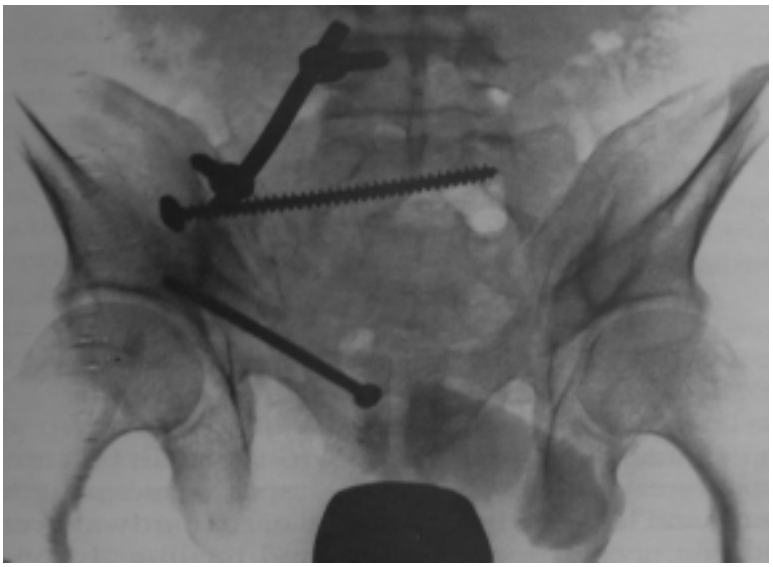

Figure 3a: Osteosynthesis: AP view.

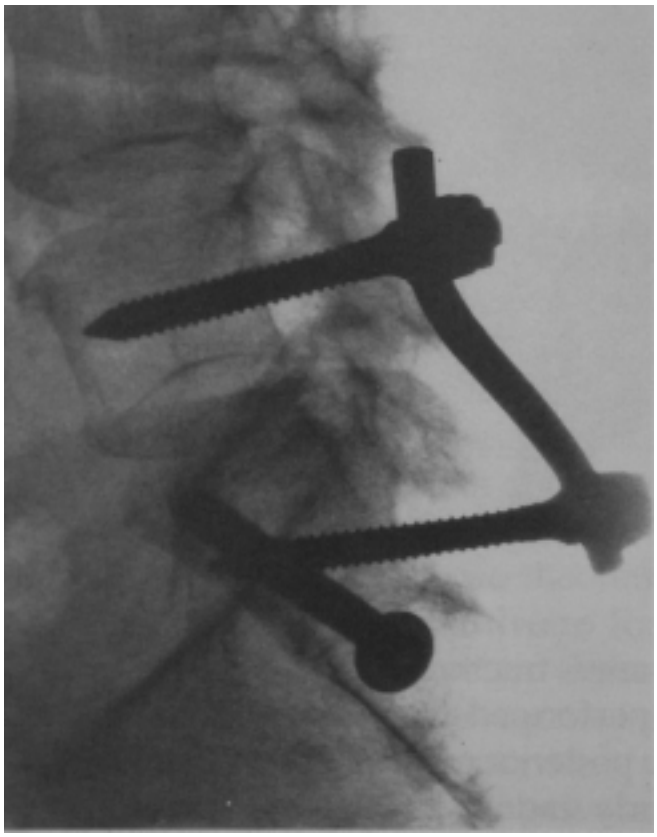

Figure 3b: Osteosynthesis: Lateral view.

altering the loads on the hardware fixation.

Triangular osteosynthesis combines multiplanar fixations, and provides additional protection against cranial migration of the injured hemipelvis by transferring lower lumbar spine loads directly to the iliac wing. The sacral fracture is then unloaded and the iliosacral screw more effectively stabilizes the fracture locally. Based on this, the triangular osteosynthesis construct is the optimal biplanar operative fixation technique for unstable sacral fractures.

Conclusion

Triangular osteosynthesis provided a significantly higher stability to the posterior pelvic ring for an unstable transforaminal sacral fracture when compared to iliosacral screw fixation alone. Pelvic fixation technique evaluations performed under cyclical loading in a single-leg stance model simulate clinical postoperative situations and demonstrate failure modes of certain fixation techniques.

Recommended Reading

Josten et al.; Chirurg 1994; 97:28. 4. Schildhauer et al.; J Orthop Trauma 1998; 12:307.

Keating et al.; J Orthop Trauma 1999; 13(2):107. 5. Simonian et al.; Clin Orthop 1996; 323:202.

Pohlemann et al.; J Orthop Trauma 1993; 7:107.

Effect of Cervical Lesions on Neural Space Integrity

SOHAIL K. MIRZA, M.D., D.J. NUCKLEY, M.A. KONODI, AND RANDY P. CHING, PH.D.

Instability is the basis for treatment of numerous acute and chronic spinal conditions such as trauma, malformations, vertebral infections, rheumatoid arthritis, primary tumors, metastases, and chronic degenerative diseases. Assessment of spinal instability, although rooted in the function-structure as well as neuro-protective capacities of the spine, does not currently include neuro-logically defensive management criteria (White, 1990). Since neurologic deficit typically dictates functional outcome, instability assessment should include a measure of the neural protective capability of the spine. Thus, we have defined and quantified this role of the spine in preventing compressive injury to the spinal cord and nerve roots as neural space integrity.

This study directly examines the relationship between structural loss in the spinal column and compression of spaces occupied by the neural elements. We created controlled lesions in the anterior cervical spine and measured the resulting changes in the space occupied by the nerve roots and spinal cord. We hypothesized that anterior cervical spine lesions result in increased stenosis of the spinal canal and intervertebral foramen indicating diminished neural space integrity with successively destructive lesions.

METHODS

Eight unembalmed human cervical spine specimens were used in a repeated measures study design to compare the effects of sequentially induced, simulated lesions on neural space integrity under physiologic loading conditions. Neural space monitoring was accomplished using unique neural-space occlusion transducers (Raynak, 1998) which, when inserted into the intervertebral foramen and spinal canal, measured their cross-sectional area. The mean age of the five females and three males was 75-years (range: 49—92-years).

Specimen Preparation

Each osteoligamentous specimen was potted inferiorly at C7 and superiorly at C3. Pins were inserted into the vertebral bodies of C6 and C4 for the attachment of 3-D motion tracking sensors (3 Space Fastrak System, Polhemus Inc., Colchester, VT). These sensors recorded the relative translational and angular orientation of vertebrae across the lesion site. After removal of the neural tissues, the intervertebral foramen occlusion transducers were inserted into the bilateral foramen of C3-4, C4-5, and C5-6, and a spinal canal occlusion transducer was inserted into the canal.

Experimental Procedure

The cervical spine was placed in a custom loading frame which loaded the specimen in bending by 1.0-Nm increments up to 4-Nm, applied in eight directions: flexion, extension, right and left lateral bending, and four off-axis bending motions. In addition to bending, axial torque was applied up to 3-Nm in 1.0-Nm increments. This full range of motion was executed for the intact case and after each sequential lesion. The lesions, created using a high-speed drill (Midas Rex, Fort Worth, TX), included the sequential

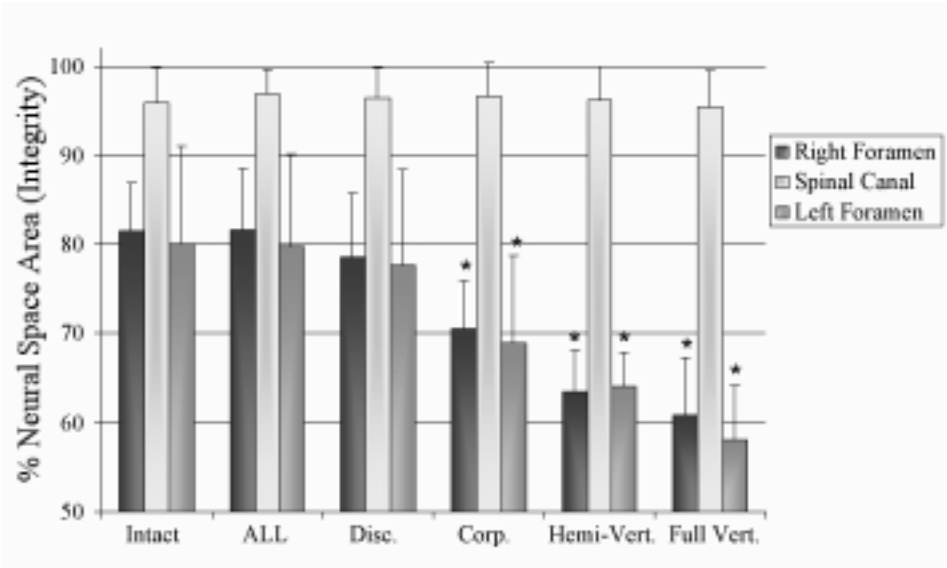

Figure 1: Effect of Extension with Anterior Lesions on the Integrity (cross-sectional area) of Spinal Neural Spaces. Percent changes in neural space cross-sectional area from neutral position are illustrated for 4-Nm of extension loading. While the spinal canal is little affected by anterior lesions, the intervertebral foramen (grouped by side) demonstrate significant changes (* denotes $p < 0.05$) compared with intact. (N=8).

transection of the following: ALL (across C4-5 disc), C4-5 disc (discectomy), C5 body (corpectomy), left anterior C5 body (hemi-vertebrectomy, and right anterior C5 body (full vertebrectomy). In addition to the eight study specimens, a control specimen was tested through six full loading cycles without lesions to determine the effects of repeated loading alone.

Data Analysis

An analysis of variance was used to evaluate differences in neural space integrity for successive lesions using blocks to evaluate the effects of motion, foraminal level and side and canal level (SPSS, SPSS Inc.). This enabled the examination of the effect of lesions on the individual neural spaces as well as the relative neural space integrity for a specific lesion.

Results

Range of Motion

Evaluation of the loading and subsequent range of motion of the intact cervical spine between the C4 and C6 vertebral bodies were not statically different from normal cervical ranges of motion reported in the literature. Classical examination of instability (using displacements) revealed that with sequential lesions, the range of motion across the lesion site (C4-6) increased in extension. In this study, extension motion across the defect increased from 12° (intact) to 21° with a discectomy lesion and up to 32° with a full anterior resection of one vertebra.

The control specimen demonstrated no statistically significant motions across C5 from the first to the sixth trial indicating that our experimental measures can be attributed to the lesions and are not a result of the repeated loading.

Spinal Canal Integrity

Changes in the spinal canal integrity were not statistically different for any lesion or motion, and in fact revealed the robustness of the spinal canal space during quasi-static loading of specimens with anterior spinal lesions.

Intervertebral Foramen Integrity

Statistically significant changes in intervertebral foramen integrity were measured for successive anterior lesions at various spinal positions. The results presented here are for the final (max.) loading case (4-Nm bending, 3-Nm rotation) for each lesion at each cervical position. Assessed against intact normal range-of-motion neural space integrity values, flexion, extension, ipsilateral bending, ipsilateral bending with flexion, and ipsilateral bending with extension resulted in significant increases in neural space stenosis ($p < 0.01$). Intervertebral foramen integrity was compromised to the greatest degree in extension (>72.7%), ipsilateral bending (>74.9%), and ipsilateral bending with extension (>70.5%) for each lesion following the corpectomy and were significant ($p < 0.0001$) compared with intact measurements. Maximum intervertebral foramen integrity deficit resulted from the vertebrectomy lesion in each position, and the greatest potential for neurologic injury with this lesion occurred with the spine loaded in extension with ipsilateral bending (58.9%).

Discussion

The current findings demonstrate significant and unique maps of neural space integrity. The effects of both anterior lesions and cervical position on the ability of the spine to protect its neural tissue were elucidated. Statistically significant intervertebral foramen integrity changes were found for various lesions and positions, while spinal canal integrity was maintained throughout these experiments. Assessment of neural space integrity that would be injurious to a patient's neural tissues remains a clinical judgment; however these data may help to enhance the accuracy and precision of this evaluation. Further delineation of the neural protective ability of the spinal column to lesions and trauma remains our focus as we attempt to define fully neural space integrity for enhanced clinical assessment of all spinal conditions.

Acknowledgement

This work was supported by grants from the Orthopaedic Research and Education Foundation and the Cervical Spine Research Society.

Recommended Reading

White III, AA, & Panjabi, M.M., Clinical Biomechanics of the Spine, JB Lippincott Co., 1990

Raynak GC, Nuckley DJ, Tencer AF, Ching RP, "Transducers for dynamic measurement of spine neural-space occlusions," Journal of Biomechanical Engineering 120(6): 787-791, 1998

Vertebroplasty with a Cavitation Drill

A.J. Mirza, M.A. Konodi, Jens R. Chapman, M.D., Carlo Bellabarba, M.D., Randy P. Ching, Ph.D., Allan F. Tencer, Ph.D., and Sohail K. Mirza, M.D.

Osteoporosis-related Vertebral Fractures. Osteoporotic fractures remain a common and difficult problem. In the United States, 10 million people have osteoporosis and 18 million are at risk of osteoporosis because of low bone mass. Despite current prevention measures and treatment strategies, approximately 1.5 million osteoporosis-related fractures occur every year in the United States, with vertebral fractures accounting for half this number. Up to 15% of women in the United States over the age of 50 will suffer from one or more vertebral fractures related to osteoporosis. Vertebral fractures are associated with substantial pain, deformity, disability, and poor quality of life in patients with osteoporosis.

Osteoporotic vertebral fractures rarely require hospitalization but often cause severe pain and functional limitation. Following acute vertebral compression fractures, up to 75% of patients continue to suffer from persistent back symptoms. Current medical and surgical treatments of vertebral body fractures offer few effective options. Conventional non-operative therapy usually entails a period of immobilization or bracing, placing patients at risk for further deterioration of bone strength and increasing the risk for additional fractures. Surgical treatment of pain and deformity in this population presents additional challenges. Operative intervention involves significant risks because of the high prevalence of co-existing medical conditions in the target population of elderly individuals. Stabilization procedures are technically difficult due to poor bone quality of the osteoporotic spine, making it difficult to achieve and retain adequate fixation of hardware. Surgical stabilization is rarely indicated and is reserved for patients with severe spinal deformity or impending neurologic impairment.

The limitations of medical and surgical treatments for vertebral compression fractures have spurred the search for other therapeutic options. A promising new technology is the reinforcement of fractured vertebrae with the percutaneous injection of bone cement: percutaneous vertebroplasty. Percutaneous vertebroplasty was developed in the late 1980´s by Galibert, Deramond, and their colleagues at the Centre Hospitalier Universitaire (Amiens, France) as a novel technique to reinforce vertebral fractures caused by osteolytic metastases and myeloma. They reported instantaneous pain relief in their patients following the injection of acrylic cement. Vertebroplasty was not performed in the United States until 1994. The procedure consists of injecting polymethylmethacrylate bone cement, usually under fluoroscopic or CT guidance, through a needle into a weakened vertebral body. The aim of the procedure is to obtain optimal vertebral filling without leakage of cement. Current indications include: metastatic lesions of the spine, multiple myeloma, symptomatic vertebral hemangiomas, and severe osteoporotic compression fractures. Indications among osteoporotic fracture patients are severe disabling pain secondary to an acute fracture or chronic pain refractory to medical therapy and bracing. Treatment of ambulatory patients and prophylactic injection of non-fractured vertebrae are more controversial indications for vertebroplasty.

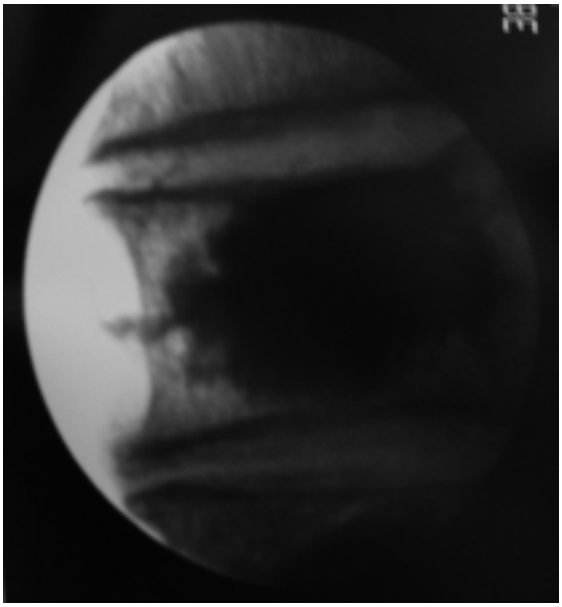

Figure 1: Leakage of cement through venous channels is a common complication in standard vertebroplasty.

Vertebroplasty

Percutaneous vertebroplasty (PV) consists of injecting acrylic cement (polymethylmethacrylate) into pathologic vertebral lesions to obtain fracture consolidation, embolization of vascular lesions, and pain relief. Lesional characteristics including location, the extent of vertebral body collapse, presence of cortical disruption, and degree of pedicle involvement should be radiographically assessed pre-operatively. Vertebroplasty is performed under general anesthesia or neuroleptanalgesia using needles of different lengths and diameters,

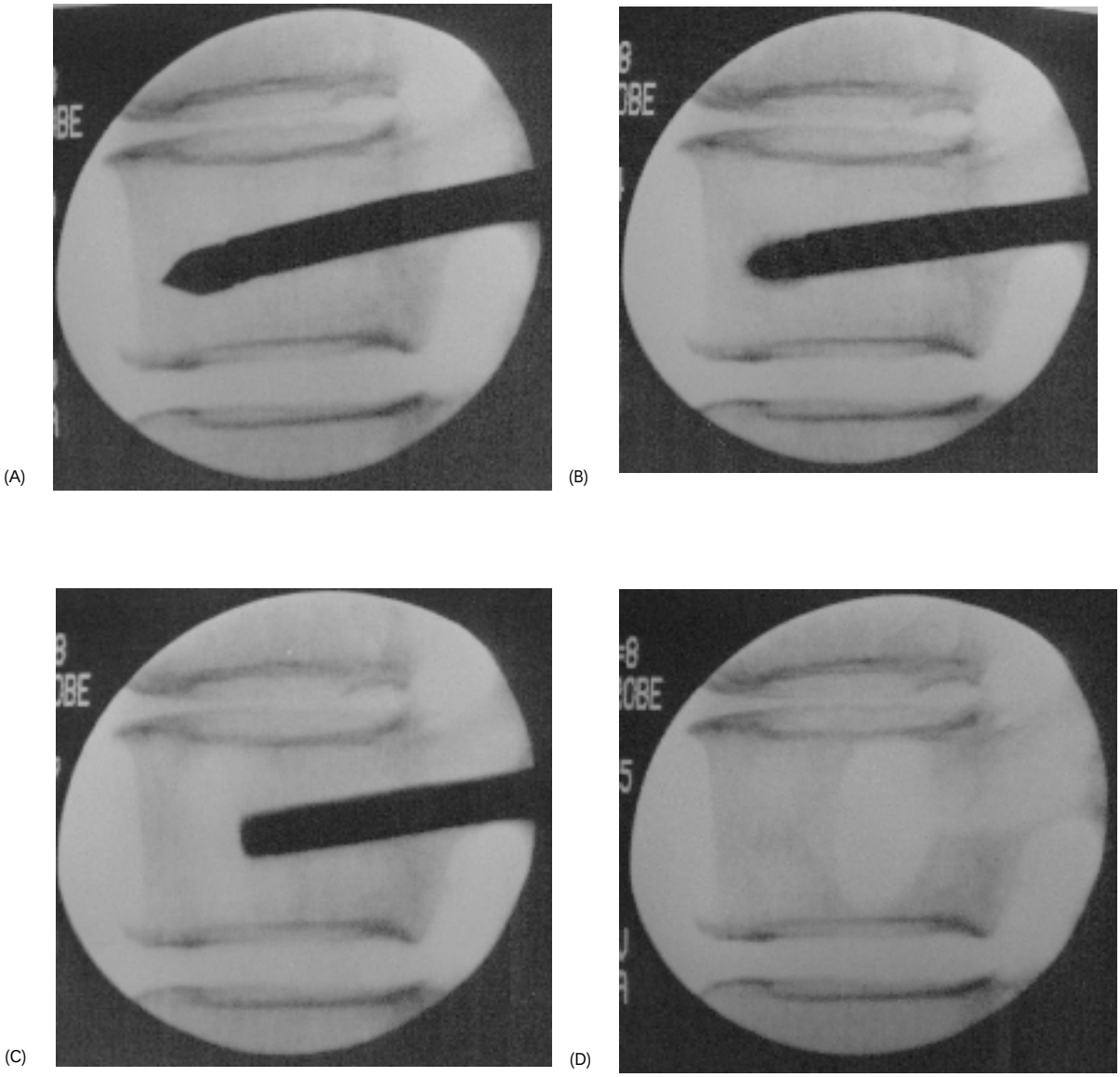

Figure 2: The cavitation drill allows the drill tip to bend to a postion perpendicular to the shaft with rotation, creating a cavity with a larger diameter than the cannulation needed to insert the drill.

depending upon the spinal level involved. Thoracic and lumbar vertebrae may be approached via a transpedicular or posterolateral route 15. The transpedicular approach avoids injury to the spinal segmental nerve and lowers the risk for paravertebral cement leakage. A posterolateral approach is most commonly used for lesions of the lumbar spine. This approach is difficult to use for thoracic lesions due to risk of pneumothorax. The posterolateral approach may result in paravertebral cement leaks during needle removal from the vertebral body. Contralateral access to the vertebral body is needed to obtain adequate filling. Cervical vertebrae are approached via an anterolateral route.

Once the needle is in optimal position, vertebral venography is recommended to identify venous drainage. After needle insertion, the acrylic cement is prepared for injection. Tantalum or barium powder is added to make solution radiopaque and improve visibility on radiographs. Some investigators have added tobramycin to their cement solution when treating immunocompromised patients. After preparation, the viscosity of the mixture gradually increases. One of the difficulties of vertebroplasty is injecting the cement when it reaches the appropriate consistency. Cement of thick consistency is difficult to inject. More free flowing cement is associated with greater risk of leakage. The injection

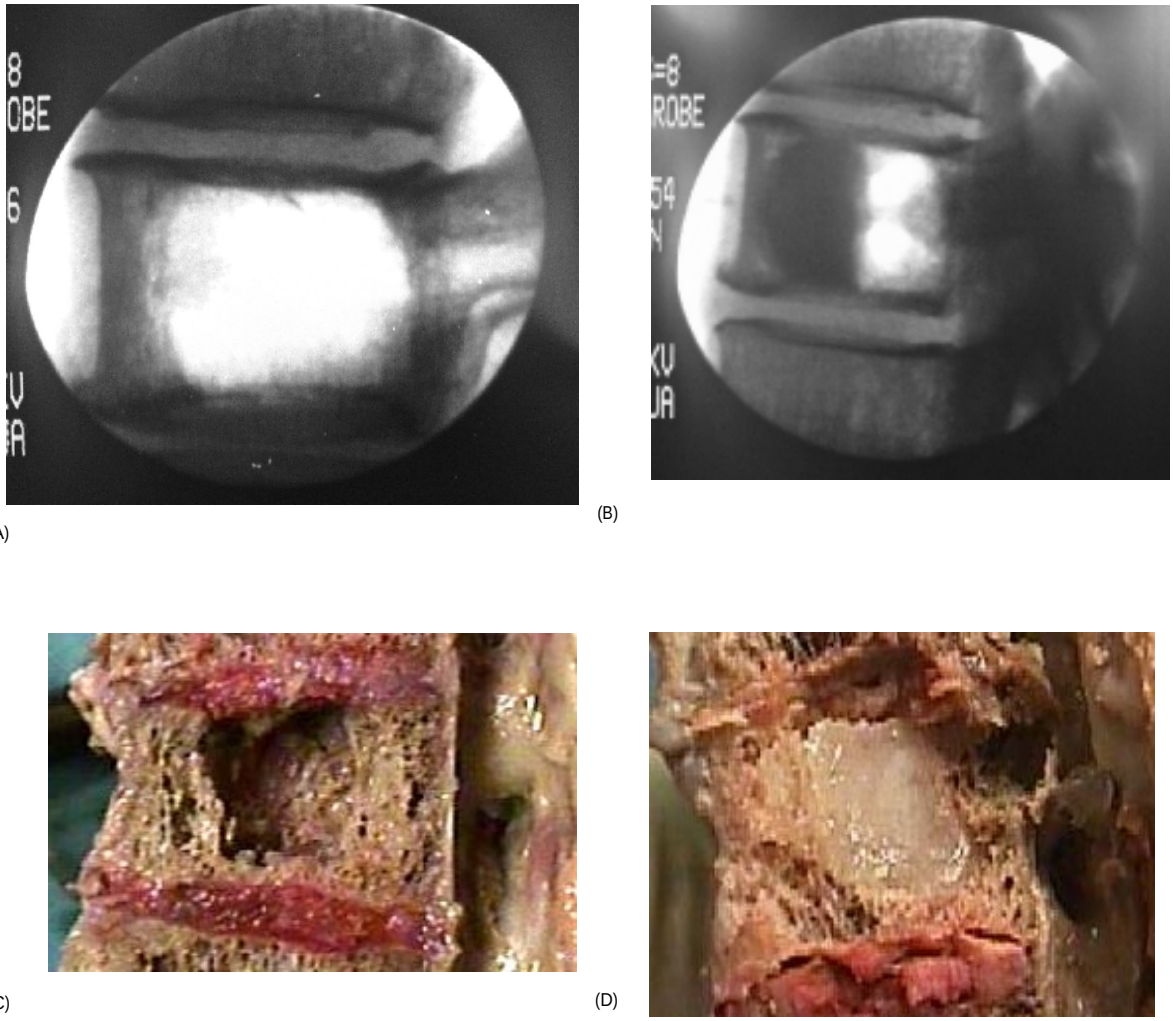

Figure 3: A large cavity allows the liquid acrylic to be delivered with drip-filling under low pressure, avoiding leaks related to cement pressurization.

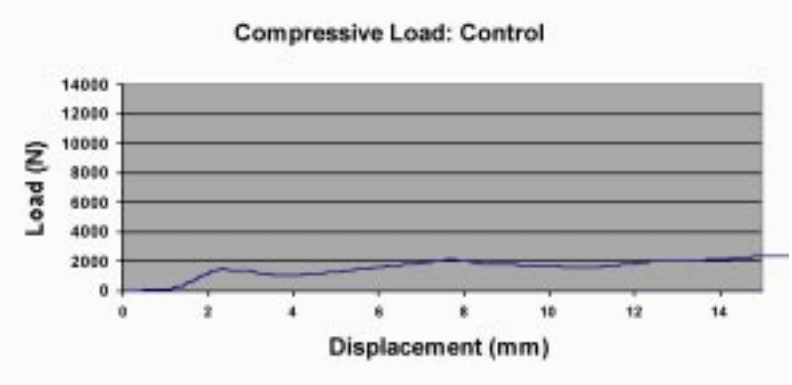

Figure 4: Typical load-displacement curve for a thoracic vertebra, showing fracture at approximately 1500 N.

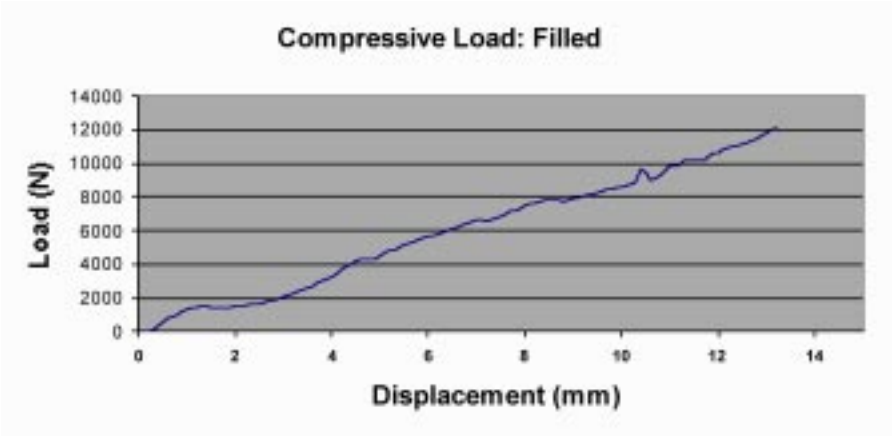

Figure 5: Load-displacement curve for a thoracic vertebra augmented with methymethacrylate, showing minimal collapse at loads exceeding physiologic thresholds.

volume can range from two to ten milliliters depending on the spinal level and the vertebral lesion. The duration of the procedure is usually between one to two hours depending on the number of vertebrae injected.

Cavitation

Cement leakage is a common occurrence with standard vertebroplasty. The viscosity and pressurization of acrylic cement necessary to permit flow during injection are often also sufficient to force cement extravasation into venous sinuses (Figure 1). In order to decrease cement extravasation, we have developed a technique to create a cavity within the vertebral body with a specialized cavitation drill. The drill has an articulated tip. The articulated tip can be angulated after insertion, permitting insertion through a small opening (Figure 2). Rotating the drill in the angulated position removes adjacent bone, creating a cylindrical cavity with a radius equal to the length of the articulated portion of the drill tip. The slurry of liquefied bone is evacuated with a suction apparatus, creating a large cavity within the vertebral body. The cavity is then filled with cement injection under low pressure, essentially "dripping" the cement into the space concurrently with suction applied through the contra-lateral pedicle opening (Figure 3). Restriction cement filling to the anterior dependent portions of the vertebral body also decreases the possibility of cement leakage into critical areas such as the spinal canal and neural foramina.

We have compared the strength of acrylic augmented vertebrae to control vertebrae with osteoporosis under compression loading. Acrylic cement augmentation prevents vertebral body compression fracture (Figure 4 and Figure 5). We are currently exploring the option of using biodegradable alternatives to acrylic cement in vertebroplasty using the cavitation drill. A biodegradable material in combination with a cavitation device may also permit percutaneous lumbar fusion in treating symptomatic degenerative disc disease. We additionally are investigating the feasibility of bone reinforcement in preventing fractures at other common sites, such as the proximal femur and distal radius.

Recommended Reading

NIH. Consensus development conference statement: Osteoporosis prevention, diagnosis, and therapy., March 27-29, 2000.

Galibert P, Deramond H, Rosat P, Le Gars D. [Preliminary note on the treatment of vertebral angioma by percutaneous acrylic vertebroplasty]. Neurochirurgie 1987; 33:166-8.

Tohmeh AG, Mathis JM, Fenton DC, Levine AM, Belkoff SM. Biomechanical efficacy of unipedicular versus bipedicular vertebroplasty for the management of osteoporotic compression fractures. Spine 1999; 24:1772-6.

Cotten A, Boutry N, Cortet B, et al. Percutaneous vertebroplasty: state of the art. Radiographics 1998; 18:311-20; discussion 320-3.

Jensen ME, Evans AJ, Mathis JM, Kallmes DF, Cloft HJ, Dion JE. Percutaneous polymethylmethacrylate vertebroplasty in the treatment of osteoporotic vertebral body compression fractures: technical aspects. AJNR Am J Neuroradiol 1997; 18:1897-904.

The Development and Validation of a Computational Foot and Ankle Model

WILLIAM R. LEDOUX, PH.D., DANIEL L. A. CAMACHO, M.D., PH.D., RANDY P. CHING, PH.D., AND BRUCE J. SANGEORZAN, M.D.

Cadaveric experiments have provided useful insights into foot biomechanics, but these protocols are frequently technically difficult, time-intensive and costly. A validated computational model of the foot can provide insights into potential outcomes before investing in cadaveric tissue. A model can complement cadaveric studies by determining quantities often inaccessible to measurement in cadaveric experiments, such as internal stresses and strains, and allow for parametric analyses to be conducted. The potential simulations with a carefully designed, rigorously validated, computational foot model include: deformities following ligamentous or neuromuscular injury, outcomes of surgical interventions, responses to impact loading, and the relative roles of various anatomic structures during normal and abnormal activities. The model may also be used as an efficient tool for the optimization of design parameters in the development of foot orthoses, performance footwear, surgical procedures or surgical hardware. A model may be a very effective teaching tool for the difficult three-dimensional motions and deformities of the foot. Finally, the model may be employed to explore complex theories of biomechanical foot function that otherwise would be difficult to study. We have developed a first generation finite element model of the human foot that is capable of simulating quiet stance.

METHODS

The geometry of the computational foot-ankle model was based upon the cadaveric foot of a 67-year-old male. No gross deformities or significant degenerative changes were evident on AP or lateral radiographs. Transverse CT images of the specimen were acquired at 1 mm intervals. The images were processed using several commercial and custom-written software packages. Each bone was reconstructed as a mesh of 4-noded quadrilateral surface shell elements, and the plantar soft tissues were reconstructed as a mesh of 8-noded hexahedral solid elements (Figure 1). The ligaments were modeled as 2-noded spring elements with endpoints tied to the bone surfaces. The plantar aponeurosis was modeled as a central spring originating from the medial tubercle on the plantar aspect of the os calcis, which then separates into three branches inserting on the plantar aspects of the 1st, 3rd, and 5th metatarsal heads. The locations of the insertions and origins of the ligaments and plantar aponeurosis were determined from cadaveric dissection and photographic anatomy atlases.

To limit the number of material property assumptions, the model was simplified by grouping certain bones together to form single rigid bodies: the tibia and fibula, the 1st through 4th metatarsals and phalanges, the 1st metatarsal and phalanges, and the navicular and three cuneiforms.

The massless springs representing the ligaments and plantar aponeurosis were assigned linear stiffnesses in tension, and no stiffness in compression. To shorten simulation times for these quasi-static analyses, linear dashpots were placed in parallel with the spring elements and assigned a linear viscous damping constant equal to 0.0005 times the linear tensile stiffness. Tensile stiffness values were taken from the literature. For ligaments without reported stiffness data, stiffnesses were computed from scaling relationships based on ligament length and/or cross sectional area as measured in the literature.

The plantar soft tissues were assigned a density of 1 g/cm3, and nearly incompressible with nonlinear stress-strain characteristics. A rubber-like material model (Ogden hyperelastic) was used for material property definition. Model constants were determined by fitting the subcalcaneal soft tissue stress-strain curve reported previously. A rigid floor plate was modeled by 144 four-noded shell elements.

The rotations of the talus, navicular, cuboid, and calcaneus, as measured during the cadaveric experiments, were used to generate performance corridors for model validation. Briefly, 11 cadaveric specimens were procured from the Department of Biological Structure of the University of Washington. The specimens were screened for gross and radiographic abnormalities. For each specimen, the soft tissue was stripped from around the tibial shaft, and an acrylic rod was placed into the intramedullary canal and cross-locked. Carbon fiber pins, 6 mm in diameter, were placed into holes drilled into the talus, navicular, cuboid, and calcaneus. Receivers for an electromagnetic motion transducer system (Fastrak 3-D, Polhemus Systems, Colchester, VT) were rigidly fastened to the ends of the carbon fiber pins. Each specimen was placed on a skid-resistant plate with the tibia and fibula oriented vertically. A 150N load was applied down the tibial shaft, and the three-dimensional motions of the talus, navicular, cuboid, and calcaneus were measured. A coordinate system was chosen such that the x, y, and z axes corresponded to eversion/inversion, dorsiflexion/plantar flexion, and internal/external rotation, respectively. A sequence of three Euler angle rotations (x, y and z) was computed for each of the four bones. These rotations were averaged over the eleven specimens to generate twelve validation corridors (mean(S.D.) for model performance.

Model simulations were executed using LS-DYNA (LSTC; Livermore, CA), an explicit, nonlinear, large-deformation finite element code, on a dual processor Dell Precision 610 workstation. The tibia was constrained to vertical motion only, and a 150N axial load was applied down the tibial shaft to simulate the cadaveric validation experiments.

RESULTS

The simulation ran for 0.4 seconds, after which steady state was reached. Model validation demonstrated good correlation between predicted and

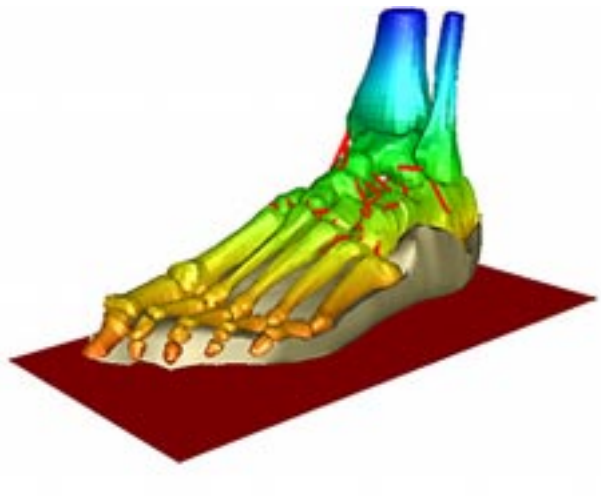

Figure 1: The anterolateral view of the finite element foot and ankle model. Pictured are the bones, ligaments, plantar soft tissue and floor.

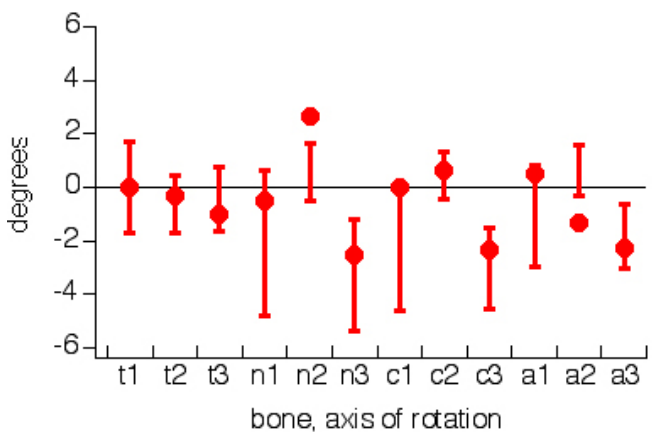

Figure 2: The motions of the hindfoot complex as predicted by the model (circles). The cadaveric data is presented as a range from the mean + one standard deviation to the mean - one standard deviation (error bars). t = talus, n = navicular, c = cuboid, a = calcaneus, 1 = eversion/inversion, 2 = dorsiflexion/plantar flexion, and 3 = internal/external rotation

experimentally measured motions of the hindfoot complex (Figure 2). When comparing the three-dimensional rotations of the tarsal bones, the computational model came with one standard deviation of the cadaveric mean for 10 out of 12 rotations and within two standard deviations of the mean for all of the rotations.

Discussion

To more efficiently study the biomechanical phenomena underlying foot structure and function, a three-dimensional, finite element model of the foot and ankle was created. This anatomically accurate, experimentally validated, foot and ankle model should ultimately provide a powerful tool for the rapid understanding, treatment and prevention of foot disease.

There are several limitations to the current model, including the exclusion of muscle (preventing accurate force application) and cartilage (preventing accurate joint space descriptions). Additionally, all ligaments were assumed to be linear (potentially underestimating stiffness). A stepwise approach to development and validation of an osteoligamentous foot model was deemed a necessary first step in efforts to develop a generalized foot model. Future additions of the model will include intrinsic and extrinsic muscle, cartilage and nonlinear ligament properties. The validation to date involved only a 150 N tibial load; data are currently being collected for tibial loads up to 600 N with Achilles tendon loads up to 300 N.

The foot architecture represented a normal, neutrally aligned foot. Parallel models of high or low arched feet are being developed. Deformable bones will be implemented to allow for calculation of foot joint forces. Finally, the model will eventually be used to simulate all of stance phase rather than just midstance.

Recommended Reading

Attarian, D. E., McCrackin, H. J., DeVito, D. P., McElhaney, J. H., Garrett, W. E., Jr., 1985. Biomechanical characteristics of human ankle ligaments. Foot Ankle 6, 54-8.

Kitaoka, H. B., Luo, Z. P., Growney, E. S., Berglund, L. J., An, K. N., 1994. Material properties of the plantar aponeurosis. Foot Ankle Int 15, 557-60.

Lemmon, D., Shiang, T. Y., Hashmi, A., Ulbrecht, J. S., Cavanagh, P. R., 1997. The effect of insoles in therapeutic footwear: A finite-element approach. Journal of Biomechanics 30, 615-620.

Sarrafian, S. K., 1993. Anatomy of the Foot and Ankle: Descriptive, Topographic, Functional. Philadelphia, PA: J. B. Lippincott.

Siegler, S., Block, J., Schneck, C. D., 1988. The mechanical characteristics of the collateral ligaments of the human ankle joint. Foot & Ankle 8, 234-42.

Mechanical Testing to Characterize the Performance of Shock Absorbing Pylons Used in Transtibial Prostheses

JOCELYN S. BERGE, B.S., GLENN K. KLUTE, PH.D., CAROL F. KALLFELZ, M.S., AND JOSEPH M. CZERNIECKI, M.D.

High frequency load components arising from heel strike during locomotion are thought to be responsible for the deleterious effects observed on the residual tissue and structures of lower limb amputees. To ameliorate these problems, prosthesis manufacturers have developed vertical shock absorbing pylons intended to attenuate the shock loads transmitted to the residual limb from the prosthesis during locomotion. Although prescribed to enhance comfort during walking and high impact activities, to date, the performance and efficacy of shock absorbing pylons is not well understood.

Research conducted on both humans and animals suggests that repetitive loading in general, and high frequency repetitive loading in particular, can be harmful to the musculoskeletal system. Such loading has been implicated in the initiation and progression of osteoarthritis, prosthetic joint loosening, low back disorders, and inflammatory autolysis of the skin leading to ulceration.

Several studies have attempted to characterize different types of shock absorbing pylons using human test subjects and/or mechanical test instruments (Miller and Childress, 1997 and Adderson et al., 1998), however, none have specifically measured the ability of a pylon to attenuate load as a function of frequency.

The purpose of this study was to measure the ability of two commonly prescribed shock absorbing pylons to attenuate load at frequencies enveloping those observed during human locomotion. The two pylons tested were the ICON™ Shock Pylon (Flex-Foot Inc., Aliso Viejo, CA) and the TT (Telescopic Torsion) Pyramid Pylon (Blatchford Endolite, Basingstoke, Hampshire, UK).

MATERIALS AND METHODS

The ICON™ Shock Pylons were outfitted, by the prosthetist, with i4, i5, i6, and i7 springs and the TT Pylons with Purple, White, and Black springs for testing. To objectively characterize the performance of each ICON™ Shock Pylon and TT Pylon, two sets of tests were performed using servo-hydraulic material testing systems (MTS Systems Corporation, Eden Prairie, MN), a pseudo-static loading and unloading test and dynamic cyclic testing.

From the pseudo-static loading and unloading test, a spring constant (k) for each pylon was determined and used to calculate the non-dimensional force results discussed below. From the dynamic cyclic testing, sinusoidal inputs were used to obtain an output non-dimensional force as a function of frequency.

Psuedo-static loading and unloading was performed on a MTS (Model 858 Bionix). The MTS was programmed to follow a 0.5 mm/s loading ramp starting at 0 mm and ending at 15 mm or 12.5 mm followed by a return ramp ending at final displacement of 0 mm for the ICON™ Shock Pylons and TT Pylons, respectively.

The dynamic cyclic testing was performed on a MTS (Model 810 High Rate). The material testing system was programmed to generate five sinusoids, starting at 1 mm offset, at each of the frequencies and peak-to-peak displacements listed (Table 1).

Frequency (Hz)	Step Size (Hz)	Peak-to-peak (mm)
0.1, 0.5-4	0.5	9
5-15	1	3
16-25	1	2
26-35	1	1
36-45	1	1
46-55	1	1
60-100	5	1 (except i5, 0.5)

Table 1: Dynamic Cyclic Testing Matrix.

RESULTS

Figure 1 represents loading/unloading curves typical for the ICON™ Shock Pylons and TT Pylons tested. As shown in Figure 1, the loading and unloading curves were fairly linear over the displacement range for the all the pylons tested.

A least squares linear fit of the loading and unloading curves was performed to determine the spring constant for each pylon. The calculated spring constants for the ICON™ Shock Pylons with i4-i7 springs were 74, 84, 96, and 112 N/mm, respectively. The calculated spring constant for the TT Pylons with Purple, White, and Black springs were 80, 110, and 140 N/mm, respectively.

Using the steady state (typically the 3rd peak of the sinusoid) peak displacement and the corresponding force from the dynamic cyclic testing data and the linear spring constants from the pseudo-static tests, non-dimensional force vs. frequency plots were obtained (Figures 2 and 3). This non-dimensional variable was developed to allow for quantification of damping present while also taking into account the nature of the testing, in which the displacement and therefore force varied with frequency.

DISCUSSION

Each pylon tested formed a hysteresis loop with a different spring constant value for the loading and unloading curves. The rectangular shape of the hysteresis loop indicated the presence of coulomb damping at loading rate of 0.5 mm/s.

Figure 2 shows that the ICON™ Shock Pylons have very little damping. The TT Pylons (Figure 3) have more

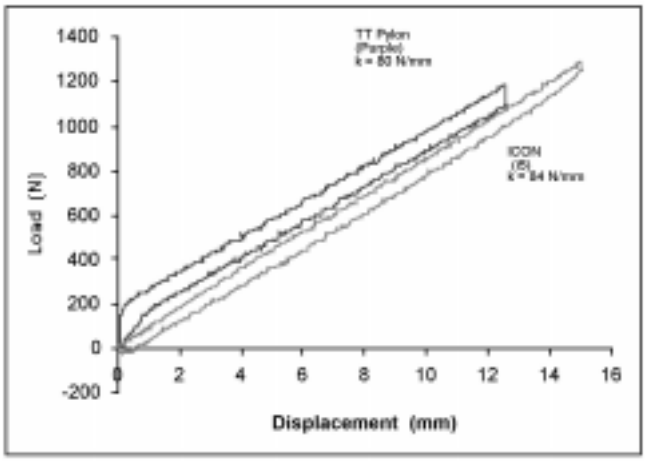

Figure 1: Loading/Unloading curves for an ICONTM Shock Pylon with an i5 spring and a TT Pylon with a Purple spring.

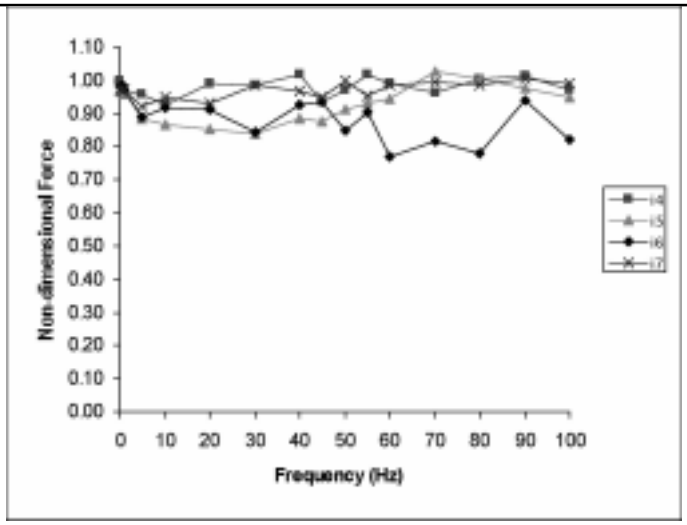

Figure 2: Non-dimensional Force vs. Frequency for the ICONTM Shock Pylons with i4-i7 springs.

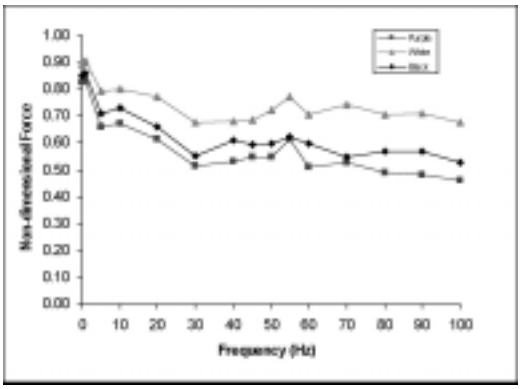

Figure 3: Non-dimensional Force vs. Frequency for TT Pylons with Purple, White, and Black springs.

damping than the ICON™ Shock Pylons and the damping tends to increase with increasing frequency.

Figure 2 also shows that the ICON™ Shock Pylons have little force attenuation over the whole frequency range tested independent of the spring installed (possible exception i6 spring). The TT Pylons (Figure 3) have more attenuation than the ICON™ Shock Pylons and the attenuation changes depending on the spring installed. Future human subject research will help to determine the magnitude of attenuation necessary to protect residual limb tissue.

Acknowledgements

Mechanical testing conducted at the Applied Biomechanics Laboratory, Harborview Medical Center, Seattle, WA. Prosthetic services provided by Martin McDowell, VA Puget Sound Health Care Systems, Seattle, WA.

Recommended Reading

Whittle, M. W. Generation and Attenuation of Transient Impulsive Forces Beneath the Foot: A Review. Gait Posture 1999;10(3), December:264-275.

Miller, L. A., and Childress, D. S. Analysis of a Vertical Compliance Prosthetic Foot. Journal of Rehabilitation Research and Development:1997;34(1), January:52-57.

Adderson, J. A., MacLeod, D. A., Kirby, R. L., and McPhail, C. L. Analysis of a Shock Absorber Used in a Transtibial Prosthesis. Proceedings, IXth World Congress of the International Society for Prosthetics and Orthotics, June 28 - July 3, 1998, Afdeling Revalidatie-Academisch Ziekenhuis, Groningen, The Netherlands.

From the VA RR&D Center of Excellence For Limb Loss Prevention & Prosthetic Engineering, VA Puget Sound Health Care Systems, Seattle Division: Bruce J Sangeorzan, Director.

The Distribution of Shoulder Replacements Among Surgeons and Hospitals is Significantly Different than that of Hip or Knee Replacements

SAMER S. HASAN, M.D., PH.D., JORDAN M. LEITH, M.D., F.R.C.S.C., KEVIN L. SMITH, M.D., AND FREDERICK A. MATSEN III, M.D.

Shoulder replacements are performed far less frequently than hip or knee replacements, but data are lacking on the proportion of 'low-volume' and 'high-volume' surgeons and hospitals performing these replacements. The frequency distribution of joint replacement surgery is of potential importance because of the observed relationship between case volume per surgeon and complication rate. Significantly higher rates of mortality, infections, revisions and complications for patients managed by 'low-volume' hip replacement surgeons have been reported.

Our hypothesis is that the frequency distribution of shoulder replacements among surgeons and hospitals is significantly different than that of hip or knee replacements.

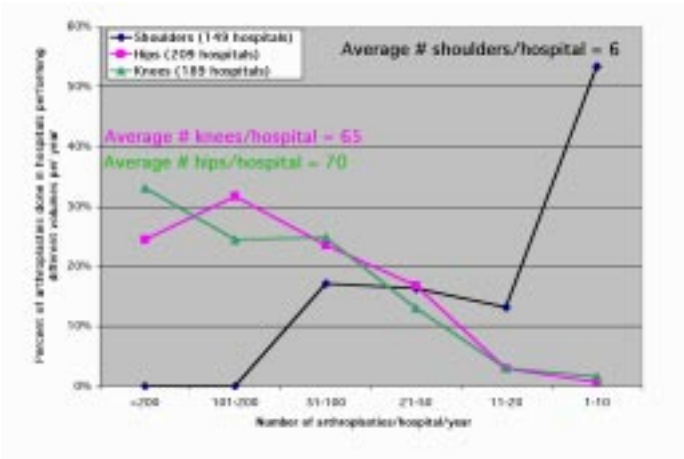

Figure 1: Distribution of hospitals in New York State stratified by the volume of shoulder, hip and knee arthroplasties done in 1998 comparing the relative percentages of each procedure for different sized groups of patients.

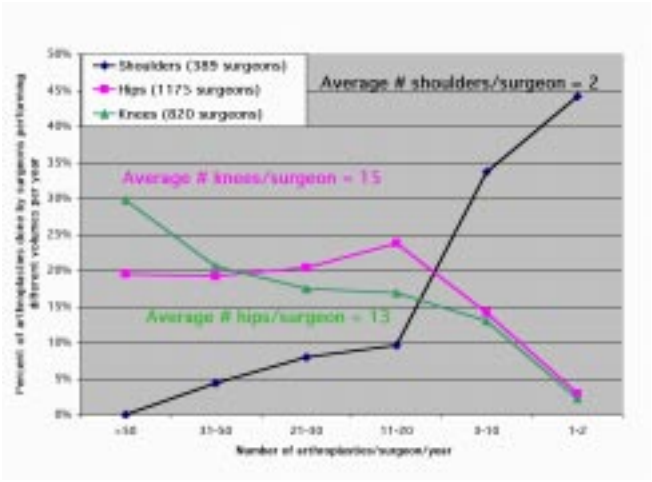

Figure 2: Distribution of surgeons in New York State stratified by the volume of shoulder, hip and knee arthroplasties done in 1998 comparing the relative percentages of each procedure for different sized groups of patients.

METHODS

The 1998 database of the Center for Medical Consumers was queried to determine the volume distribution among surgeons and hospitals in New York State for 1) total/partial shoulder replacements, 2) total/partial hip replacements, and 3) total knee replacements.

The database is accessible online at: www.medicalconsumers.org/Performance_Reports.

RESULTS

The database demonstrated that in 1998, 14,644 hip replacements, 12,328 knee replacements and 902 shoulder replacements were performed by 1175, 820, and 389 surgeons, respectively. Over 40% of hip or knee replacement surgeons in New York State performed 10 or more replacements. In contrast, among shoulder replacement surgeons, only 10 or less than 3% performed 10 or more shoulder replacements and 78% performed only one or two.

Only 7 hospitals witnessed 20 or more shoulder replacements in 1998, compared with over 76% and 66% of hospitals for hip and knee replacements, respectively. Over 25% of hospitals in which shoulder replacements are performed witnessed only a single procedure.

By chi square analysis, the distribution of shoulder replacements among surgeons and hospitals was statistically different than that of hip ($p < .0001$) or knee replacements ($p < .0001$).

	Hip N (%)	Knee	Shoulder
# Replacements	14844	12328	902
# Surgeons	1175	820	389
#Replacements/Surgeon	12.5	15.0	2.3
# Surgeons performing > 10 Replacements	458 (49.0)	340 (41.5)	10 (2.6)
# Surgeons performing 1-2 Replacements	361 (30.7)	209 (25.5)	304 (78.2)
# Hospitals	209	189	149
#Replacements/Hospital	70.1	65.2	6.1
# Hospitals performing > 20 replacements	160 (76.6)	125 (66.1)	7 (4.7)
# Hospitals performing ≤ 20 replacements	49 (23.4)	64 (33.9)	142 (95.3)

Table 1: Hip, knee, and shoulder replacement data for New York State in 1998.

Discussion

In the US in 1998 there were 17,571 AAOS members and 270,000 hip replacements, 265,000 knee replacements, and 17,468 shoulder replacements performed (of which 6822 were total shoulder replacements). On average, it would take each AAOS member over 125 years to accumulate 50 total shoulder replacements, compared with 3 years to accumulate 50 total knee or hip replacements.

In New York State, 12 of the 16 highest volume shoulder surgeons were members of ASES and 7 of the 8 highest volume hospitals were a site of residency education.

The infrequency with which shoulder replacement is performed is concerning because 'low-volume' providers may produce outcomes inferior to those of 'high-volume' providers. This has been borne out in studies of outcomes following hip and knee replacement.

Conclusions

Three-quarters of shoulder replacement surgeons in New York State performed only 1 or 2 shoulder replacements in 1998 and only 10 surgeons performed 10 or more.

Hereditary Multiple Exostoses: Is there a Correlation Between Phenotype and Genotype?

GREGORY A. SCHMALE, M.D., ERNEST U. CONRAD III, M.D., AND WENDY H. RASKIND, M.D., PH.D.

Exostoses are cartilage capped outgrowths of metaphyseal bone that may arise from defects in the perichondral ring at the physes of long bones. Primary locations of exostoses include the distal femur, proximal tibia, and proximal humerus, though lesions of the scapula, phalanges, and vertebrae are not uncommon. Hereditary multiple exostoses (HME) is an autosomal dominant condition affecting approximately 1/50,000 persons in the Western U.S., with estimated penetrance of 95%, variable expressivity, and a rate of malignant degeneration of around 2%. The periarticular location of exostoses may lead more frequently to disability, with rates of forearm and lower extremity bowing and shortening approaching 40%. The prominence of these cartilage lesions may also lead to soft tissue impingement and painful snapping of tendons with joint motion.

Three different loci for the gene defects leading to HME have been proposed - EXT1, EXT2 and EXT3 on chromosomes 8, 11, and 19, respectively. Mutations in EXT1 or EXT2 have been found in eight of the families previously identified at the UW. Linkage could be assigned to EXT1 or EXT2 in an additional six families, although no mutations have been identified to date. The mutations identified include frame-shifts from insertions and deletions, and nonsense and missense mutations from substitutions. EXT1 and EXT2 are thought to have tumor suppressor activity. Tumor suppressor genes are recessive in nature, being rendered inactive by mutations of both normal copies of the gene. The relatively high incidence of chondrosarcomas with loss of heterozygosity at EXT1 or EXT2 supports the notion of tumor suppressor behavior of EXT1 and EXT2.

The variability in expression of HME results in a broad range of severity of affected members within a family. This makes comparisons between families all the more difficult. Correlation between the chromosomal locations and phenotypes of affected individuals has not been reported. This study looks to examine the phenotypes of affected members in eight of these fourteen families with the hope of identifying patterns of expression of EXT1 and EXT2.

Physical exams were performed and blood was drawn under the approval of the University of Washington Human Subjects Committee. A modified functional assessment scale of the Musculoskeletal Tumor Society was used to establish degree of involvement, as previously reported. This scale was based on five primary factors: motion, strength, pain, activity, and upper and lower limb deformities (Table 1). As phenotype may be best reflected by deformity, that one factor was reported separately as well. The radiographs of the left knee of patient 6, in family HME2, are representative of the typical involvement about the knee in HME. This patient's function was only fair and deformity moderate because of bowing and shortening of the forearms.

Table 2 includes the functional assessments and deformities for members of seven families with identified or high probability gene mutations in chromosome 8, and for members of one family with an identified gene defect in chromosome 11. The data is condensed in Table 3. Though the data is limited, there is less severe involvement with better function and milder deformity in family HME08, having a gene defect on chromosome 11, in EXT2.

Though these numbers are small, they suggest that there may be a trend towards less severe involvement in

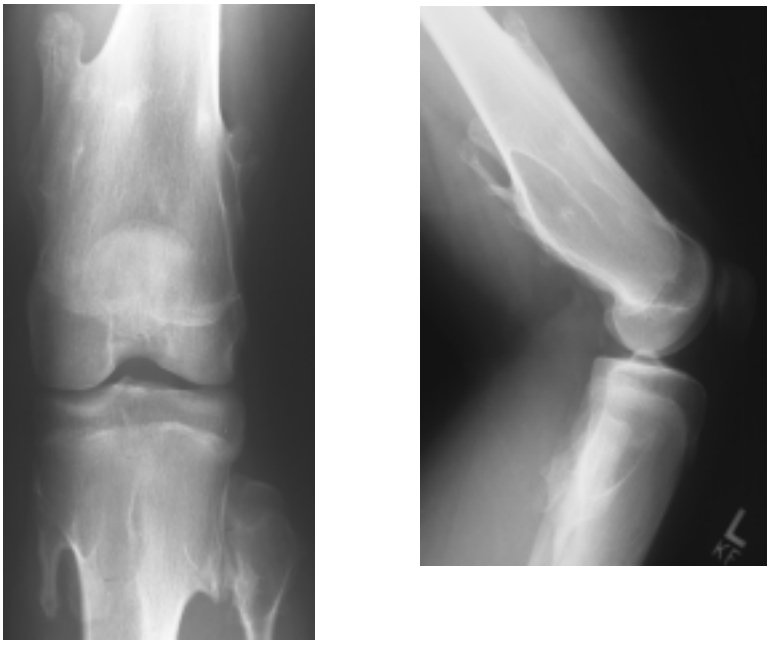

Figure 1: AP and lateral views of the left knee of patient 6, HME02-4, at age 13. Multiple exostoses of the distal femur, proximal tibia, and proximal fibula are present, though little loss of function or deformity about the knees was noted.

Rating	1. Motion (% of Total Normal Joint Motion)	2. Strength	3. Pain	4. Functional Activity	5. Deformity*			
					Forearm Bowing Shortening	Knee Shortening	Leg varus/valgus	
Excellent	>90%	5/5	None	No restrictions	None	None	0-5°	None
Good	60-90%	4/5	Mild (occ meds)	Recreational restrictions	Mild	< 1cm	5-10°	< 1cm
Fair	30-60%	3/5	Moderate (weekly meds)	Partial disability	Moder-ate	1-2cm	10-20°	1-3cm
Poor	<30%	1-2/5	Severe (narcotics or daily meds)	Total disability	Severe	> 2cm	> 20°	> 3cm

* The deformity grade is determined by the lowest score given for any of the four components.

Overall Grade	Criteria
Excellent	At least four of five primary factors are excellent
Good	Lowest rating is good on four of five primary factors
Fair	Lowest rating is fair on four of five primary factors
Poor	At least two of the five primary factors are rated poor

Table 1: Functional assessment scale for HME based on five primary factors.

Patient ID	Family-pt	Chromosome 8 defect (EXT1)	Chromosome 11 defect (EXT2)	Function (Excellent, good, fair, poor)	Deformity (none, mild, moderate, severe)
1	HME01-1	yes		E	None
2	HME01-2	yes		P	Severe
3	HME02-1	yes		E	Moderate
4	HME02-2	yes		P	Severe
5	HME02-3	yes		P	Severe
6	HME02-4	yes		F	Severe
7	HME02-5	yes		F	Severe
8	HME02-6	yes		P	Severe
9	HME02-7	yes		F	Mild
10	HME02-8	yes		E	None
11	HME02-9	yes		E	None
12	HME02-10	yes		E	None
13	HME07-1	yes		G	Mild
14	HME07-2	yes		P	Severe
15	HME07-3	yes		P	Severe
16	HME09-1	yes		F	Severe
17	HME09-2	yes		E	None
18	HME09-3	yes		E	None
19	HME09-4	yes		P	Severe
20	HME09-5	yes		G	Mild
21	HME16-1	yes		F	Moderate
22	HME16-2	yes		E	None
23	HME16-3	yes		E	Mild
24	HME17-1	yes		E	None
25	HME17-2	yes		E	None
26	HME28-1	yes		P	Severe
27	HME08-1		yes	E	None
28	HME08-2		yes	E	Moderate
29	HME08-3		yes	F	Severe
30	HME08-4		yes	G	None
31	HME08-5		yes	F	Moderate
32	HME08-6		yes	E	None
33	HME08-7		yes	F	Severe
34	HME08-8		yes	E	None
35	HME08-9		yes	E	None

Table 2: Phenotypes of 35 patients in eight families for whom genotypes are known.

	EXT1		EXT2
Functional Assessment			
Excellent	11		5
Good	2		1
Fair	5		3
Poor	8		0
Deformity			
None	9		5
Mild	4		0
Moderate	2		2
Severe	11		2

Table 3: Summary of phenotypes for EXT1 and EXT2.

families with EXT2. Expanding the database of patients and family members with HME should help establish more reliable associations between phenotype and genotype, and perhaps suggest guidelines for the prediction of severity of disease in some affected individuals.

Recommended Reading

Schmale, G. A., E. U. Conrad, 3rd, et al. (1994). The natural history of hereditary multiple exostoses. J Bone Joint Surg Am 76(7): 986-92.

Hennekam, R. C. (1991). Hereditary multiple exostoses. J Med Genet 28(4): 262-6.

Hecht, J. T., D. Hogue, et al. (1997). Hereditary multiple exostoses (EXT): mutational studies of familial EXT1 cases and EXT-associated malignancies. Am J Hum Genet 60(1): 80-6.

Raskind, W. H., E. U. Conrad, 3rd, et al. (1998). Evaluation of locus heterogeneity and EXT1 mutations in 34 families with hereditary multiple exostoses. Hum Mutat 11(3): 231-9.

Cook, A., W. Raskind, et al. (1993). Genetic heterogeneity in families with hereditary multiple exostoses.‰ Am J Hum Genet 53(1): 71-9.

Philippe, C., D. E. Porter, et al. (1997). Mutation screening of the EXT1 and EXT2 genes in patients with hereditary multiple exostoses. Am J Hum Genet 61(3): 520-8.

Raskind, W. H., E. U. Conrad, et al. (1995). Loss of heterozygosity in chondrosarcomas for markers linked to hereditary multiple exostoses loci on chromosomes 8 and 11. Am J Hum Genet 56(5): 1132-9.

Intralesional Treatment of Symptomatic Enchondromas and Low-Grade Chondrosarcomas

SCOTT HELMERS, M.D. AND ERNEST U. CONRAD III, M.D.

Typical treatment for symptomatic cartilage lesions, particularly low-grade chondrosarcomas, in this country has been wide surgical resection. Most of these studies have cited unacceptably high local recurrence rates (up to 60%) and greater difficulty in performing limb salvage surgery with intralesional surgical treatment. However, even these studies found no differences in long-term (20-year) survival for intralesional surgery compared to wide resection (68% versus 66%) for chondrosarcoma. In the European literature, other authors have reported good success in treating low-grade cartilaginous neoplasms with intralesional surgery.

The purpose of our study is to report our experience at the University of Washington Medical Center with intralesional treatment of symptomatic enchondromas and low-grade chondrosarcomas.

MATERIALS AND METHODS

A retrospective review was conducted on all patients with low-grade cartilaginous neoplasms at the University of Washington Medical Center from January 1992 to November 2000. Patients with either prior surgical treatment or metastases at time of diagnosis were excluded. In addition, we excluded those patients with frankly high-grade cartilage lesions or extensive soft-tissue masses that were treated with surgical resection. All patients in this review were treated with intralesional surgery. One hundred thirty patients were identified: forty-nine patients with low-grade chondrosarcoma and 81 patients with symptomatic enchondromas. The diagnosis was confirmed both by histological and radiographic examination.

Our technique for intralesional surgery involved wide surgical exposure, to allow adequate visualization of the affected bone. The tumor was removed grossly with meticulous curettage. The bony surfaces were then burred with a high speed burr to bleeding normal bone. The bone was then treated with cryotherapy using a liquid nitrogen spray gun. The bone was frozen and then allowed to thaw, and this cycle was repeated three times. The bony defect was then filled using polymethylmethacrylate bone cement or allograft cancellous chips, depending on the patient's preference and need for immediate stability. All wounds were primarily closed over drains.

Patients were followed every two months with repeat clinical examination and imaging until healing of their bone grafts were demonstrated radiographically. Long-term follow-up was done every six to 12 months with repeat clinical and radiographic examination, including plain radiographs and either magnetic resonance imaging or computerized tomography. The average follow-up was 49 months (range three to 110 months).

RESULTS

One hundred thirty patients were identified with low-grade chondrosarcomas or symptomatic enchondromas. At the time of latest clinical follow-up, there were nine patients (6.9%) identified with the local recurrences, four patients (4.9%) with symptomatic enchondromas and five patients (10.2%) with low-grade chondrosarcomas (Figure 1). Age of patient, sex, size, and duration of symptoms were not identified as significant risk factors for local recurrence. Location, primarily intrapelvic, was identified as a significant risk factor for local recurrence with four of eight (50%) intrapelvic lesions experiencing local recurrences. Each of the local recurrences required additional surgery; six were treated with repeat curettage, and three with radical resection surgery and reconstruction. There were no deaths from disease, and no distant metastases at time of latest follow-up.

DISCUSSION

Most American literature has opposed intralesional treatment for symptomatic cartilaginous neoplasms. Eriksson in his review of the management of chondrosarcomas strongly recommended wide surgical resection for all chondrosarcomas. Similarly, Azzarelli recommended wide surgical resection for all chondrosarcomas due to unacceptably high local recurrence rates-as high as 60%-with intralesional treatment compared to only 11% with radical surgery. Azzarelli's review included 55 chondrosarcomas, composed of 14 intermediate-grade tumors, 23 high grades, and 12 with "undetermined" grades. When compared to our study, only the six patients with low-grade chondrosarcomas would be treated with intralesional surgery at our facility. When stratifying their data according to histological grade, there was only a 20% local recurrence rate in low-grade chondrosarcomas. Ozaki's review followed 26 chondrosarcoma patients treated with intralesional surgery for an average of 12 years. Their cohort included eight patients with intermediate-grade chondrosarcoma, and four patients with high-grade chondrosarcoma. They reported a 93% local recurrence rate with intralesional surgery, compared to a 46% local recurrence rate with marginal or wide resection. Ozaki also noted greater difficulty in performing limb-salvage surgery after intralesional treatment. Like Azzarelli's review, almost half of the patients in this study (46%) had intermediate- or high-grade tumors. This prompted Marco in his recent article in the *Journal of the American Academy of Orthopaedic Surgeons* to strongly recommended wide surgical resection and allograft or prosthetic reconstruction for all chondrosarcomas including low-grade lesions.

Even in these studies, there has been no evidence to suggest any significant differences in long-term survival with intralesional surgery when compared to wide resection chondrosarcomas. In Ozaki's review, he found the 20-year survival rate for intralesional chondrosarcoma surgery was 68%

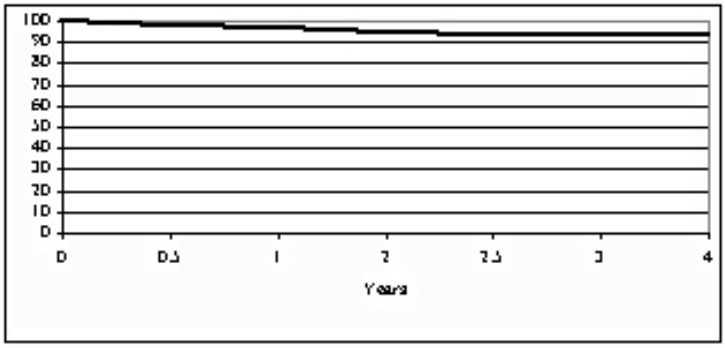

Figure 1: Local Recurrence.

compared with 66% for radical resection. We found similar findings in our review, with no distant metastases and no deaths from disease with short-term (average four-year) follow-up.

In contrast, Bauer reported his results with 40 patients with enchondromas and 40 patients with low-grade chondrosarcomas treated with intralesional surgery followed for an average of 6.5 years. He noted four local recurrences (5%), one in the enchondroma group (2.5%) and three in the chondrosarcoma group (7.5%). As with the other studies, there were no metastases. Bauer concluded that enchondromas and low-grade chondrosarcomas should be treated with limited surgery.

Schreuder reported his results in treating three chondroblastomas, 14 enchondromas, and nine low-grade chondrosarcoma followed for an average of two years. He noted no local recurrences and concluded intralesional treatment equal to marginal resection.

Our results were similar to those of Bauer and Schreuder with a 6.9% local-recurrence rate and no evidence of metastases with short-term follow-up when treating low-grade cartilaginous neoplasms.

We would conclude that intralesional treatment of low-grade cartilaginous neoplasms has an acceptably low local recurrence rate (6.9%) and no increased threat of systemic disease. This method of treatment avoids the morbidity associated with radical resection and reconstruction without jeopardizing limb or patient survival. This mode of treatment requires meticulous technique with adequate exposure, curettage, high-speed burring, cryotherapy, bone grafting/cementation, and close clinical and imaging follow-up.

Recommended Reading

Azzarelli A, Gennari L, Quagliuolo V, Bonfanti G, Cerasoli S, Bufalino R. Chondrosarcoma—55 unreported cases: epidemiology, surgical treatment and prognostic factors. Eur J Surg Oncol. 1986 Jun; 12(2): 165-8.

Bauer HC, Brosjo O, Kreicbergs A, Lindholm J. Low risk of recurrence of enchondroma and low-grade chondrosarcoma in extremities. 80 patients followed for 2-25 years. Acta Orthop Scand. 1995 Jun; 66(3): 283-8.

Eriksson AI, Schiller A, Mankin HJ. The management of chondrosarcoma of bone. Clin Orthop. 1980 Nov-Dec; (153): 44-66.

Lee FY, Mankin HJ, Fondren G, Gebhardt MC, Springfield DS, Rosenberg AE, Jennings LC. Chondrosarcoma of bone: an assessment of outcome. J Bone Joint Surg Am. 1999 Mar; 81(3): 326-38.

Marco RA, Gitelis S, Brebach GT, Healey JH. Cartilage tumors: evaluation and treatment. J Am Acad Orthop Surg. 2000 Sep;8(5): 292-304.

Ozaki T, Lindner N, Hillmann A, Rodl R, Blasius S, Winkelmann W. Influence of intralesional surgery on treatment outcome of chondrosarcoma. Cancer. 1996 Apr 1; 77(7): 1292-7

The Orthopedic Implications of Chemotherapy to Growth in Children

SCOTT HELMERS, M.D. AND ERNEST U. CONRAD III, M.D.

Over the past several decades, the incidence of childhood malignancies has increased. Modern cancer treatment regimens are more intense and involve multiple drugs, resulting in greater long-term survival. Although children can tolerate the acute side effects of chemotherapy better than adults, the growing child is more susceptible to the long-term results of chemotherapy. With an estimated one in one thousand 20-year-olds being a childhood cancer survivor, it is essential that every orthopedic surgeon who manages these survivors understands the long-term effects of chemotherapy. Therefore, the purpose of our review is to summarize the effects of chemotherapy on growth, and its implications to the orthopedic surgeon who may care for these patients.

METHODS

We conducted a literature review through PubMed, a National Library of Medicine database. We searched all articles in the English language that dealt with the effects of chemotherapy upon growth and the growing skeleton. Thirty-one articles were identified, of which 18 specifically addressed the effects of chemotherapy on growth.

RESULTS

Poor nutrition, infections, radiation, corticosteroids, and the disease itself are well known causes of diminished growth during cancer treatment. The significant role of chemotherapy in growth inhibition has only been established during the past ten to 15 years. Although the exact mechanism by which chemotherapy impairs growth is not known, most authors believe it is due to impairment of growth hormone. One study found growth hormone deficiencies were common (47%) after chemotherapy treatment and led to growth impairment. This has led some to recommend growth hormone treatment for affected children. Another study demonstrated that chemotherapeutic agents (doxorubicin, actinomycin D, cisplatin) had a direct effect on animal growth plate chondrocytes in vitro, suggesting direct toxicity of chemotherapy on the growing skeleton.

Even though the exact mechanism by which chemotherapy impairs growth may not be known, its effects have been well established. Several studies have shown impairment of growth during chemotherapy treatment that lasts as long as the treatment. Children most often dropped one standard deviation in height, corresponding to four centimeters, from before treatment to peak impairment during treatment (Figure 1). After chemotherapy treatment concludes, multiple studies have demonstrated "catch-up growth," with increased growth and growth velocity. Most "catch-up growth" occurred in the first two years after the end of chemotherapy. This phenomenon was accompanied by delayed puberty and delayed skeletal maturation, particularly when chemotherapy treatment occurred in the prepubertal period. After "catch-up growth," these children most often had normal overall height and stature by four to five years following the conclusion of all treatment.

DISCUSSION

It is essential that the orthopedic surgeon who may treat these children -- particularly for any limb length issues -- understand these effects of chemotherapy. Limb length inequalities are common, particularly for patients with histories of extremity tumors. These patients often require limb equalizing procedures, contralateral epiphysiodesis, contralateral shortening, or ipsilateral lengthening. The timing of these surgeries is usually based upon "normal" growth curves; however, these children often have delayed puberty and skeletal maturation, making timing a challenge. These surgeries often are delayed by one to two years to account for "catch-up growth" and delayed maturation. Therefore, any orthopedic surgeon treating these children must appreciate and account for the temporal relationship between chemotherapy treatment and growth.

RECOMMENDED READING

Berglund G, Karlberg J, Marky I, Mellander L. A longitudinal study of growth in children with acute lymphoblastic leukemia. Acta Paediatr Scand 1985 Jul; 74(4): 530-3.

Berry DH, Elders MJ, Crist W, Land V, Lui V, Sexauer AC, Dickinson L. Growth in children with acute lymphocytic leukemia: a Pediatric Oncology Group study. Med Pediatr Oncol 1983; 11(1): 39-45.

Birkebaek NH, Clausen N. Height and weight pattern up to 20 years after treatment for acute lymphoblastic leukaemia. Arch Dis Child 1998 Aug; 79(2): 161-4.

Cicognani A, Cacciari E, Rosito P, Mancini AF, Carla G, Mandini M, Paolucci G. Longitudinal growth and final height in long-term survivors of childhood leukaemia. Eur J Pediatr 1994 Oct; 153(10): 726-30.

Clayton PE, Shalet SM, Morris-Jones PH, Price DA. Growth in children treated for acute lymphoblastic leukaemia. Lancet 1988 Feb 27; 1(8583): 460-2.

Davies HA, Didcock E, Didi M, Ogilvy-Stuart A, Wales JK, Shalet SM. Growth, puberty and obesity after treatment for leukaemia. Acta Paediatr Suppl 1995 Sep; 411:45-50; discussion 51.

Glasser DB, Duane K, Lane JM, Healey JH, Caparros-Sison B. The effect of chemotherapy on growth in the skeletally immature individual. Clin Orthop 1991 Jan;(262): 93-100.

Groot-Loonen JJ, Otten BJ, van t' Hof MA, Lippens RJ, Stoelinga GB. Chemotherapy plays a major role in the inhibition of catch-up growth during maintenance therapy for childhood acute lymphoblastic leukemia. Pediatrics 1995 Oct; 96(4 Pt 1): 693-5.

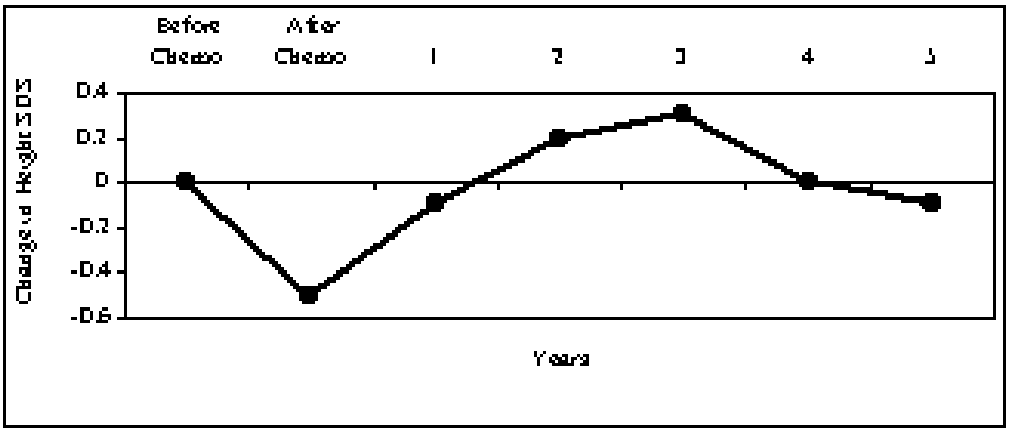

Figure 1: Cumulative Changes in Height with Chemotherapy.

Hokken-Koelega AC, van Doorn JW, Hahlen K, Stijnen T, de Muinck Keizer-Schrama SM, Drop SL. Long-term effects of treatment for acute lymphoblastic leukemia with and without cranial irradiation on growth and puberty: a comparative study. Pediatr Res 1993 Jun; 33(6): 577-82.

Holm K, Nysom K, Hertz H, Muller J. Normal final height after treatment for acute lymphoblastic leukemia without irradiation. Acta Paediatr 1994 Dec; 83(12): 1287-90.

Logghe KA, Bourguignon JP, Craen M, Benoit Y. Factors contributing to the impairment of growth in children with acute lymphoblastic leukemia. Horm Res 1988; 30(2-3): 62-7.

Marky I, Samuelsson BO, Mellander L, Karlberg J. Longitudinal growth in children with non-Hodgkin's lymphoma and children with acute lymphoblastic leukemia: comparison between unirradiated and irradiated patients. Med Pediatr Oncol 1991; 19(2): 96-9.

Olshan JS, Gubernick J, Packer RJ, D'Angio GJ, Goldwein JW, Willi SM, Moshang T Jr. The effects of adjuvant chemotherapy on growth in children with medulloblastoma. Cancer 1992 Oct 1; 70(7): 2013-7.

Roman J, Villaizan CJ, Garcia-Foncillas J, Azcona C, Salvador J, Sierrasesumaga L. Chemotherapy-induced growth hormone deficiency in children with cancer. Med Pediatr Oncol 1995 Aug; 25(2): 90-5.

Sato J, Ninomiya T, Tsuda Y, Komazawa M, Nagata K, Iwai A, Nishikawa K, Maeda H, Ohmiya A, Ohta M, et al. Analysis of growth failure in children treated for acute lymphoblastic leukemia. Int J Hematol 1992 Dec; 56(3): 205-12.

Sklar C, Mertens A, Walter A, Mitchell D, Nesbit M, O'Leary M, Hutchinson R, Meadows A, Robison L. Final height after treatment for childhood acute lymphoblastic leukemia: comparison of no cranial irradiation with 1800 and 2400 centigrays of cranial irradiation. J Pediatr 1993 Jul; 123(1): 59-64.

Tamminga RY, Kamps WA, Drayer NM, Humphrey GB. Longitudinal anthropometric study in children with acute lymphoblastic leukaemia. Acta Paediatr 1992 Jan; 81(1): 61-5.

Van Leeuwen BL, Kamps WA, Jansen HW, Hoekstra HJ. The effect of chemotherapy on the growing skeleton. Cancer Treat Rev 2000 Oct; 26(5): 363-76.

Technique of Scapulothoracic Fusion in Facioscapulohumeral Muscular Dystrophy

MOHAMMAD DIAB, M.D. AND FREDERIC SHAPIRO, M.D.

Facioscapulohumeral muscular dystrophy (FSHMD) is an autosomal dominant disorder with a frequency of 1 in 20,000, 95% penetrance by 20 years of age, and a 5-10% new mutation rate. The disorder initially affects the muscles of the face, shoulder and arm, and progresses to involve the muscles of the pelvic girdle and lower limbs. In the infantile variant, a more severe disorder presenting in the first year of life, the clinical presentation includes extramuscular disease such as sensorineural hearing loss and retinal vasculopathy. While FSHMD has been linked to chromosome 4q35, non-linkage in a small number of families illustrates its genetic heterogeneity.

Figure 1: Pre- and post-operative shoulder abduction in the same patient.

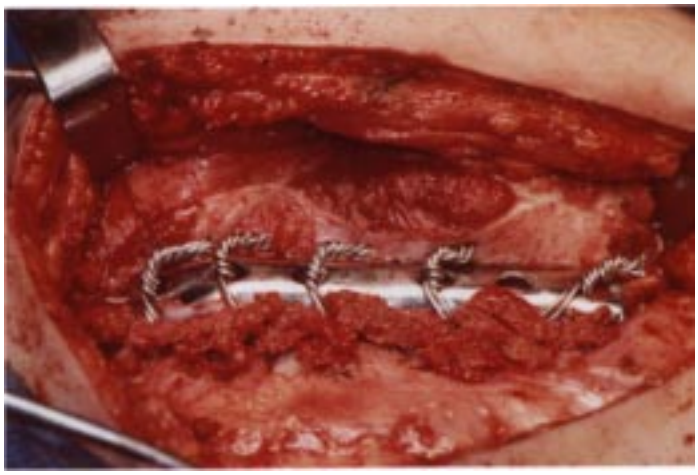

Figure 2: Operative technique: scapulocostal fixation with doubled 16 guage cerclage wires and limited contact dynamic compression plate.

Weakness of the muscles of the shoulder, including the serratus anterior, trapezius, levator scapulæ, rhomboid major and minor, and latissimus dorsi, leads to instability of the scapula during shoulder motion. The deltoid muscle, which originates from the clavicle and scapula and inserts into an eminence on the lateral surface of the humeral shaft, is relatively spared. Activation of the deltoid muscle leads to movement of its site of origin at the scapula, which is not retained against the thorax and becomes more mobile than the humerus. The scapula rotates cephalad and away from the chest wall, to produce winging. Traction on the muscles which insert into the vertebral border of the scapula is painful. Because of its mechanical disadvantage, the deltoid muscle rapidly fatigues. Affected individuals complain of an unacceptable winging deformity and inability to perform overhead activities, such as combing the hair. Stabilization of the scapula improves the appearance of the shoulder, alleviates pain and allows for functional abduction of the upper limb.

We describe a technique of scapulothoracic fusion for adolescent and infantile FSHMD that is effective, straight forward, relatively uncomplicated and avoids restrictive postoperative immobilization.

MATERIALS AND METHODS

We performed 12 scapulothoracic fusions in 3 girls (1 bilateral, 1 unilateral) and 5 boys (3 unilateral and 2 bilateral). One girl was affected by the infantile form. Average age at operation was 15 yr. 2 mo. (range 11 yr. 4 mo.-18 yr. 10 mo.). Average follow-up was 5 yr. 1 mo. (range 12 mo.-11 yr. 1 mo.).

The patient is placed prone. The forequarter is draped free. A linear incision is made over the vertebral border of the scapula. The trapezius muscle is cut in line with the cutaneous incision. Dorsally, levator scapulæ, rhomboid major and minor,

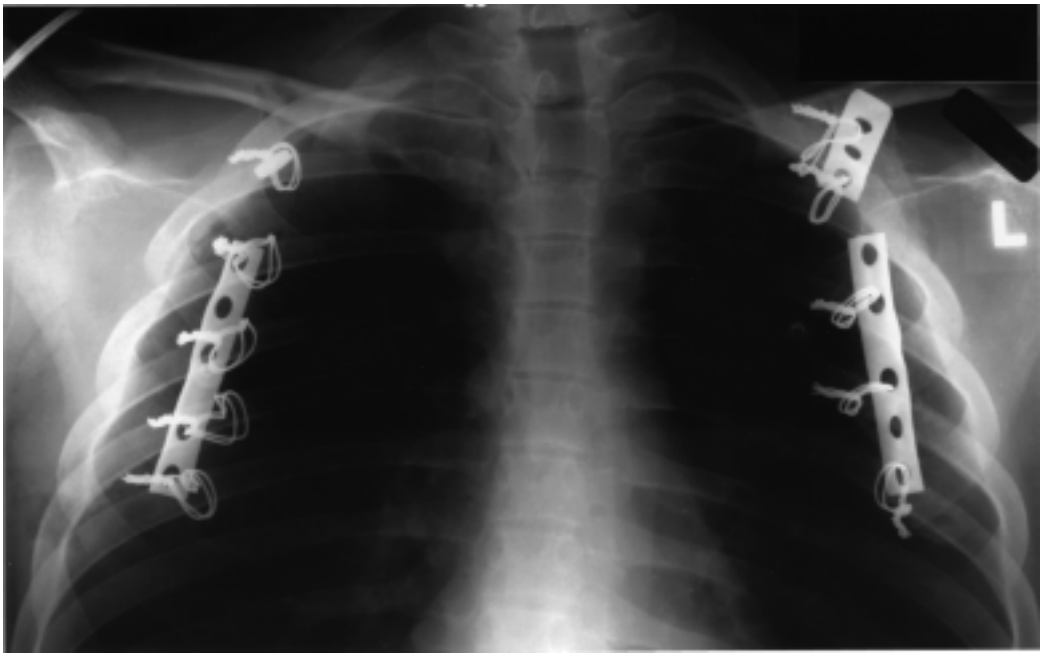

Figure 3: Postoperative röntgenogramme showing position of scapula and internal fixation. Doubled washers were used on the right because the supraspinatus fossa did not accommodate a two-hook semitabular plate.

supraspinatus, infraspinatus and teres major muscles are released from their sites of origin. Ventrally, serratus anterior muscle is released, and an approximately 4 cm strip of subscapularis muscle is excised, permitting direct apposition of the vertebral border of the scapula against subjacent ribs. Ribs for fusion, typically the second to seventh, are exposed subperiosteally from neck to posterior angle. Autogenous osseous graft is harvested from the posterior iliac crest. The deep surface of the scapula and the external surface of the ribs are decorticated by means of a motorized burr. Doubled 16 gauge stainless steel wires are passed around each rib and through opposite channels in the vertebral border of the scapula and the base of the scapular spine. In the supraspinatus and infraspinatus fossæ, doubled washers or a plate are used to reinforce the thin scapular bone. The wires are tightened sequentially to compress scapula against ribs, with interposition of the osseous graft. A Valsalva maneuver is performed to evaluate for pleural puncture. The thoracic and posterior iliac wounds are closed routinely.

The postoperative course consists of 3 phases: sling and swathe immobilization of the shoulder and upper limb for 4 weeks, followed by sling with active and passive range of motion of the elbow for 4 weeks, followed by progression to full active and passive range of motion of the shoulder without sling over 4 weeks. No cast immobilization is necessary.

Results

After scapulothoracic fusion, all patients were relieved of pain and were satisfied with the cosmetic result. Shoulder abduction improved from 80° (60°-90°) to an average of 115° (105°-160°). There were no cases of non-union, pleural puncture, implant failure, wound complication or donor site morbidity. There were 2 cases of prominent wires: at the time of implant removal, union was complete. The 11 patients with adolescent FSHMD maintained their correction. The patient with infantile FSHMD lost abduction from 105° to 90° as a result of increasing deltoid weakness at 2 years after operation.

Discussion

Scapular stabilization without fusion, including scapulopexy to a contralateral, uninvolved scapula, construction of fascial slings, and muscle transfer to restrict but not eliminate scapular motion, have required prolonged immobilization and have met with progressive loss of stability. Previous attempts at fusion of the scapula to the thorax by means of screws required spica cast immobilization, and were complicated by prominent implants, rib fracture due to stress concentration and pleural irritation by the implants.

We performed scapulothoracic fusion in patients with adolescent and infantile FSHMD utilizing wire and washer or plate fixation, autogenous iliac osseous graft, and rapid postoperative mobilization. The only morbidity was implant prominence necessitating removal in 2 patients. In all patients, scapular stabilization eliminated scapular winging and alleviated periomal pain. In the patients with adolescent FSHMD, the procedure resulted in functional shoulder abduction. Progressive weakening of the deltoid muscle in the patient with infantile FSHMD has led to partial loss of the gain in shoulder abduction (105/90). We recommend

scapulothoracic fusion as an effective, reproducible and safe procedure in adolescent FSHMD, but counsel patients with infantile FSHMD that while pain may be eliminated and appearance may be improved, initial gain of shoulder motion may not be permanent.

Recommended Reading

Landouzy, L.T.J., Dejerine, J.J. De la myopathie héréditaire, débutant, dans l'enfance, par la face, sans alteration du système nerveux. Compt. Rend. Hebomadaires Seances Acad. Sci., 98:53, 1884.

Putti, V. L'osteodesis intersacpolare in un caso di mipoatia atrofica progressiva. Arch. Ortop., 23:319, 1906.

Wijmenga, C., Frants, R.R., Brouwer, O.F., Moerer, P., Weber, J.L., Pagberg, G.W. Location of the facioscapulohumeral muscular dystrophy gene on chromosome 4. Lancet, 336:651, 1990.

Van der Maarel, S.M., Deidda, G., Lemmers, R.J.L.F. De novo facioscapulohumeral muscular dystrophy. Frequent somatic mosaicism, sex dependent phenotype, and the role of mitotic transchromosomal repeat interaction between chromosomes 4 and 10. Am. J. Hum. Genet. 66:26-35, 2000.

Effects of Growth Factors in Combination on In Vivo Flexor Tendon Healing

CHRISTOPHER H. ALLAN, M.D., SANG-GIL P. LEE, M.D., ROBERT A. MINTZER, B.S., HO-JUNG KANG, M.D., AND DANIEL P. MASS, M.D.

Surgical repair of injured flexor tendons in Zone II of the hand is often complicated by formation of adhesions between the repaired tendons and the surrounding flexor sheath, resulting in limited excursion and a stiff digit. Early motion has been popularized in an attempt to prevent adhesions, but this increases the risk of rupture of the repair. Recently many investigators have attempted to improve flexor tendon healing with various growth factors. Most research in this area has been done on extrasynovial tendons such as the Achilles, with much less study devoted to tendons within a sheath. Studies in our laboratory and others have shown activity of platelet-derived growth factor BB (PDGF-BB) in stimulating cell division of tendon fibroblasts and of transforming growth factor beta-one (TGF-B1) in stimulating collagen and extracellular matrix production. We hypothesized that delivery of PDGF-BB to an injured flexor tendon in the early phase would stimulate increased cell division, and that delivery of TGF-B1 subsequent to this would stimulate increased collagen production and lead to more rapid and stronger repair.

METHODS

We modified a hemitransection technique of Manske et al which eliminates the need for a technically challenging repair of the rabbit flexor digitorum profundus tendon and which allows the animal freedom of movement of the operated limb, while still allowing for evaluation of healing tissue. Pilot data confirmed that one-half of the flexor tendon retained sufficient strength to allow normal activity of the animal.

Twenty-four New Zealand White rabbits were randomized into two groups. Operative transection of one-half of the FDP of each right forepaw digit was performed under loupe magnification for each group, beginning at the midline raphe and exiting straight laterally to leave one-half of the tendon longitudinally intact. The experimental group underwent injection of platelet-derived growth factor (PDGF-BB; 100ng/ml) at day zero and day two and transforming growth factor (TGF-B1; 20 ng/ml) at days four and six. The concentrations used were in the middle range of concentrations found to be effective in our own and other previous studies. The control group received injections of carrier vehicle in the same volumes and at the same time periods. Animals were allowed free use of the operated extremity and were killed at seven weeks. The flexor digitorum profundus was dissected intact from common flexor tendon to insertion into the distal phalanx of each digit of the operated paws (Figure 1).

Measurement of coronal and sagittal diameter of the tendons at the wound site were performed under sixteen times magnification using electronic digital calipers (MAX-CAL) and selecting the narrowest point at the healing site for measurement, and cross-sectional area of reparative tissue was calculated (Figure 2).

A #11 scalpel blade was used under sixteen power magnification to make a transverse cut through the one-half of the tendon not previously cut at surgery, making this cut at the same level as the prior one, using the midline raphe as a guide. In this way the healing tissue at the wound site was isolated so that tensiometric measurement of strength of the reparative tissue only could be performed. We selected the two radial-sided tendons for evaluation because these tend to be slightly larger and therefore easier to manipulate during biomechanical testing. Specimens were photographed under sixteen-power magnification using Kodak Elite II100 slide film and a Minolta XDII 35mm camera attached to the camera port of the operating microscope (Wild) after creating the hemitransection at the level of the wound. This was performed because of the few instances where detection of the original surgical laceration was difficult, so that correlation could later be made between tensiometric results and site of laceration. Both AP and lateral views were obtained.

After hemitransection of the index and middle ray FDP tendons, the entire tendon specimen (common FDP origin, four tendons, and four toenails with FDP insertions intact) was placed in specially-designed jaws and tendon-retention apparatus on a custom-

Figure 1: FDP Dissected from Paw.

Figure 2: Healed Laceration Site.

Figure 3: Tensiometric Force Testing of Healing Tendon.

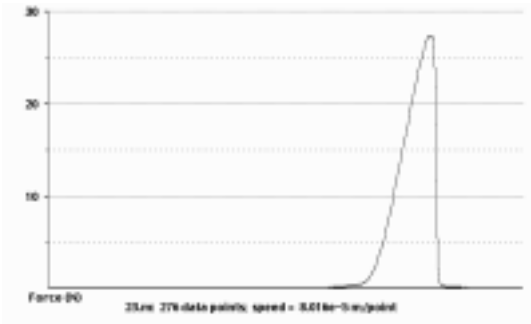

Figure 4: Sample Force Curve Derived from Tensiometry.

designed tensiometer. Each specimen was placed dorsal side up. First the index and then the middle ray FDP tendons were clamped securely into the apparatus and then pulled to failure at a constant rate of one mm per second (Figure 3). Curves of force vs. distance were derived from data points obtained every one-sixtieth of a second using a software program created in our lab (Figure 4). All dissection, photography, hemitransection, and tensiometric testing took place with copious and liberal use of 0.9% normal saline to prevent drying of specimens.

Results

Nineteen of 24 original control and 22 of 24 experimental group tendons underwent evaluation. The mean cross-sectional area of reparative tissue was 0.628 mm2 for control and 0.573 mm2 for experimental group tendons. The mean force to disruption per unit area was 42.788 N/mm2 for control and 39.967 N/mm2 for experimental group tendons. No statistical differences between the groups were identified for these parameters.

Discussion

We conclude that PDGF-BB and TGF-B1 injected into the flexor sheath at four time periods after partial tendon laceration did not lead to measurable differences in amount or strength of reparative tissue at seven weeks. While it is possible that the growth factors or concentrations chosen have no significant effect on tendon healing, it is also possible that an alternative in vivo model would yield different results. In particular the mode of delivery and the model of injury used in this study deserve attention and we intend to modify these in future studies. Recent work has suggested growth factor-coated suture can elute significant levels of cytokine over several weeks, and this strategy could be combined with a complete transection and repair model.

In summary, growth factors stimulate cell proliferation and collagen production. PDGF-BB and TGF-B1 are found early in flexor tendon healing, associated with these molecular events. Addition of these factors in supraphysiologic doses at or before the time of their expression in injured tendons has been hypothesized to increase tendon repair strength. This study does not support this hypothesis, but the limitations of the study suggest alternative approaches which we are currently pursuing.

Recommended Reading

Allan C., Kordylewska A., Shumway S., and Mass D.: PDGF-BB Stimulates Proliferation of Rabbit Flexor Tendon Fibroblasts. Ortho Trans., 18:3, 920, 1994.

Robbins JR, Evanko SP, Vogel KG: Mechanical loading and TGF-beta regulate proteoglycan synthesis in tendon. Arch Biochem Biophys 1997 Jun 15;342(2):203-11.

Duffy FJ, Seiler JG, Gelberman RH, Hergrueter CA: Growth factors and canine flexor tendon healing: initial studies in uninjured and repair models. J Hand Surg [Am] 1995 Jul;20(4):645-9.

Kubota H, Manske PR, Aoki M, Pruitt DL, Larson BJ: Effect of motion and tension on injured flexor tendons in chickens. J Hand Surg [Am] 1996 May; 21(3):456-63.

Rohrich RJ, Trott SA, Love M, Beran SJ, Orenstein HH: Mersilene suture as a vehicle for delivery of growth factors in tendon repair. Plast Reconstr Surg 1999 Nov; 104(6):1713-7.

The authors gratefully acknowledge grant funding from the American Society for Surgery of the Hand (ASSH) in support of this research.

Randomized Prospective Trial of Active versus Passive Motion after Zone II Flexor Tendon Repair

THOMAS E. TRUMBLE, M.D., RICHARD S. IDLER, M.D., JAMES W. STRICKLAND, M.D.,
PETER J. STERN, M.D., SHELLY SAILER, O.T.R./C.H.T., AND MARY M. GILBERT-ANDERSON, M.A.

The controversy surrounding flexor tendon repairs and rehabilitation dates back over a hundred years ago to the early studies by Paget and Adams. In 1928 the founding father of American hand surgery, Sterling Bunnell, wrote "if flexor tendons are severed in the finger the usual place opposite the proximal phalanx, one cannot join them together by sutures with success, as the junction will become adherent in the narrow fixed channel and will not slip. It is better to remove the tendons entirely from the finger and graft in a new tendon smooth throughout its length". However, this repair technique, which excises the lacerated tendon and replaces it with a graft has been plagued by several problems including the delay for wound healing prior to tendon grafting, the need to harvest a graft, and results that lacked full digit flexion. The area of injury that is most likely to result in a poor result is Zone II which is also known as "no-man's land" because there are two tendons within the sheath resulting in an extremely large surface area for adhesions to form and restrict tendon motion.This study uses a stronger repair technique so that the patients can start active motion with their own muscle control rather than relying on passive motion as done by the patient's other hand or by the hand therapist. There is a theoretical trade off between passive motion rehabilitation protocols which result in less digit motion but a lower tendon rupture rate and active motion therapy resulting in greater motion but a theoretically increased rate of tendon rupture. This study is the first to prospectively compare active versus passive motion for the rehabilitation of patients with flexor tendon laceration using a standardized repair technique and standardized functional outcome tests. Purpose: This study evaluated the patient outcome following Zone II flexor tendon repair using range of motion as well as dexterity tests and questionnaires to determine whether active versus passive motion provided the greatest patient satisfaction and digit motion.

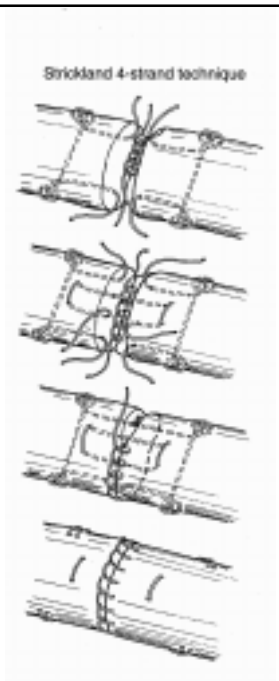

Figure 1: The 4- strand technique offers greater strength compared to earlier 2-strand suture repairs.

Figure 2: The tenodesis splint allows wrist extension and decreases the force of finger flexion during active motion exercises.

METHODS

A standardized 4-strand tendon repair with a running epitenon suture was used in this study. Our own biomechanical study as well as a large body of clinical and experimental evidence suggest that this technique provides the strength necessary to avoid the risk of tendon rupture during the critical first three weeks with active exercises while still minimizing the amount of suture material in the repair. Flexor tendon lacerations were randomized to active versus passive hand therapy after the surgery has been performed to eliminate the possibility of surgeon bias during the repair.

STUDY DESIGN

1. Prospective randomized clinical trial
2. Multicenter
3. Effectiveness study
4. Follow up for one year per patient from injury
5. Outcome study using validated questionnaires
6. Outcome study using validated functional tests
7. Cost analysis of treatment

Patients in each injury group were randomized to either passive or to an active plus passive rehabilitation program. The tendon repairs were performed in a standardized fashion using a technique popularized by one of the principal investigators using two core sutures and a running epitenon suture.

INCLUSION CRITERIA

1. Patients with a zone I or II flexor tendon injury involving the hand with or without a concomitant nerve injury.
2. Injuries < 2 weeks old prior to surgery
3. Patients > 12 years old and < 75 years old.
4. Patients receiving therapy within one week from the time of surgery.

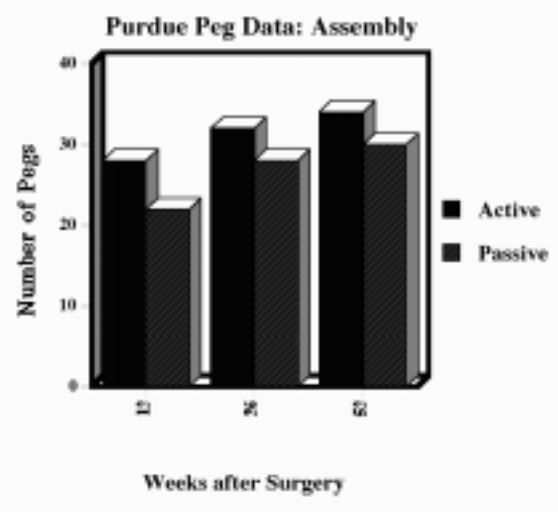

Figure 3: The patients with active motion therapy had greater finger dexterity when measured by the Purdue Pegboard test compared to patients with passive motion therapy.

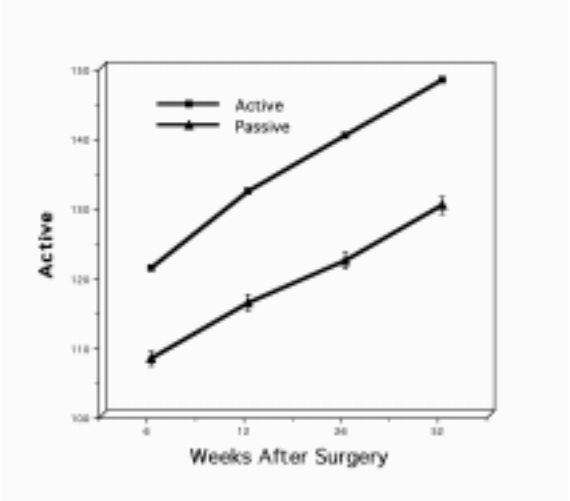

Figure 4: The patients with active motion therapy had greater digit motion than patients with passive motion.

Exclusion Criteria

(i.e. not randomized but followed in the same manner):

1. Patients with wound infections at the time of presentation.
2. Patients with concomitant fractures of the injured digit as this dramatically increases scar formation.
3. Patients with digit ischemia requiring immediate arterial repair.
4. Patients who have a psychiatric history, head injury, substance abuse or evidence of cognitive deficits that would decrease compliance with hand therapy.
5. Patients with medical problems that preclude any anesthetic required for surgery.
6. Concomitant disorders, e.g. severe arthritis that limits hand motion.
7. Patients with severe crushing injuries that prevent primary tendon repair.
8. Patients < 12 years old or > 75 years old. These patients have been shown to perform poorly with therapy.
9. Only one flexor tendon in a digit was repaired.

Patient Enrollment

After the patient was identified as having a flexor tendon laceration by the emergency or trauma room personnel, the patient was scheduled for surgical repair of all flexor tendon injuries using the 4-strand technique (Figure 1).

Other variables included in the study were the presence of a nerve injury and whether the injury was sharp or crushing in nature.

Passive Range of Motion for Rehabilitation of Flexor Tendon Laceration:

The patient starts passive exercises as described by Duran, flexing the digits into the palm using the opposite hand and then actively extending to the limits of the static splint. Flex and hold exercises are not started until 5 weeks after surgery and active flexion did not start until 6 weeks after surgery.

Active Range of Motion for Rehabilitation of Flexor Tendon Laceration:

The patient starts active exercises by having the patients bend the digits into the palm without any resistance using a hinged or tenodesis splint (Figure 2). During the initial exercises the patient should perform "flex and hold" exercises 3-4 times to reduce edema followed by active flexion exercises.

Hand Function Tests:

In addition to strength measurements with grip and pinch strength, the sensation was measured using two point discrimination fine filaments. The finger motion was measured and the Jebsen's Hand Function Score and the Purdue Pegboard Test were used to assess the dexterity of the hand.

Please see Table 1 for demographic data.

Results

Patient Satisfaction as Evaluated by the DASH Questionnaire:

The DASH scores significantly improved from a mean score of 3.4 to a final score of 1.3. There was no significant difference between the active and passive motion groups. The DASH score did correlate with number of digits involved ($p<.05$) as well as the presence of nerve injuries ($p<.05$).

Hand Dexterity:

Patients with active motion scored better on the Purdue Pegboard and Jebson Taylor tests at three, six and twelve months following the surgery (Figure 3, $p<.05$)

Range of Motion:

The patients with the active range of motion had greater motion than the patients in the passive group at 6, 12,

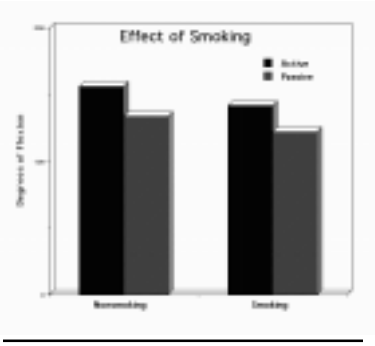

Figure 5: The patients who smoked had less digit motion than did non-smoking patients.

26, and 52 week follow up points. At final follow up, the patients in the passive motion group averaged 130° of motion as compared to 148° in the active group ($p<.01$). The patients had smaller PIP joint flexion contractures in the active group (8°) as compared to the passive group (23°, $p<.05$) (Figure 4). The same was true for the DIP joint where the passive range of motion group had greater flexion contractures (22°) as compared to the patients in the active group (10°, $p<.05$).

The Effect of Nerve Injury:

The patients with nerve injuries demonstrated improvement in their sensibility during the course of the follow up period. There was no significant difference between the patients in the active motion group 3.44 versus the patients in the passive group 3.22. The digits with nerve injury had less overall active motion as compared to the digits without nerve injury. The digits with nerve injury also had greater PIP joint flexion contracture and DIP joint flexion contracture ($p<.05$) as compared to patients without nerve injuries.

The Effect of the Mechanism Injury: Sharp Versus Crush Injury:

There was no significant difference in the mechanism of injury between the active versus the passive motion groups. As a combined group the patients with crush injuries had less active motion than the patients with a sharp injury ($p<.05$).

Effect of Smoking:

Smoking had a significant impact on the patient's range of motion regardless of whether of the patients had active motion or passive motion ($p<.05$).

Please see Table 2 for complications.

Discussion

Controlled Active Motion Therapy:

This therapy demonstrated improved results with respect to overall active motion as well as the ability to minimize PIP and DIP joint flexion contractures as compared to passive motion only. Hand dexterity was better in the active therapy group. The incidence of complications was similar between the two groups with tendon rupture occurring in one patient in each group. Because the injury often involved only a single digit in most patients, the DASH questionnaire did not appear to be able to provide a sensitive means of differentiating between the patients in the two different treatment groups. The patients with sharp injuries had greater overall active motion with smaller flexion contractures as compared to the crush injury. The patients with nerve injury generally had a wider laceration and usually had a laceration down to bone as compared to patients with only tendon lacerations. It is not clear whether the fact that the sensory feedback or the overall magnitude of the injury that effects final functional outcome with concomitant nerve injury. Smoking had a significant negative effect on digit motion.

Conclusion

In conclusion, a combination of controlled active motion plus passive motion for the rehabilitation of patients with Zone II flexor tendon injuries, appears to be a safe and effective technique that helps to optimize overall motion. Patients still were short of regaining a full motion, and the challenge of achieving full hand function following a flexor tendon injury remains.

Therapy	Active	Passive
Digits	33	33
Nerve Lacerations	15	16
Crush Injuries	8	5
Male	16	17
Work related	7	7

Table 1: Demographic Data.

Complication	Treatment	Active	Passive
Rupture	Repair	1/33	1/33
Adhesions	Tenolysis	2/33	5/33

Table 2: Complications.

Recommended Reading

Silfverskiold, K. L.; May, E. J.; and Oden, A.: Factors affecting results after flexor tendon repair in zone II: a multivariate prospective analysis. J Hand Surg Am, 18(4):654-62, 1993.

Strickland, J. W.: Flexor Tendon Repair: Indiana method. Indiana Hand Center Newsletter, 1(1):1-19, 1993.

Thurman, R. T.; Trumble, T. E.; Hanel, D. P.; Tencer, A. F.; and Kiser, P. K.: Two-, four-, and six-strand zone II flexor tendon repairs: an in situ biomechanical comparison using a cadaver model. J Hand Surg [Am], 23(2):261-5, 1998.

Wagner, W. F., Jr.; Carroll, C. t.; Strickland, J. W.; Heck, D. A.; and Toombs, J. P.: A biomechanical comparison of techniques of flexor tendon repair. J Hand Surg Am, 19(6):979-83, 1994.

Department of Orthopaedics and Sports Medicine Faculty

Frederick A. Matsen III, M.D.
Professor and Chair

Christopher H. Allan, M.D.
Assistant Professor

David Barei, M.D.
Assistant Professor

Carlo Bellabarba, M.D.
Assistant Professor

Stephen K. Benirschke, M.D.
Associate Professor

James D. Bruckner, M.D.
Associate Professor

Howard A. Chansky, M.D.
Assistant Professor

Jens R. Chapman, M.D.
Associate Professor

Randal P. Ching, Ph.D.
Assistant Professor

John M. Clark, Jr., M.D., Ph.D.
Associate Professor

Ernest U. Conrad III, M.D.
Professor

Mohammad Diab, M.D.
Assistant Professor

David R. Eyre, Ph.D.
Professor

Theodore K. Greenlee, Jr., M.D.
Associate Professor

Ted Gross, Ph.D.
Associate Professor

Douglas P. Hanel, M.D.
Associate Professor

Sigvard T. Hansen, Jr., M.D.
Professor

M. Bradford Henley, M.D.
Associate Professor

Nancy J. Kadel, M.D.
Assistant Professor

Roger V. Larson, M.D.
Associate Professor

William J. Mills, M.D.
Assistant Professor

Sohail K. Mirza, M.D.
Assistant Professor

Vincent S. Mosca, M.D.
Associate Professor

Sean E. Nork, M.D.
Assistant Professor

John O'Kane, M.D.
Assistant Professor

Milton L. Routt, Jr., M.D.
Associate Professor

Bruce J. Sangeorzan, M.D.
Professor

Gregory A. Schmale, M.D.
Assistant Professor

John A. Sidles, Ph.D.
Professor

Peter T. Simonian, M.D.
Associate Professor

Douglas G. Smith, M.D.
Associate Professor

Kevin L. Smith, M.D.
Assistant Professor

Kit M. Song, M.D.
Assistant Professor

Sundar Srinivasan, Ph.D.
Research Assistant Professor

Lynn T. Staheli, M.D.
Professor Emeritus

Carol C. Teitz, M.D.
Professor

Allan F. Tencer, Ph.D.
Professor

Thomas E. Trumble, M.D.
Professor

Jiann-Jiu Wu, Ph.D.
Research Associate Professor

Liu Yang, Ph.D.
Research Assistant Professor

Adjunct Faculty

Basia R. Belza, R.N., Ph.D.
Associate Professor, Physiological Nursing

Jack W. Berryman, Ph.D.
Professor, Medical History & Ethics

Charles H. Chesnut, M.D.
Professor, Nuclear Medicine

Eva M. Escobedo, M.D.
Assistant Professor, Radiology

Gregory C. Gardner, M.D.
Associate Professor, Rheumatology

Thurman Gillespy, M.D.
Associate Professor, Radiology

Daniel O. Graney, Ph.D.
Associate Professor, Biological Structure

John C. Hunter, M.D.
Associate Professor, Radiology

Frederick A. Mann, M.D.
Professor, Radiology

David W. Newell, M.D.
Professor, Neuroscience

Susan M. Ott, M.D.
Associate Professor, Division of Metabolism

Wendy Raskind, M.D., Ph.D.
Associate Professor, General Internal Medicine

Michael L. Richardson, M.D.
Professor, Radiology

Christopher I. Shaffrey, M.D.
Associate Professor, Neuroscience

Robert B. Schoene, M.D.
Professor, Medicine

Peter A. Simkin, M.D.
Professor, Medicine

Tony J. Wilson, M.D.
Professor, Radiology

Joint Faculty

John E. Olerud, M.D.
Professor, Division of Dermatology

Nathan J. Smith, M.D.
Professor Emeritus, Pediatrics

Michael D. Strong, Ph.D.
Research Professor, Surgery

Nicholas B. Vedder, M.D.
Associate Professor, Plastic Surgery

Clinical Faculty

Sarah E. Jackins, R.P.T.
Assistant Professor, Rehab Medicine

UNIVERSITY
OF WASHINGTON
SCHOOL OF
MEDICINE

Department of Orthopaedics
and Sports Medicine
University of Washington
1959 N.E. Pacific Street
Box 356500
Seattle, Washington 98195-6500
Phone: (206) 543-3690
Fax: (206) 685-3139

Affiliated Institutions

Children's Hospital and
Regional Medical Center
4800 Sand Point Way NE
Seattle, WA 98105
(206) 526-2000

Harborview Medical Center
325 Ninth Avenue
Seattle, WA 98104
(206) 731-3462

University of Washington
Medical Center
Bone and Joint Center
4245 Roosevelt Way NE
Seattle, WA 98105
(206) 598-4288

VA Puget Sound Health Care System
1660 South Columbian Way
Seattle, WA 98108
(206) 764-2215

Incoming Residents

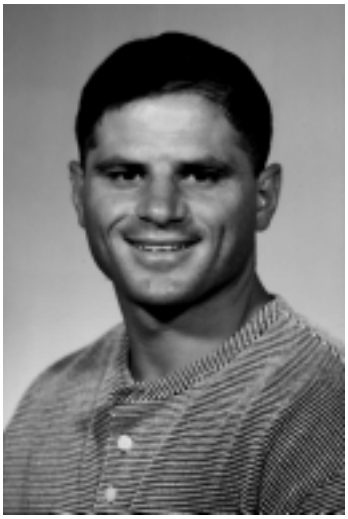

Anthony Buoncristiani: Tony attended UC-Davis and received his BS degree in Physiology. He received his medical degree from USC. After completing a surgical internship at the Naval Medical Ctr. in San Diego he began serving his military obligation to the Navy as a flight surgeon. He is currently completing a surgical internship at the University of Washington. His interests outside of medicine include running, cycling, marathons and triathlons.

Wren McCallister: Wren attended the University of Washington where he received a BA in both Economics and Biochemistry. Wren also received his MD degree from the University of Washington. He is currently completing his surgical internship at the University of Washington. In his spare time he enjoys baseball, golf and reading.

Timothy O'Mara: Tim received his BS degree in Biomedical Engineering from USC. He received his MD from the University of Nevada. He is completing his surgical internship at the University of Washington. Tim enjoys Abalone diving, swimming and running in his spare time.

Waqqar Khan-Farooqi: Waqqar received his BS degree in Biological Sciences from Stanford. He also earned his MD degree from Stanford. He is currently completing a surgical internship at the University of Washington. Personal interests include basketball, hiking and mountain bicycling.

David Stevens: David received his BA in Spanish from Brigham Young University. He received his MD from the University of Texas-Southwestern. He is currently completing his surgical internship at the University of Washington. His interests outside of medicine include automotive mechanics, computer electronics and skiing.

Graduating Residents
Class of 2001

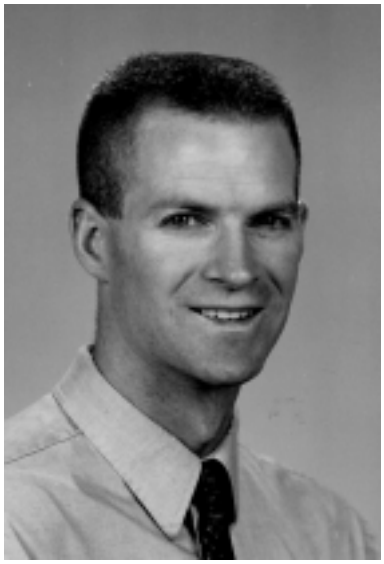

Richard Bransford, M.D., following his residency he will be doing a spine fellowship at the University of Washington Medical Center and Harborview Medical Center. In the future, he intends to return to his home in Kenya to live and work.

Fred Huang, M.D., will pursue a career in private practice at Valley Orthopaedic Associates in Renton, Washington, after completing his residency.

Michael Metcalf, M.D., will participate in a fellowship at the Mississippi Sports Medicine Clinic. He hopes to join a private practice in Park City, Utah.

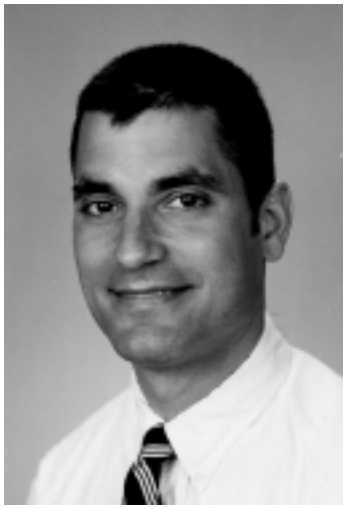

Matthew Camuso, M.D. will be doing a traumatology fellowship at Harborview Medical Center. Thereafter, he will spend four years on active duty with the US Navy, as part of his Health Professions Scholarship.

Eric Novack, M.D., will be part of a general orthopaedic practice in Scottsdale, Arizona.

2001 Department of Orthopaedics
New Faculty

David Barei, M.D.

David Barei recently joined the Orthopaedic & Sports Medicine faculty at Harborview as an Assistant Professor specializing in trauma surgery. Dr. Barei received his undergraduate education from the University of Western Ontario in London, Canada, and received his medical degree from the University of Ottawa. His internship was spent at St. Joseph's Health Centre, University of Toronto. He completed his residency at the Ottawa Hospital, University of Ottawa. Following residency, Dr. Barei completed two clinical fellowships at the Ottawa Hospital, one in joint arthroplasty and one in foot & ankle surgery. He received twelve months of advanced clinical experience in trauma surgery at Harborview Medical Center. Dr. Barei sees patients at Harborview Medical Center.

Ted S. Gross, Ph.D.

Ted S. Gross, Ph.D. recently joined the Orthopaedic & Sports Medicine faculty as an Associate Professor and Director of the Orthopaedic Science Laboratories (OSL) at Harborview. Dr. Gross received his undergraduate education from the Trinity University in Texas, his MS in Sports Biomechanics from Pennsylvania State University, and his Ph.D. in mechanical engineering from State University of New York at Stony Brook. Following graduate work, Dr. Gross did a Post-Doctoral Fellowship at the McCaig Centre for Joint Injury and Arthritis in Calgary, Canada. His specific area of research interest is the study of how bone cells and bone tissue perceive and respond to physical stimuli. Applications of this basic bone biological research include improved fracture healing, novel strategies to mitigate bone loss associated with disuse or space flight, and non-invasive, low magnitude, exercise strategies to counteract bone loss associated with aging and menopause. As Director of the OSL, Dr. Gross is charged with developing a unique, collaborative, multi-disciplinary research facility that interfaces biology and mechanics.

Gregory A. Schmale, M.D.

Dr. Schmale received his medical degree from the University of Washington in 1994 and completed an orthopaedic residency at the University of North Carolina at Chapel Hill in 1999. He pursued subspecialty training in pediatric orthopaedics at the Children's Hospital in Denver. Dr. Schmale has an interest in both adult and pediatric orthopaedics, including basic fracture care, sports medicine, spinal deformity, and congenital and developmental conditions such as club foot and dysplasia of the hip. He is active in research related to growth abnormalities of the knee and the treatment of hip disease in patients with cerebral palsy. Dr. Schmale sees patients on the Eastside at UW Physicians Neighborhood Clinics in Woodinville and Bellevue, as well as at Children's Hospital and Regional Medical Center in Seattle.

Research Grants
Department of Orthopaedics and Sports Medicine

National Institutes of Health (NIH)

Augmentation of Peak Bone Mass
Ted S. Gross, Ph.D.

Collagens of Cartilage and the Intervertebral Disc
David R. Eyre, Ph.D.

Disuse Induced Osteocyte Hypoxia
Ted S. Gross, Ph.D.

Imaging of Molecules by Oscillator-Coupled Resonance
John A. Sidles, Ph.D.

Outcomes Following Limb Reconstruction Vs Amputation
Douglas G. Smith, M.D.

Pathology of Inborn Skeletal Diseases
David R. Eyre, Ph.D.

Skeletal Dysplasias
David R. Eyre, Ph.D.

Veterans Affairs Medical Center Review Grants

Effect of Motor Imbalance on Bony Deformity and Plantar Pressure
Bruce J. Sangeorzan, M.D.

Rehabilitation Research and Development Center of Excellence for Limb Loss Prevention and Prosthetic Engineering
Bruce J. Sangeorzan, M.D.

Centers for Disease Control

Age-Related Cervical Spine Mechanics and Injury Tolerance
Randal P. Ching, Ph.D.

Low Speed Cervical Whiplash Injury
Allan F. Tencer, Ph.D.

Orthopaedic Research and Education Foundation (OREF)

Collaborative Opportunities in Orthopaedic Traumatology Research
Frederick A. Matsen III, M.D.

Research Grants
Department of Orthopaedics and Sports Medicine

Orthopaedic Research and Education Foundation (OREF)

Neural Instability of the Cervical Spine
Sohail K. Mirza, M.D.

Kappa Delta Award
Bruce J. Sangeorzan, M.D.

Overcoming Nerve Defect by Growth Factor Stimulated Regeneration Along Intact Nerves
Thomas E. Trumble, M.D.
Ben Dubois, M.D.

Reproductive Hormone Effects on ACL Strength
Emma Woodhouse, M.D.
Peter T. Simonian, M.D.

Toward Clinical Application of the Intact Nerve Bridge Technique: Longer Term Study in a Rabbit Model
Thomas E. Trumble, M.D.
Wren V. McCallister, M.D.

The Shoulder Function and Health Status of Individuals with Documented Rotator Cuff Tears Before and After Treatment: A Multicentered Prospective Study
Frederick A. Matsen III, M.D.

American Orthopaedic Foot & Ankle Society

Development of a Self Administered Outcome Tool for the Foot and Ankle
Bruce J. Sangeorzan, M.D.

American Society for Surgery of the Hand

Axonal Sprouting from Intact Peripheral Nerves
Thomas E. Trumble, M.D.

Prospective Randomized Clinical Trial of Hand Therapy Following Carpal Tunnel Surgery
Thomas E. Trumble, M.D.

Using Intact Nerve to Bridge Peripheral Nerve Defects: An Alternative to the Use of Nerve Grafts
Thomas E. Trumble, M.D.

Research Grants
Department of Orthopaedics and Sports Medicine

Genetics Institute

A Feasibility and Safety Study of rhBMP-2/ACS and Allograft Compared to Autogenous Bone Graft for Patients with Severe Tibial Shaft Fractures
Sohail K. Mirza, M.D.

Epidemiology Research and Information Center

Relationship Among Deformity, Pressure and Ulcer Formation in Diabetic Feet
Bruce J. Sangeorzan, M.D.

National Highway Traffic Safety Administration

Age-Dependent Properties of the Spine
Randal P. Ching, Ph.D.

Neck Mechanics and Injury Tolerance as a Function of Developmental Age
Randal P. Ching, Ph.D.

Pfizer, Inc.

Pfizer Study
David R. Eyre, Ph.D.

Spinal Dynamics Corp.

BRD Functional Disc Space Prosthesis Development Project
Randal P. Ching, Ph.D.

Functional Intervertebral Disc Space Prosthesis Development Project
Randal P. Ching, Ph.D.

Spinal Dynamics Baboon Testing
Randal P. Ching, Ph.D.

National Childhood Cancer Foundation

Children's Cancer Group
Ernest U. Conrad III, M.D.

Research Grants
Department of Orthopaedics and Sports Medicine

The Boeing Company

Randomized Clinical Trial of Open versus Endoscopic Carpal Tunnel Release and Hand Therapy Comparing Patient Satisfaction: Functional Outcome and Cost Effectiveness
Thomas E. Trumble, M.D.

Wyeth-Ayerst Clinical Research

Safety and Efficacy of Two Intravenous Dosages of GAR-936 for Complicated Skin Infections: A Prospective Randomized Trial
William J. Mills, M.D.

Ostex International, Inc.

Molecular Markers of Connective Tissue Degradation
David R. Eyre, Ph.D.

Royalty Research Fund

Vertebral Strength Following Percutaneous Vertebroplasty: A Comparison Between the Standard Technique and a Novel Approach to Stabilizing Osteoporotic Vertebrae
Sohail K. Mirza, M.D.

Zymogenetics

An Analysis of Collagen Synthesized by Zfgf5 Treated Chondrocytes
David R. Eyre, Ph.D.
Russell J. Fernandes, Ph.D.

Ethicon

Role of Bone in Cartilage Transplantation
Peter T. Simonian, M.D.

United States Air Force Research Laboratory

Pilot Study: Human Tensile Neck Injury Tolerance
Randal P. Ching, Ph.D.

Research Grants
Department of Orthopaedics and Sports Medicine

DePuy Orthopaedics, Inc.

THA Range Of Motion Study
Randal P. Ching, Ph.D.

The Physical Medicine Research Foundation

Development of a Device to Reduce Whiplash Motion of the Cervical Spine
Allan F. Tencer, Ph.D.

National Leukemia Research Foundation

TLS/ERG fusion protein in leukemia
Liu Yang, Ph.D.

Contributors to Departmental Research and Education

APRIL 2000 THROUGH MARCH 2001

We express our appreciation to all who have contributed to the work of the Department of Orthopaedics and Sports Medicine over the past year. Your assistance makes possible special research activities, educational programs, and other projects that we could not offer without this extra support from our alumni, faculty, and friends in the community. We owe a special thanks to the University of Washington Resident Alumni who have made significant contributions to help further the education of our current residents.

Friends of Orthopaedics

Aircast
Christopher Allan
Marylin J. Alvine
Eamonn J. Anderson
Harold Anderson
Nick Anderson
Roger Arms
Aventis Pharmaceuticals
Allan Bach
Marjorie Bakamus
Sam Baker
Ballard Orthopaedic & Fracture Clinic
William & Lauren Barrett
Timothy Beals
Christian Bean
Carlo Bellabarba
Paul Benca
Steve Benirschke
Donald & Helen Bonomi
Ray Bouchey
P.G. Bowman
Andrew Bronstein
James D. Bruckner
Ernest Burgess
Darla Carnevali
Carnevali Enterprises
Susan Cero
Howard A. Chansky
Randy Ching
Gary Clancey
John Clark
Michael Coe
Lisa Conaghan
Ernest U. Conrad
Wayne Coutter
David Deneka
Robert Dennis
DePuy Orthopaedics
Mohammad Diab
Richard Dimond
Oriente Ditano
D-Square Electronics
Lenord Ely
Donald & Sarah Ericksen
Edward & Cynthia Farrar
Thomas Fischer
Flouroscan
Harold Forney
Richard & Joy Garner
Tom Green
Thomas Gritzka
Ken & Marian Hampton
Douglas P. Hanel
Sigvard Hansen
Hansjorg Wyss AO Medical Foundation
Healthwise
James Helm
John Hendrickson
Joel Hoekema
Cindy Houser
Kevin Hughes
Dan Jones
Nancy Kadel
David Karges
Tom Karnezis
Carlton Keck
Edith & Herbert Kelp
Harvey W. Kelp
Betty Killoran
Richard Kirby
Jonathan L. Knight
Labbeemint
Roger Larson
David G. Levinsohn
Robert Littleton
Vito Loguidice
R.H. Goodwin
Thomas Green
Theodore Greenlee
Ted Gross
John Hendrickson

Friends of Orthopaedics

Diana Jansen
R.E. Mackenzie
Marteinn Magnusson
Joan & Maxine Malmassari
Gil Mar
Frederick A. Matsen III
Gregory May
John McCaffery
Merck
Joseph Mezistrano
Microsoft
John Michelotti
William Mills
Sohail Mirza
Peter Mitchell
Mitek
John A. Miyano
Vincent Mosca
David R. Nank
Ann Nelson
Sean Nork
William Obremsky
John O'Kane
Mark Olson
William L. Oppenheim
Orthologic
Lawrence Page
Carol Peterson
Gregg Pleger
Colin Poole
Brett Quigley
Rainier Surgical
Gregory Rafijah
Steven Ratcliff
Jim Reiff
Mark Remington
Kenneth Robel
John Robertson
Raymond Robinson
Roland Rogers
M.L. Chip Routt
John T. Sack (Seattle Hand Surgery)
Michael Sailer
Rita L. Sandler
Bruce Sangeorzan
Mr. and Mrs. Sarah Sato
Paul & Connie Schlimgen
Gregory Schmale
Lynn & Jean Seaward
Richard Semon
Peter Simonian
Doug Smith
Kevin Smith
James Sobenski
Kit Song
Lyle Sorenson
Jeannia Stanley
Elaine Stevenson
John Stewart
Jeff Stickney
Ed Stokel
Don Striplin
Synthes Spine
Marisol Summers
Ilene Swanson
James Swanson
Mr. & Mrs. Kilip Swanson
Steven Sun
Marc & Beth Swiontkowski
Carol C. Teitz
Allan Tencer
Michael Thorpe
David Thull
Irving Tobin
Thomas Trumble
Martin Tullus
Tyco/Surgical Dynamics
Jim Vahey
J. Eric Vanderhooft
Nicholas B. Vedder
Robert Veith
Theodore Wagner
William F. Wagner
Karin L. Wahlstrom
Donald Warren
Pamela Warren
Patrick Warren
Beverly Wilson
Peter Wise
Neil Wells
John West III
Jay A. Winzenried
Brodie Wood
Robert L. Wood
Jiann-Jiu Wu
Zimmer
Joseph D. Zuckerman

Alumni at the 2001 AAOS

Here are a couple of photos taken at the Friday evening UW Orthopaedic Alumni gathering at the San Francisco Academy Meeting, wonderfully organized as usual by Lyle Sorensen. How many of these folks can you identify? Be there next year in Dallas!